

1937

Stresses in the curved beam under loads normal to the plane of its axis

Robert Burrus Buckner Moorman
Iowa State College

Follow this and additional works at: <https://lib.dr.iastate.edu/rtd>

 Part of the [Civil Engineering Commons](#)

Recommended Citation

Moorman, Robert Burrus Buckner, "Stresses in the curved beam under loads normal to the plane of its axis " (1937). *Retrospective Theses and Dissertations*. 14122.
<https://lib.dr.iastate.edu/rtd/14122>

This Dissertation is brought to you for free and open access by the Iowa State University Capstones, Theses and Dissertations at Iowa State University Digital Repository. It has been accepted for inclusion in Retrospective Theses and Dissertations by an authorized administrator of Iowa State University Digital Repository. For more information, please contact digirep@iastate.edu.

INFORMATION TO USERS

This manuscript has been reproduced from the microfilm master. UMI films the text directly from the original or copy submitted. Thus, some thesis and dissertation copies are in typewriter face, while others may be from any type of computer printer.

The quality of this reproduction is dependent upon the quality of the copy submitted. Broken or indistinct print, colored or poor quality illustrations and photographs, print bleedthrough, substandard margins, and improper alignment can adversely affect reproduction.

In the unlikely event that the author did not send UMI a complete manuscript and there are missing pages, these will be noted. Also, if unauthorized copyright material had to be removed, a note will indicate the deletion.

Oversize materials (e.g., maps, drawings, charts) are reproduced by sectioning the original, beginning at the upper left-hand corner and continuing from left to right in equal sections with small overlaps.

ProQuest Information and Learning
300 North Zeeb Road, Ann Arbor, MI 48106-1346 USA
800-521-0600

UMI[®]

NOTE TO USERS

This reproduction is the best copy available.

UMI[®]

STRESSES IN THE CURVED BEAM
UNDER LOADS NORMAL TO THE PLANE OF ITS AXIS

by

Robert Burrus Buckner Moorman

A Thesis Submitted to the Graduate Faculty
for the Degree of

DOCTOR OF PHILOSOPHY

Major Subject Structural Engineering

Approved:

Signature was redacted for privacy.

In charge of Major work

Signature was redacted for privacy.

Head of Major Department

Signature was redacted for privacy.

Dean of Graduate College

Iowa State College

1937

UMI Number: DP13380

UMI[®]

UMI Microform DP13380

Copyright 2005 by ProQuest Information and Learning Company.
All rights reserved. This microform edition is protected against
unauthorized copying under Title 17, United States Code.

ProQuest information and Learning Company
300 North Zeeb Road
P.O. Box 1346
Ann Arbor, MI 48106-1346

TABLE OF CONTENTS		Page
I.	INTRODUCTION	8
II.	HISTORICAL	11
III.	ANALYSIS OF CURVED BEAM BY METHOD OF WORK INVOLVING ONLY BENDING MOMENT, TWISTING MOMENT AND VERTICAL SHEAR	14
	A. General	14
	B. Notation	15
	C. Assumptions	17
	D. Derivation.	17
IV.	EXPERIMENTS ON A CURVED ROD OF CIRCULAR- ARC PLAN	30
	A. Tests	30
	B. Analytical.	33
	C. Discussion.	56
V.	ANALYSIS OF CIRCULAR-ARC CURVED BEAM OF I-FORM	57
	A. General	57
	B. Notation	58
	C. Assumptions	60
	D. Derivation.	60
VI.	EXPERIMENTS ON AN I-BEAM BENT TO A SEMI- CIRCLE	73
	A. General	73
	B. Materials	73
	C. Constants	75

	Page
D. Method of Procedure	77
E. Annealing of I-beam	79
F. Results	90
VII. CONCLUSIONS.	104
A. Analysis of Curved Beam by Method of Work Involving only Bending Moment, Twisting Moment and Shear, with Tests on a Curved Rod.	104
B. Analysis of the Circular-Arc Beam of I-Form and Tests on the I-Beam	104
VIII. SUMMARY.	107
IX. LITERATURE CITED	108
X. ACKNOWLEDGMENT	110.
APPENDIX A	111
APPENDIX B	115

	Page
I. Computations of x and y Distances. . .	54
II. Computations of Values for Influence Lines, Bending Moment, Twisting Moment and Shear	35
III. Values of Influence Ordinates for Bending Moment and Twisting Moment at Quarter- Point - Arc 180°	43
IV. Values of Influence Ordinates for Bending Moment and Twisting Moment at Quarter- Point - Arc 144°	44
V. Constants of Integration in Terms of P to be used in Equation (54)	76
VI. Deflections of Center of Beam Due to a Load of 500 pounds.	85

	Page
1. Left Segment of Beam	18
2. Distances - u and v	21
3. Right Segment of Beam.	21
4. Curved Rod in Place	32
5. Influence Line for Bending Moment at \mathcal{C} - Arc 180° .	45
6. Influence Line for Twisting Moment at \mathcal{C} - Arc 180°	46
7. Influence Line for Shear at \mathcal{C} - Arc 180°	47
8. Influence Line for Bending Moment at Quarter- Point - Arc 180°	48
9. Influence Line for Twisting Moment at Quarter- Point - Arc 180°	49
10. Influence Line for Bending Moment at \mathcal{C} - Arc 144° .	50
11. Influence Line for Twisting Moment at \mathcal{C} - Arc 144°	51
12. Influence Line for Shear at \mathcal{C} - Arc 144°	52
13. Influence Line for Bending Moment at Quarter- Point - Arc 144°	53
14. Influence Line for Twisting Moment at Quarter- Point - Arc 144°	54
15. Other Test Data - Arc 180°	55
16. Forces Acting on Elemental Length of I-Beam	61

	Page
17. Displacements v , y and z	64
18. Relative Displacements of Points 1 and 2.	65
19. q_m and \mathcal{U}	66
20. General View of Experimental Set-up	74
21. Huggenberger Tensometers in Place	78
22. General View During Annealing of Beam	81
23. Outer Fiber Stress T_I for $\alpha=90^\circ$, $\beta=90^\circ$	86
24. Outer Fiber Stress T_O for $\alpha=90^\circ$, $\beta=90^\circ$	87
25. Outer Fiber Stress B_I for $\alpha=90^\circ$, $\beta=90^\circ$	88
26. Outer Fiber Stress B_O for $\alpha=90^\circ$, $\beta=90^\circ$	89
27. Outer Fiber Stress T_I for $\alpha=75^\circ$, $\beta=105^\circ$	90
28. Outer Fiber Stress T_O for $\alpha=75^\circ$, $\beta=105^\circ$	91
29. Outer Fiber Stress B_I for $\alpha=75^\circ$, $\beta=105^\circ$	92
30. Outer Fiber Stress B_O for $\alpha=75^\circ$, $\beta=105^\circ$	93
31. Outer Fiber Stress T_I for $\alpha=45^\circ$, $\beta=135^\circ$	94
32. Outer Fiber Stress T_O for $\alpha=45^\circ$, $\beta=135^\circ$	95
33. Outer Fiber Stress B_I for $\alpha=45^\circ$, $\beta=135^\circ$	96
34. Outer Fiber Stress B_O for $\alpha=45^\circ$, $\beta=135^\circ$	97
35. Values of z for $\alpha=90^\circ$ and $\beta=90^\circ$	98
36. Values of z for $\alpha=75^\circ$ and $\beta=105^\circ$	99
37. Values of z for $\alpha=45^\circ$ and $\beta=135^\circ$	100
38. Twisting Moment - $\alpha=90^\circ$ and $\beta=90^\circ$	101
39. Twisting Moment - $\alpha=75^\circ$ and $\beta=105^\circ$	102

	Page
40. Twisting Moment - $\alpha = 45^\circ$ and $\beta = 135^\circ$	103
41. Change in Curvature	112
42. Outer Fiber Stress T_I for Quarter-Point Loads	116
43. Outer Fiber Stress T_O for Quarter-Point Loads	117
44. Outer Fiber Stress B_I for Quarter-Point Loads	118
45. Outer Fiber Stress B_O for Quarter-Point Loads	119

I. INTRODUCTION

The horizontally curved beam has a variety of uses such as in the design of elevated tanks and balconies of theatres and auditoriums. According to Young and Hughes (15) bridge girders have been built of circular-arc plan. The principles of analysis of the horizontally curved beam may be applied to the arch rib with a lateral wind load. It has also been found expedient to use the curved beam for corners of buildings where it is desired to omit columns.

The problem of the curved beam is a three dimensional one. It involves bending moment, torque and shear. A general solution which could cover all cases would be very complicated. One complicating factor is the measure of torsional rigidity. Another complication is introduced by the fact that for certain cross-sections of beam, particularly those of I-form, there are bending moments induced in planes parallel to the plane of the axis of the beam which cannot readily be determined by the use of statics. If the simplifying assumption is made that the

unit angle of twist varies as the total torque, regardless of the length of the member, then a general solution may be expedited. There remains then only the bending moment, torque and shear for which to solve. However, an analysis of this type is not applicable to a curved beam when its shape is such that additional bending moments may be induced in planes parallel to the plane of the axis of the beam.

A special solution is necessary for a curved beam of I cross-section. In this case there exists a bending moment in the plane of each of the flanges. The bending moment in one flange is equal to the bending moment in the other flange but of opposite sign. When analyzing the beam, if we imagine the beam cut at any section these two moments cancel the effects of one another. Consequently, it is necessary to depend upon displacements when solving for these induced bending moments. There is also a shear which accompanies each of these moments. This shear contributes to the total twisting moment in that the total twisting moment is equal to this shear times the depth of the beam, or more properly the distance between the centroids of the flanges, plus the pure torsion. The curved beam of I cross-section also has bending moment, twisting moment and vertical shear acting upon it.

The objectives of this thesis are, first, to present an analysis for a curved beam of any plan in which there is little or no bending moment induced in planes parallel to the plane of the axis of the beam; second, to present an analysis of the circular-arc beam of I cross-section which is loaded by single concentrated loads; and third, to present the results of experiments for comparison with the algebraic analyses.

In connection with these analyses experimental investigations were conducted on a curved round rod of steel and a curved I-beam. The I-beam was bent cold and tested, both in the unannealed and annealed conditions.

II. HISTORICAL

The problem of the beam curved in plan has been treated by a number of investigators. The first work on the curved beam was by Grashof (5). He dealt with the circular ring cut at a section with two equal and opposite loads applied at the cut ends.

The majority of investigators have used the circular-arc for the plan of the beam and have assumed that the unit angle of twist varies directly as the total twisting moment, regardless of the shape of the cross-section. Mayer (9) treated the girder of half-circular plan with unsymmetrical loads and a uniform load. Federhof (3) did the same but extended the work to include influence lines. Gibson and Ritchie (4) published a book on the circular-arc bow girder in which are given curves of bending moments and twisting moments to be used for various values of subtended arc. They presented the results of experiments conducted on a number of commercial steel sections which were tested in order to determine the torsional rigidity of these sections. Kannenberg (7) treated the circular-

arc beam on which the loads were symmetrically placed.

St. Hessler (12) worked on the circular-arc curved beam with fixed ends and loaded with uniform and symmetrically placed loads. He also derived formulas for the analysis of circular-arc beams with uniform loads in which the beams were on three and four equally spaced supports (13).

Worch (16) treated examples of curved beams made up of straight pieces and having several intermediate supports. Hailer (6) analyzed a special case of a beam whose plan was made up of a straight piece and a quadrant of a circle and loaded uniformly. Oesterblom (10) treated the circular-arc girder with uniformly distributed loads and presented curves of bending moment and twisting moment for various values of the elastic constants.

Pippard and Barrow (11) treated the curved girder with fixed ends. The curve of the girder could have any plan form, i.e., it was not limited to the circular-arc shape. The procedure recommended for the analysis of the non-circular shape involved the use of a planimeter or Simpson's rule for determining areas. The first analysis developed in this thesis eliminates this inconvenience and expresses the bending moment, twisting moment and shear in general terms.

All of the work mentioned above neglected the special treatment necessary for curved beams of I cross-section. Andrée (1) was the first to treat the beam of I-form. Unold (14) published the most complete treatment of circular-arc curved girders and included a summary of the work done on this problem prior to 1922. In the second analysis of this thesis his treatment of the circular-arc beam of I cross-section has been extended to apply to the beam with unsymmetrical concentrated loads and experiments were conducted for comparison with the analysis.

An uncertainty in a problem of this nature is the determination of a suitable torsion factor for irregular cross-sections. Along this line experiments have been conducted by Ritchie (4) and by Young and Hughes (15). An attempt was made by these investigators to determine a suitable relation between the experimental value of the torsion factor and the polar moment of inertia of the sections tested, but the results were not entirely satisfactory. Lyse and Johnston (8) conducted an extensive investigation on commercial steel sections in which the experimental values of the torsion factor were compared with the results of work using the membrane analogy. This investigation was found to be quite satisfactory and consequently the information has been made available to the engineering profession in a steel handbook (2).

III. ANALYSIS OF CURVED BEAM BY METHOD OF WORK INVOLVING
ONLY BENDING MOMENT, TWISTING MOMENT
AND VERTICAL SHEAR

A. General

The analysis developed in this chapter follows somewhat the procedure presented by Pippard and Barrow (11), but the solutions are extended to include formulas for bending moment, twisting moment and shear in general terms. Where it is possible terms are combined in order to expedite the work necessary for practical application.

The formulas derived in this chapter are applicable to a curved beam with fixed ends and a plan of any shape. Needless to say, the application becomes simplified for the case in which the plan of the beam is symmetrical.

In solving for the redundants we imagine the beam cut at any section, C, (see Fig. 1) and such forces are applied as to again produce continuity. In this case the beam is cut along the YZ-plane. At the cut end are placed a bending moment, twisting moment and shear, designated by the characters M_c , T_c and V_c , respectively.

The equation for work is written and by taking partial derivatives of the work with respect to M_c , T_c and V_c and equating each partial derivative to zero, three equations are obtained involving the three unknowns.

In the case of the unsymmetrical beam the section, C , should be taken at the right support. Then all terms with the subscript R would vanish, as they are used to indicate functions on the right segment of the beam. The bending moment, twisting moment and shear at the right support would then be given by the formulas for M_c , T_c and V_c , respectively.

B. Notation

The following notation is used in Chapters III and IV.

The subscripts L and R designate the left segment and the right segment, respectively, of the beam.

θ angle which the tangent to the left segment of the beam axis makes with the Y -axis (Fig. 1b).

ϕ angle, corresponding to θ , for the right segment of the beam.

- M_C , T_C and V_C bending moment, twisting moment and shear, respectively, at C necessary to produce continuity.
- ds elemental length of the beam axis.
- M , T bending moment and twisting moment, respectively, at any section on the beam.
- m_x moment, at any section, in the X-direction due to the applied loads.
- m_y moment, at any section, in the Y-direction due to the applied loads.
- E modulus of elasticity in tension.
- I moment of inertia.
- G modulus of elasticity in shear.
- K a torsion constant; polar moment of inertia for circular section.
- EI flexural rigidity.
- GK torsional rigidity.
- x distance from C to section under consideration in X-direction.
- y distance from C to section under consideration in Y-direction.
- W work.

C. Assumptions

The following assumptions are made.

1. Hooke's law applies.
2. The deformations are small so that it may be said (approximately) for angular deformations that $\alpha = \sin \alpha = \tan \alpha$, where α is the angular deformation.
3. The angle of twist per unit length of beam varies

as $\frac{T}{GK}$.

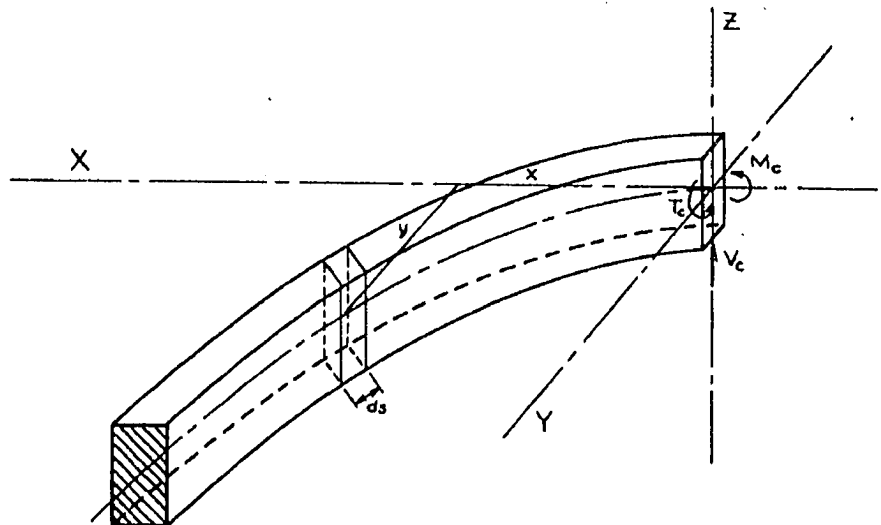
4. The angle of bending per unit length of beam varies as $\frac{M}{EI}$.

D. Derivation

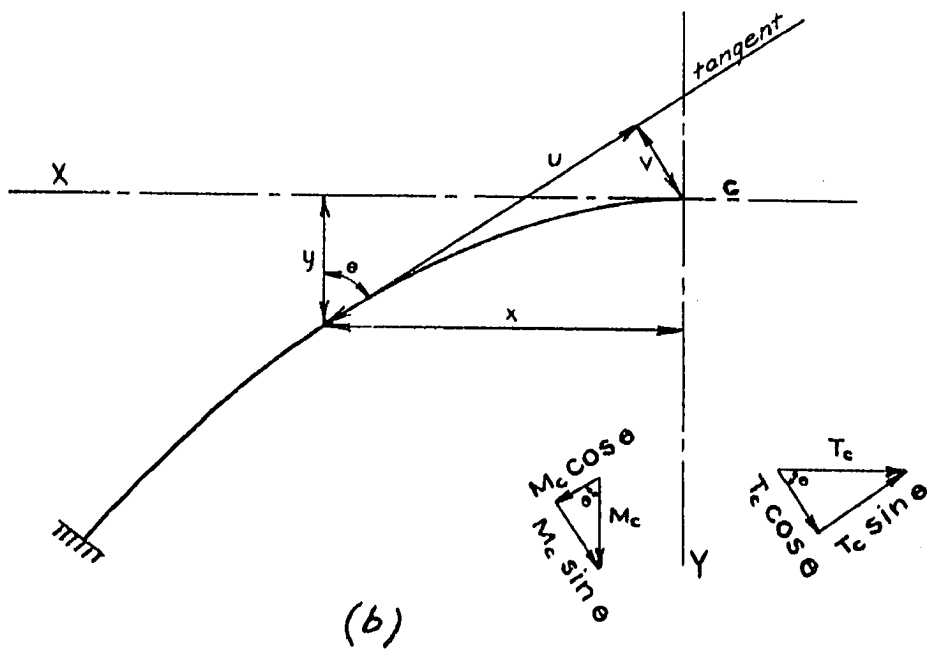
Figure 1a, a view of the left segment of the beam, shows the positions of the X-, Y- and Z-axes. The YZ-plane cuts the beam at C. At the cut end the positive directions of bending moment, twisting moment and shear are indicated.

Figure 1b shows the line diagram of the left segment of the beam with the angle θ and x- and y- distances.

In order to express the bending and twisting moments, due to the shear V_c , at any section in terms of the



(a)



(b)

FIG. 1. LEFT SEGMENT OF BEAM.

coordinates x and y it is necessary to express the distances u and v (Fig. 1b) in terms of x and y . The distance u is from C to the section under consideration along a tangent at the section. The perpendicular distance from C to the tangent at the section is taken as v .

Figure 2 shows the portion of the beam between C and any section. From the figure we see that

$$\begin{aligned}v &= AC = AB - BC = DE - BC \\ &= x \cos \theta - y \sin \theta\end{aligned}$$

and

$$\begin{aligned}u &= AF = AD + DF = BE + DF \\ &= x \sin \theta + y \cos \theta\end{aligned}$$

Now, the bending moment and twisting moment at any point along the left segment of the axis of the beam may be expressed as follows:

$$\begin{aligned}M_L &= M_C \sin \theta + V_C u + T_C \cos \theta + m_{x_L} \sin \theta + m_{y_L} \cos \theta \\ &= M_C \sin \theta + V_C (x \sin \theta + y \cos \theta) + T_C \cos \theta \\ &\quad + m_{x_L} \sin \theta + m_{y_L} \cos \theta\end{aligned}\tag{1}$$

and

$$T_L = -M_C \cos \theta - V_C v + T_C \sin \theta - m_{x_L} \cos \theta + m_{y_L} \sin \theta$$

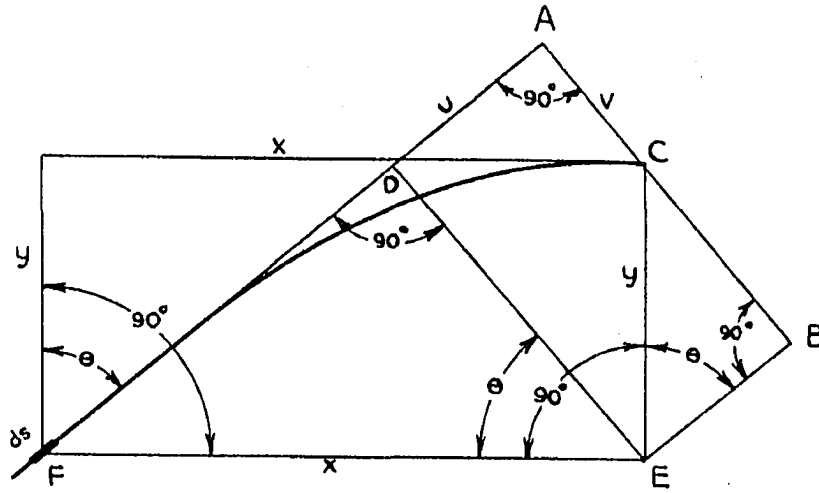


FIG. 2. DISTANCES u AND v .

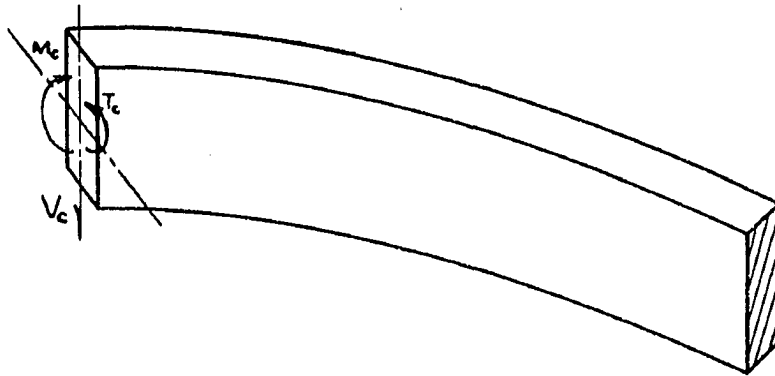


FIG. 3. RIGHT SEGMENT OF BEAM.

$$\begin{aligned} &= -M_c \cos \theta - V_c (x \cos \theta - y \sin \theta) + T_c \sin \theta \\ &\quad -m_{x_L} \cos \theta + m_{y_L} \sin \theta \end{aligned} \tag{2}$$

In a similar manner the expressions for bending moment and twisting moment may be written for the right segment of the beam. Figure 3 shows the right segment of the beam with the positive directions of M_c , T_c and V_c indicated. In order to have continuity the value of M_c on the left segment of the beam must be equal to the value on the right segment. The values of T_c and V_c on the left segment of the beam must be equal to those on the right segment but of opposite sign. The expressions for bending moment and twisting moment for the right segment of the beam may be written as follows:

$$\begin{aligned} M_R &= M_c \sin \phi - V_c u - T_c \cos \phi + m_{x_r} \sin \phi + m_{y_r} \cos \phi \\ &= M_c \sin \phi - V_c (x \sin \phi + y \cos \phi) - T_c \cos \phi + m_{x_r} \sin \phi + m_{y_r} \cos \phi \end{aligned} \quad (3)$$

and

$$\begin{aligned} T_R &= -M_c \cos \phi + V_c v - T_c \sin \phi - m_{x_r} \cos \phi + m_{y_r} \sin \phi \\ &= -M_c \cos \phi + V_c (x \cos \phi - y \sin \phi) - T_c \sin \phi - m_{x_r} \cos \phi + m_{y_r} \sin \phi \end{aligned} \quad (4)$$

Neglecting the work of the vertical shear the equation for work may be written

$$W = \int \frac{M_L^2 ds}{2EI} + \int \frac{T_L^2 ds}{2GK} + \int \frac{M_R^2 ds}{2EI} + \int \frac{T_R^2 ds}{2GK} \quad (5)$$

Then the work W may be differentiated with respect to each of the variables M_c, T_c and V_c , giving

$$\frac{\partial W}{\partial M_c} = \int \frac{M_L ds}{EI} \frac{\partial M_L}{\partial M_c} + \int \frac{T_L ds}{GK} \frac{\partial T_L}{\partial M_c} + \int \frac{M_R ds}{EI} \frac{\partial M_R}{\partial M_c} + \int \frac{T_R ds}{GK} \frac{\partial T_R}{\partial M_c} \quad (6)$$

$$\frac{\partial W}{\partial T_c} = \int \frac{M_L ds}{EI} \frac{\partial M_L}{\partial T_c} + \int \frac{T_L ds}{GK} \frac{\partial T_L}{\partial T_c} + \int \frac{M_R ds}{EI} \frac{\partial M_R}{\partial T_c} + \int \frac{T_R ds}{GK} \frac{\partial T_R}{\partial T_c} \quad (7)$$

$$\frac{\partial W}{\partial V_c} = \int \frac{M_L ds}{EI} \frac{\partial M_L}{\partial V_c} + \int \frac{T_L ds}{GK} \frac{\partial T_L}{\partial V_c} + \int \frac{M_R ds}{EI} \frac{\partial M_R}{\partial V_c} + \int \frac{T_R ds}{GK} \frac{\partial T_R}{\partial V_c} \quad (8)$$

or

$$\frac{\partial W}{\partial M_c} = \int M_L \sin \theta \frac{ds}{EI} - \int T_L \cos \theta \frac{ds}{GK} + \int M_R \sin \phi \frac{ds}{EI} - \int T_R \cos \phi \frac{ds}{GK} = 0 \quad (9)$$

$$\frac{\partial W}{\partial T_c} = \int M_L \cos \theta \frac{ds}{EI} + \int T_L \sin \theta \frac{ds}{GK} - \int M_R \cos \phi \frac{ds}{EI} - \int T_R \sin \phi \frac{ds}{GK} = 0 \quad (10)$$

$$\begin{aligned} \frac{\partial W}{\partial V_c} &= \int M_L (x \sin \theta + y \cos \theta) \frac{ds}{EI} - \int T_L (x \cos \theta - y \sin \theta) \frac{ds}{GK} \\ &\quad - \int M_R (x \sin \phi + y \cos \phi) \frac{ds}{EI} + \int T_R (x \cos \phi - y \sin \phi) \frac{ds}{GK} = 0 \end{aligned} \quad (11)$$

Substituting equations (1), (2), (3) and (4) in equations (9), (10) and (11) we have

$$\sum [M_c \sin \theta + V_c (x \sin \theta + y \cos \theta) + T_c \cos \theta + m_{x_L} \sin \theta + m_{y_L} \cos \theta] \frac{\sin \theta ds}{EI} -$$

$$\sum [M_c \sin \theta + V_c (x \sin \theta + y \cos \theta) + T_c \cos \theta + m_{x_L} \sin \theta + m_{y_L} \cos \theta] \frac{\cos \theta ds}{EI} +$$

$$\sum [M_c \sin \theta + V_c (x \sin \theta + y \cos \theta) + T_c \cos \theta + m_{x_L} \sin \theta + m_{y_L} \cos \theta] (x \sin \theta +$$

For symmetrical structures ϕ may be taken equal to θ and

$$2M_c \sum \left(\frac{\sin^2 \theta ds}{EI} + \frac{\cos^2 \theta ds}{GK} \right) + \sum (m_{x_L} + m_{x_R}) \sin^2 \theta \frac{ds}{EI} + \sum (m_{y_L} + m_{y_R}) \cos^2 \theta \frac{ds}{EI}$$

$$2V_c \sum [x \sin \theta \cos \theta \left(\frac{1}{EI} - \frac{1}{GK} \right) ds + y \left(\frac{\cos^2 \theta}{EI} + \frac{\sin^2 \theta}{GK} \right) ds] + 2T_c \sum \left(\frac{\cos^2 \theta}{EI} + \frac{\sin^2 \theta}{GK} \right) ds$$

$$2V_c \sum [(x \sin \theta + y \cos \theta)^2 \frac{ds}{EI} + (x \cos \theta - y \sin \theta)^2 \frac{ds}{GK}] + 2T_c \sum [\cos \theta (x \sin \theta + y \cos \theta) ds + \sin \theta (x \cos \theta - y \sin \theta) ds]$$

Solving for M_c from equation (15) we have

$$M_c = - \frac{\sum (m_{x_L} + m_{x_R}) \left(\frac{\sin^2 \theta ds}{EI} + \frac{\cos^2 \theta ds}{GK} \right) + \sum (m_{y_L} + m_{y_R}) \cos^2 \theta \frac{ds}{EI}}{2 \sum \left(\frac{\sin^2 \theta ds}{EI} + \frac{\cos^2 \theta ds}{GK} \right)}$$

From determinants we have

$$\left. \begin{aligned} V_c a + T_c b + c &= 0 \\ V_c d + T_c e + f &= 0 \end{aligned} \right\} V_c =$$

$$V_c = \frac{-2 \sum [\cos \theta (x \sin \theta + y \cos \theta) \frac{ds}{EI} - \sin \theta (x \cos \theta - y \sin \theta) \frac{ds}{GK}]}{\{ 2 \sum [x \sin \theta \cos \theta ds + y (\cos^2 \theta ds + \sin^2 \theta ds)] \}}$$

$$V_c = \frac{- \left\{ \sum [x \sin \theta \cos \theta \left(\frac{ds}{EI} - \frac{ds}{GK} \right) + y \left(\frac{\cos^2 \theta ds}{EI} + \frac{\sin^2 \theta ds}{GK} \right)] \right\}}{2 \left\{ \sum [x \sin \theta \cos \theta ds + y (\cos^2 \theta ds + \sin^2 \theta ds)] \right\}}$$

$$T_c = \frac{- \left\{ \sum [x \sin \theta \cos \theta \left(\frac{ds}{EI} - \frac{ds}{GK} \right) + y \left(\frac{\cos^2 \theta ds}{EI} + \frac{\sin^2 \theta ds}{GK} \right)] \right\}}{2 \left\{ \sum [x \sin \theta \cos \theta ds + y (\cos^2 \theta ds + \sin^2 \theta ds)] \right\}}$$

$$\frac{1}{s} - \sum [-M_c \cos \theta - V_c (x \cos \theta - y \sin \theta) + T_c \sin \theta - m_{x_L} \cos \theta + m_{y_L} \sin \theta] \frac{\cos \theta ds}{GK} +$$

$$\frac{1}{s} + \sum [-M_c \cos \theta - V_c (x \cos \theta - y \sin \theta) + T_c \sin \theta - m_{x_L} \cos \theta + m_{y_L} \sin \theta] \frac{\sin \theta ds}{GK} -$$

$$\theta + y \cos \theta) \frac{ds}{EI} - \sum [-M_c \cos \theta - V_c (x \cos \theta - y \sin \theta) + T_c \sin \theta - m_{x_L} \cos \theta + m_{y_L} \sin \theta]$$

and the above equations may be written

$$) \sin \theta \cos \theta \frac{ds}{EI} + \sum (m_{x_L} + m_{x_R}) \cos^2 \theta \frac{ds}{GK} - \sum (m_{y_L} + m_{y_R}) \sin \theta \cos \theta \frac{ds}{GK} = 0$$

$$+ \frac{\sin^2 \theta}{GK} ds + \sum (m_{x_L} - m_{x_R}) \sin \theta \cos \theta (EI - GK) ds + \sum (m_{y_L} - m_{y_R}) (\frac{\cos^2 \theta}{EI} +$$

$$x \sin \theta + y \cos \theta) \frac{ds}{EI} - \sin \theta (x \cos \theta - y \sin \theta) \frac{ds}{GK}] + \sum (m_{x_L} - m_{x_R}) [\sin \theta (x \sin \theta +$$

$$\sin \theta \cos \theta (\frac{ds}{EI} - \frac{ds}{GK})$$

(18)

$$V_c = \frac{-ec + bf}{ae - db} \text{ and } T_c = \frac{-af + dc}{ae - db} \text{ Using this form in solving for } V_c \text{ a}$$

$$) \frac{ds}{GK}] \left\{ \sum [(m_{x_L} - m_{x_R}) \sin \theta \cos \theta (\frac{ds}{EI} - \frac{ds}{GK}) + (m_{y_L} - m_{y_R}) (\frac{\cos^2 \theta ds}{EI} + \frac{\sin^2 \theta ds}{GK})] \right\}$$

$$\sin \theta \cos \theta (\frac{ds}{EI} - \frac{ds}{GK}) + y (\frac{\cos^2 \theta ds}{EI} + \frac{\sin^2 \theta ds}{GK}) \left\{ 2 \sum [\cos \theta (x \sin \theta + y \cos \theta) \frac{ds}{EI} - \sin \theta ($$

$$- m_{x_R}) \sin \theta \cos \theta (\frac{ds}{EI} - \frac{ds}{GK}) + (m_{y_L} - m_{y_R}) (\frac{\cos^2 \theta ds}{EI} + \frac{\sin^2 \theta ds}{GK}) \right\} + \left\{ \sum (\frac{\cos^2 \theta ds}{EI} +$$

$$\sin \theta \cos \theta (\frac{ds}{EI} - \frac{ds}{GK}) + y (\frac{\cos^2 \theta ds}{EI} + \frac{\sin^2 \theta ds}{GK}) \right\}^2 - \left\{ \sum [x^2 (\frac{\sin^2 \theta ds}{EI} + \frac{\cos^2 \theta ds}{GK}) +$$

$$(m_{x_L} - m_{x_R}) x (\frac{\sin^2 \theta ds}{EI} + \frac{\cos^2 \theta ds}{GK}) + (m_{x_L} - m_{x_R}) y \sin \theta \cos \theta (\frac{ds}{EI} - \frac{ds}{GK}) + (m_{y_L} - m_{y_R}) x \sin \theta \cos \theta$$

$$\left\{ \sum [x \sin \theta \cos \theta (\frac{ds}{EI} - \frac{ds}{GK}) + y (\frac{\cos^2 \theta ds}{EI} + \frac{\sin^2 \theta ds}{GK}) \right\}^2 - 2 \left\{ \sum [x^2 (\frac{\sin^2 \theta ds}{EI} + \frac{\cos^2 \theta ds}{GK}) +$$

$$\frac{\cos \theta ds}{GK} + \sum [M_c \sin \phi - V_c (x \sin \phi + y \cos \phi) - T_c \cos \phi + m_{x_R} \sin \phi + m_{y_R} \cos \phi] \frac{\sin \phi}{EI}$$

$$\frac{\sin \theta ds}{GK} - \sum [M_c \sin \phi - V_c (x \sin \phi + y \cos \phi) - T_c \cos \phi + m_{x_R} \sin \phi + m_{y_R} \cos \phi] \frac{\cos \phi}{EI}$$

$$+ m_{y_L} \sin \theta] (x \cos \theta - y \sin \theta) \frac{ds}{GK} - \sum [M_c \sin \phi - V_c (x \sin \phi + y \cos \phi) - T_c \cos \phi + m_{x_R}$$

$$= 0 \quad (15)$$

$$\left(\frac{\cos^2 \theta}{EI} + \frac{\sin^2 \theta}{GK} \right) ds = 0 \quad (16)$$

$$(x \sin \theta + y \cos \theta) \frac{ds}{EI} + \cos \theta (x \cos \theta - y \sin \theta) \frac{ds}{GK} + \sum (m_{y_L} - m_{y_R}) [\cos \theta (x \sin \theta -$$

for V_c and T_c we have

$$+ \frac{\sin^2 \theta ds}{GK}]] + \left\{ 2 \sum \left(\frac{\cos^2 \theta ds}{EI} + \frac{\sin^2 \theta ds}{GK} \right) \right\} \left\{ \sum \left\{ (m_{x_L} - m_{x_R}) \sin \theta + (m_{y_L} - m_{y_R}) \cos \theta - \sin \theta (x \cos \theta - y \sin \theta) \frac{ds}{GK} \right\} - \left\{ 2 \sum \left[(x \sin \theta + y \cos \theta)^2 \frac{ds}{EI} + (x \cos \theta - y \sin \theta) \right. \right. \right.$$

$$\left. \left. \frac{\cos^2 \theta ds}{EI} + \frac{\sin^2 \theta ds}{GK} \right] \right\} \left\{ \sum \left[(m_{x_L} - m_{x_R}) x \left(\frac{\sin^2 \theta ds}{EI} + \frac{\cos^2 \theta ds}{GK} \right) + (m_{x_L} - m_{x_R}) y \sin \theta \right. \right.$$

$$\left. \left. \frac{\cos^2 \theta ds}{GK} \right] + 2xy \sin \theta \cos \theta \left(\frac{ds}{EI} - \frac{ds}{GK} \right) + y^2 \left(\frac{\cos^2 \theta ds}{EI} + \frac{\sin^2 \theta ds}{GK} \right) \right\} \left\{ 2 \sum \left(\frac{\cos^2 \theta}{EI} \right. \right.$$

$$\left. \left. x \sin \theta \cos \theta \left(\frac{ds}{EI} - \frac{ds}{GK} \right) + (m_{y_L} - m_{y_R}) y \left(\frac{\cos^2 \theta ds}{EI} + \frac{\sin^2 \theta ds}{GK} \right) \right] \right\} + \left\{ \sum \left[x^2 \left(\frac{\sin^2 \theta ds}{EI} + \frac{\cos^2 \theta ds}{GK} \right) \right. \right.$$

$$\left. \left. \frac{\cos^2 \theta ds}{GK} \right] + 2xy \sin \theta \cos \theta \left(\frac{ds}{EI} - \frac{ds}{GK} \right) + y^2 \left(\frac{\cos^2 \theta ds}{EI} + \frac{\sin^2 \theta ds}{GK} \right) \right\} \left\{ \sum \left(\frac{\cos^2 \theta ds}{EI} + \frac{\sin^2 \theta ds}{GK} \right) \right\}$$

$$\phi] \frac{\sin \phi ds}{EI} + \sum [M_c \cos \phi - V_c (x \cos \phi - y \sin \phi) + T_c \sin \phi + m_{xR} \cos \phi - m_{yR} \sin \phi]$$

$$\phi] \frac{\cos \phi ds}{EI} + \sum [M_c \cos \phi - V_c (x \cos \phi - y \sin \phi) + T_c \sin \phi + m_{xR} \cos \phi - m_{yR} \sin \phi]$$

$$\cos \phi + m_{xR} \sin \phi + m_{yR} \cos \phi] (x \sin \phi + y \cos \phi) \frac{ds}{EI} - \sum [M_c \cos \phi - V_c (x \cos \phi - y \sin \phi) +$$

$$(x \sin \theta + y \cos \theta) \frac{ds}{EI} - \sin \theta (x \cos \theta - y \sin \theta) \frac{ds}{GK}] = 0 \quad (17)$$

$$+ (m_{yL} - m_{yR}) \cos \theta \} (x \sin \theta + y \cos \theta) \frac{ds}{EI} + \sum \{ (m_{xL} - m_{xR}) \cos \theta + (-m_{yL} - m_{yR}) \sin \theta \} (x \cos \theta - y \sin \theta) \frac{ds}{GK} \} \left\{ 2 \left[\left(\frac{\cos^2 \theta ds}{EI} + \frac{\sin^2 \theta ds}{GK} \right) \right] \right\}$$

$$+ (m_{yL} - m_{yR}) y \sin \theta \cos \theta \left(\frac{ds}{EI} - \frac{ds}{GK} \right) + (m_{xL} - m_{xR}) x \sin \theta \cos \theta \left(\frac{ds}{EI} - \frac{ds}{GK} \right) + (m_{yL} - m_{yR}) y \left(\frac{\cos^2 \theta ds}{EI} + \frac{\sin^2 \theta ds}{GK} \right) \}$$

$$\left(\frac{\cos^2 \theta ds}{GK} \right) + 2xy \sin \theta \cos \theta \left(\frac{ds}{EI} - \frac{ds}{GK} \right) + y^2 \left(\frac{\cos^2 \theta ds}{EI} + \frac{\sin^2 \theta ds}{GK} \right) \} \left\{ \left[(m_{xL} - m_{xR}) \sin \theta \right] \left(\frac{\cos^2 \theta ds}{EI} + \frac{\sin^2 \theta ds}{GK} \right) \right\}$$

$$[\sin \phi + m_{x_R} \cos \phi - m_{y_R} \sin \phi] \frac{\cos \phi ds}{GK} = 0 \quad (12)$$

$$[\sin \phi + m_{x_R} \cos \phi - m_{y_R} \sin \phi] \frac{\sin \phi ds}{GK} = 0 \quad (13)$$

$$[\sin \phi - V_c (x \cos \phi - y \sin \phi) + T_c \sin \phi + m_{x_R} \cos \phi - m_{y_R} \sin \phi] (x \cos \phi - y \sin \phi) \frac{ds}{GK} = 0 \quad (14)$$

(17)

$$\underline{-m_{x_L} \cos \theta + (-m_{y_L} + m_{y_R}) \sin \theta \} (x \cos \theta - y \sin \theta) \frac{ds}{GK} \}$$

$$\underline{\frac{ds}{GK} + (m_{y_L} - m_{y_R}) y \left(\frac{\cos^2 \theta ds}{EI} + \frac{\sin^2 \theta ds}{GK} \right) \} \} \quad (19)$$

$$\underline{\frac{ds}{GK} \} \} \left\{ \left[(m_{x_L} - m_{x_R}) \sin \theta \cos \theta \left(\frac{ds}{EI} - \frac{ds}{GK} \right) + (m_{y_L} - m_{y_R}) \left(\frac{\cos^2 \theta ds}{EI} + \frac{\sin^2 \theta ds}{GK} \right) \right] \right\} \quad (20)$$

For a symmetrical structure the coefficients of V_c and T_c , in equation (12), cancel so that one may solve directly for M_c . Then the two remaining equations (13) and (14) each have two unknowns which can readily be determined.

Let

$$\sin \theta \cos \theta \left(\frac{ds}{EI} - \frac{ds}{GK} \right) = b \quad (21)$$

$$\frac{\sin^2 \theta ds}{EI} + \frac{\cos^2 \theta ds}{GK} = c \quad (22)$$

and

$$\frac{\cos^2 \theta ds}{EI} + \frac{\sin^2 \theta ds}{GK} = d \quad (23)$$

the expressions for M_c , V_c and T_c may be rewritten

$$M_c = -\frac{\sum(m_{x_L} + m_{x_R})c + \sum(m_{y_L} + m_{y_R})b}{2\sum c} \quad (24)$$

$$V_c = \frac{-(\sum(xb+yd))(\sum[(m_{x_L} - m_{x_R})b + (m_{y_L} - m_{y_R})d]) + (\sum d)(\sum[(m_{x_L} - m_{x_R})(xc+yb) + (m_{x_L} - m_{y_R})(xb+yd)])}{2(\sum(xb+yd))^2 - 2(\sum(x^2c + 2xyb + y^2d))(\sum d)} \quad (25)$$

$$T_c = \frac{-(\sum(xb+yd))(\sum[(m_{x_L} - m_{x_R})(xc+yb) + (m_{y_L} - m_{y_R})(xb+yd)]) + (\sum(x^2c + 2xyb + y^2d))(\sum[(m_{x_L} - m_{x_R})b + (m_{y_L} - m_{y_R})d])}{2(\sum(xb+yd))^2 - 2(\sum(x^2c + 2xyb + y^2d))(\sum d)} \quad (26)$$

If one is interested in drawing influence lines and loads only the left half of the structure $m_{x_R} = m_{y_R} = 0$ and equations (24), (25), and (26) may be written

$$M_c = -\frac{\sum m_{x_L}c + \sum m_{y_L}b}{2\sum c} \quad (27)$$

$$V_c = \frac{-(\sum(xb+yd))(\sum(m_{x_L}b + m_{y_L}d)) + (\sum d)(\sum[m_{x_L}(xc+yb) + m_{y_L}(xb+yd)])}{2(\sum(xb+yd))^2 - 2(\sum(x^2c + 2xyb + y^2d))(\sum d)} \quad (28)$$

$$T_c = \frac{-(\sum(xb+yd))(\sum[m_{x_L}(xc+yb) + m_{y_L}(xb+yd)]) + (\sum(x^2c + 2xyb + y^2d))(\sum(m_{x_L}b + m_{y_L}d))}{2(\sum(xb+yd))^2 - 2(\sum(x^2c + 2xyb + y^2d))(\sum d)} \quad (29)$$

To further simplify equations (28) and (29) the following substitutions may be made:

$$\text{let} \quad (xc + yb) = D$$

$$\text{and} \quad (xb + yd) = B$$

Then

$$M_c = - \frac{\sum m_{x_L} c + \sum m_{y_L} b}{2 \sum c} \quad (30)$$

$$V_c = \frac{-(\sum B)(\sum(m_{x_L} b + m_{y_L} d)) + (\sum d)(\sum(m_{x_L} D + m_{y_L} B))}{2(\sum B)^2 - 2(\sum(xD + yB))(\sum d)} \quad (31)$$

$$T_c = \frac{-(\sum B)(\sum(m_{x_L} D + m_{y_L} B)) + (\sum(xD + yB))(\sum(m_{x_L} b + m_{y_L} d))}{2(\sum B)^2 - 2(\sum(xD + yB))(\sum d)} \quad (32)$$

In order to facilitate the computations in the solutions of an actual case the expressions for b, c and d may be rewritten as follows:

$$\begin{aligned} b &= \sin \theta \cos \theta \left(\frac{ds}{EI} - \frac{ds}{GK} \right) = \frac{\sin 2\theta}{2} \left(\frac{1}{EI} - \frac{1}{GK} \right) ds \\ &= \frac{\sin 2\theta}{2 EI} (1-n) ds \end{aligned} \quad (33)$$

$$\text{where } n = \frac{EI}{GK}$$

$$\begin{aligned}c &= \sin^2 \theta \frac{ds}{EI} + \cos^2 \theta \frac{ds}{GK} = (1 - \cos 2 \theta) \frac{ds}{2EI} \\ &+ (1 + \cos 2 \theta) \frac{ds}{2GK} \\ &= \left(\frac{1}{EI} + \frac{1}{GK}\right) \frac{ds}{2} - \cos 2 \theta \left(\frac{1}{EI} - \frac{1}{GK}\right) \frac{ds}{2} \\ &= (1 + n) \frac{ds}{2EI} - (1 - n) \frac{\cos 2 \theta ds}{2 EI}\end{aligned}\tag{34}$$

and

$$\begin{aligned}d &= \frac{\cos^2 \theta ds}{EI} + \frac{\sin^2 \theta ds}{GK} = (1 + \cos 2 \theta) \frac{ds}{2EI} \\ &- (1 - \cos 2 \theta) \frac{ds}{2GK} \\ &= (1 + n) \frac{ds}{2EI} + (1 - n) \frac{\cos 2 \theta ds}{2 EI}\end{aligned}\tag{35}$$

In the case of a load at the center of the beam, with the section C taken at the center, V_c and T_c are equal to zero and the expression for M_c may be simplified to

$$M_c = - \frac{\sum m_{x_L} c + \sum m_{y_L} b}{2 \sum c}$$

In the case of a unit load at C

$$2 m_{x_L} = -x$$

and

$$2 m_{y_L} = -y$$

and since

$xc + yb = D$ we then have

$$M_c = \frac{\sum D}{2 \sum c} \quad (36)$$

For the case of an unsymmetrical beam, take the section C at the right support. Then M_c , T_c and V_c are the bending moment, twisting moment and shear, respectively, at the right support. Expressions for M_c , T_c and V_c then may be written

$$M_c = \frac{R}{N}$$

$$T_c = \frac{S}{N}$$

and

$$V_c = \frac{Q}{N}$$

where

$$N = (\sum c) (\sum B)^2 + (\sum d) (\sum D)^2 + (\sum b)^2 (\sum (xD + yb)) \\ - (\sum c) (\sum d) (\sum (xD + yB)) - 2(\sum D) (\sum b) (\sum B)$$

$$R = F(\sum B)^2 + H(\sum (xD + yB)) (\sum b) + J(\sum d)(\sum D) \\ - F(\sum (xD + yB))(\sum d) - H(\sum D)(\sum B) - J(\sum b)(\sum B)$$

$$S = F(\sum (xD + yB))(\sum b) + H(\sum D)^2 + J(\sum c)(\sum B) \\ - F(\sum B)(\sum D) - H(\sum (xD + yB))(\sum c) - J(\sum b)(\sum D)$$

$$Q = F(\sum d)(\sum D) + H(\sum B)(\sum c) + J(\sum b)^2 - F(\sum b)(\sum B) \\ - H(\sum b)(\sum D) - J(\sum d)(\sum c)$$

$$F = - \sum m_x c - \sum m_y b$$

$$H = - \sum m_x b - \sum m_y d$$

$$J = - \sum m_x D - \sum m_y B$$

The other symbols are as previously defined.

In order to determine the bending moment and twisting moment at any section the above values of M_c , T_c and V_c should be substituted in equations (1) and (2).

IV. EXPERIMENTS ON A CURVED ROD OF CIRCULAR-ARC PLAN.

A. Tests

An application of the theory presented in Chapter III is demonstrated by the analysis and testing of a $3/4$ inch round rod of medium open hearth steel. The rod was bent into a semi-circle with a center line radius of $14\frac{1}{2}$ inches and with 5 inches of each end left straight and then threaded. Each end of the rod had two square head nuts for anchorage purposes. Each nut at the beginning of the arc had a hole drilled through it and through the rod, then a pin was driven into the hole so as to lock the nut on the rod and thus prevent turning.

The bent rod was fastened to a 15 inch channel (a part of the steel framework in the laboratory) by means of two $3/8$ inch plates and eight $3/4$ inch bolts. As described above, the nuts on the test specimen were fixed in such a way as to simulate a fixed end condition when the rod was clamped in place. Loads were then applied at right angles to the plane of the axis of the rod.

Two Huggenberger tensometers were used for measuring strains due to bending moment, and a troptometer on a 1 inch gage length for measuring angles of twist due to torque. (Fig. 4). The troptometer arm made contact with the plunger of a $\frac{1}{10,000}$ inch dial about $1\frac{3}{4}$ inches from the axis of the rod.

A modulus of elasticity in tension of 30,000,000 p.s.i. was obtained from tests of the coupon cut from the same piece as the rod. Using a 10 inch gage length the modulus of elasticity in shear was found to be 10,100,000 p.s.i.

At different times the gages were attached at the quarter-point and at the center. The load, the maximum of which was slightly over 83 lbs., was placed at various points along the length of the rod and observations made. The results of these tests are shown in Figs. 5, 6, 8 and 9. The gages were also placed as near the support as possible and the results of the observations are shown in Fig. 15 (a) and (b).

The rod was later cut to form a subtended arc of 144° and then tested. The results of the tests are shown in Figs. 10, 11, 13 and 14.

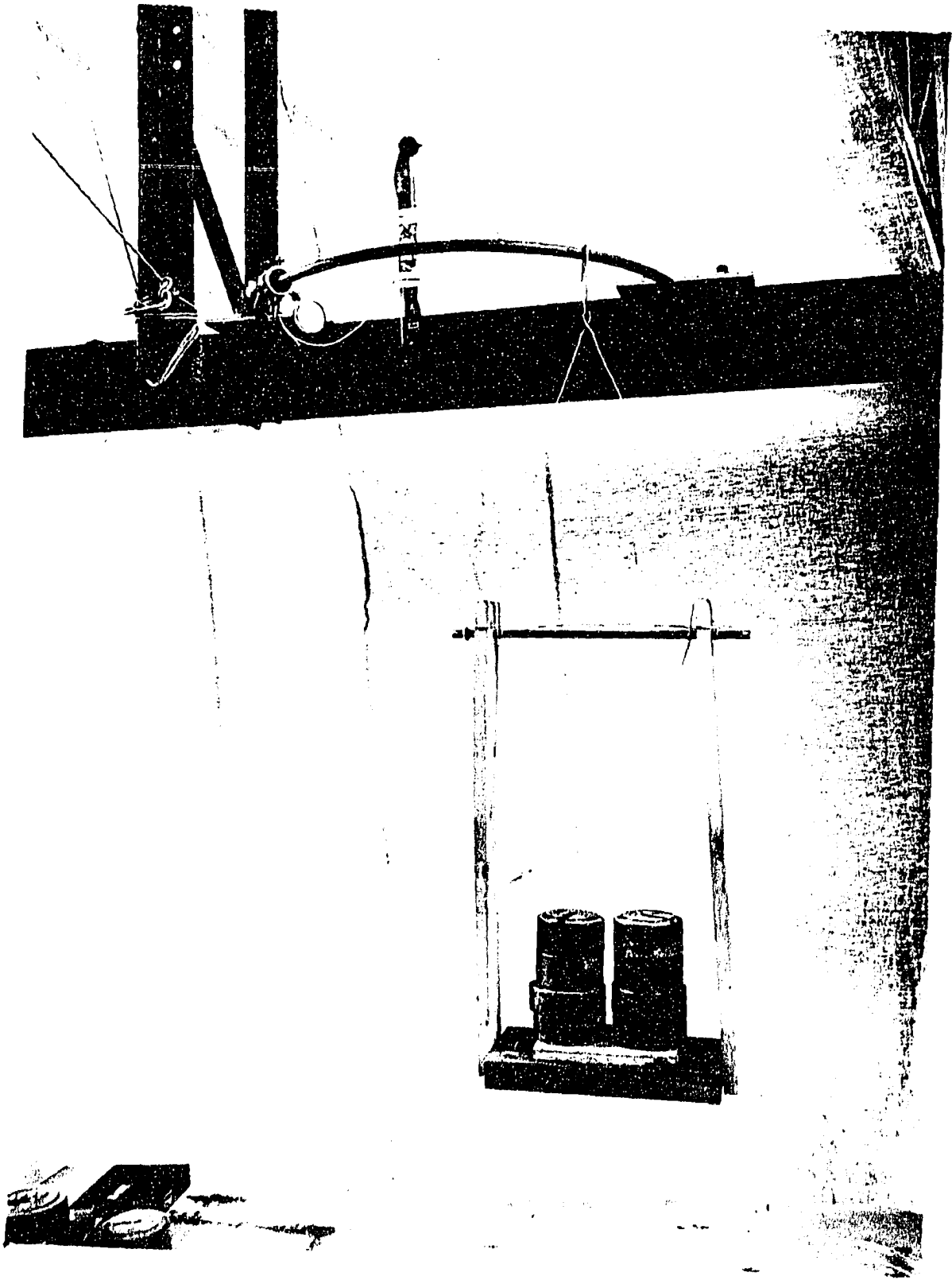


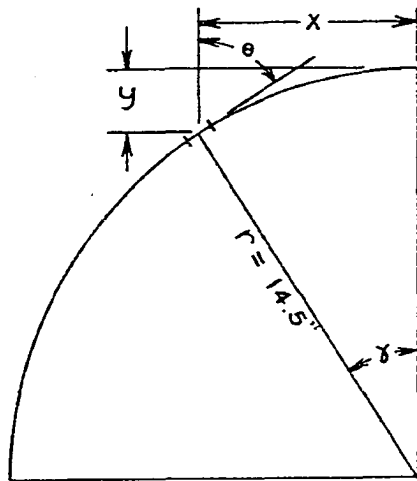
Fig. 4 Curved Rod in Place.

B. Analytical

Tables I, II, III and IV indicate the procedure followed in obtaining information for drawing influence lines for bending moment, twisting moment and shear for the curved rod. This information is given in detail so that the form might be followed in the case where the rod or beam has a non-circular plan. Each half of the rod was divided into 15 equal sections. The distances used in the computations were measured to the center of the sections. The values of M_c , T_c and V_c recorded in Tables III and IV were obtained by substituting the proper quantities in equations (30), (31) and (32).

Figures 5, 6, 7, 8 and 9 show influence lines drawn for bending moment, twisting moment and shear for an arc of 180° . Figures 10, 11, 12, 13 and 14 show the influence lines for an arc of 144° . The results of the tests are plotted in these figures for comparison with the theoretical values.

TABLE I. COMPUTATIONS OF X AND y DISTANCES.



δ	SIN δ	COS δ	1-COS δ	X r SIN δ	Y $r(1-\text{COS } \delta)$
3°	0.05234	0.99863	0.00137	0.75893	0.01987
9°	0.15643	0.98769	0.01231	2.26824	0.17850
15°	0.25882	0.96593	0.03407	3.75289	0.49402
21°	0.35837	0.93358	0.06642	5.19637	0.96309
27°	0.45399	0.89101	0.10899	6.58286	1.58036
33°	0.54464	0.83867	0.16133	7.89728	2.33929
39°	0.62932	0.77715	0.22285	9.12514	3.23133
45°	0.70711	0.70711	0.29289	10.25310	4.24691
51°	0.77715	0.62932	0.37068	11.26868	5.37486
57°	0.83867	0.54464	0.45536	12.16072	6.60272
63°	0.89101	0.45399	0.54601	12.91965	7.91715
69°	0.93358	0.35837	0.64163	13.53691	9.30364
75°	0.96593	0.25882	0.74118	14.00599	10.74711
81°	0.98769	0.15643	0.84357	14.32151	12.23177
87°	0.99863	0.05234	0.94766	14.48014	13.74107
90°	1.00000	0.00000	1.00000	14.50000	14.50000

TABLE II.

COMPUTATIONS OF VALUES
BENDING MOMENT, TWISTI

$$\begin{aligned} \text{RADIUS} &= 14.5'' & \frac{1-n}{2} &= -0.2425 & c &= \frac{1+n}{2} \\ n &= \frac{EI}{GK} = 1.485 & \frac{1+n}{2} &= +1.2425 & d &= \frac{1+n}{2} \end{aligned}$$

SEC.	SIN 2θ	COS 2θ	x	y	$\frac{1-n}{2} \sin 2\theta$	$\frac{1-n}{2} \cos 2\theta$	c	d
1	0.10453	-0.99452	0.75893	0.01987	-0.02535	0.24117	1.00133	1.4836
2	0.30902	-0.95106	2.26824	0.17850	-0.07494	0.23063	1.01187	1.4731
3	0.50000	-0.86603	3.75289	0.49402	-0.12125	0.21001	1.03249	1.4521
4	0.66913	-0.74314	5.19637	0.96309	-0.16226	0.18021	1.06229	1.4227
5	0.80902	-0.58779	6.58286	1.58036	-0.19619	0.14254	1.09996	1.3850
6	0.91355	-0.40674	7.89728	2.33929	-0.22154	0.09863	1.14387	1.3411
7	0.97815	-0.20791	9.12514	3.23133	-0.23720	0.05042	1.19208	1.2921
8	1.00000	-0.0000	10.25310	4.24691	-0.24250	0.00000	1.24250	1.2421
9	0.97815	+0.20791	11.26868	5.37486	-0.23720	-0.05042	1.29292	1.1921
10	0.91355	+0.40674	12.16072	6.60272	-0.22154	-0.09863	1.34113	1.1438
11	0.80902	+0.58779	12.91965	7.91715	-0.19619	-0.14254	1.38504	1.0999
12	0.66913	+0.74314	13.53691	9.30364	-0.16226	-0.18021	1.42271	1.0621
Σ							14.22819	15.5911
13	0.50000	+0.86603	14.00599	10.74711	-0.12125	-0.21001	1.45251	1.0321
14	0.30902	+0.95106	14.32151	12.23177	-0.07494	-0.23063	1.47313	1.0118
15	0.10453	+0.99452	14.48014	13.74107	-0.02535	-0.24117	1.48367	1.0013
Σ							18.63750	18.6371

VALUES OF VALUES FOR INFLUENCE LINES, —
 MOMENT, TWISTING MOMENT, AND SHEAR.

1.2425 $c = \frac{1+n}{2} - \frac{1-n}{2} \cos 2\theta$ $B = xb + yd$

1.2425 $d = \frac{1+n}{2} + \frac{1-n}{2} \cos 2\theta$ $D = xc + yb$

2θ	c	d	xb	yd	B	D	yB	xD
117	1.00133	1.48367	-0.01924	0.02948	0.01024	0.75944	0.00020	0.57636
063	1.01187	1.47313	-0.16998	0.26295	0.09297	2.28179	0.01660	5.17565
001	1.03249	1.45251	-0.45504	0.71757	0.26253	3.81492	0.12970	14.31698
021	1.06229	1.42271	-0.84316	1.37020	0.52704	5.36378	0.50759	27.87219
254	1.09996	1.38504	-1.29149	2.18886	0.89737	6.93083	1.41817	45.62468
863	1.14387	1.34113	-1.74956	3.13729	1.38773	8.51522	3.24630	67.24708
042	1.19208	1.29292	-2.16448	4.17785	2.01337	10.11143	6.50586	92.26621
000	1.24250	1.24250	-2.48638	5.27679	2.79041	11.70960	11.85062	120.05970
042	1.29292	1.19208	-2.67293	6.40726	3.73433	13.29458	20.07150	149.81237
863	1.34113	1.14387	-2.69409	7.55265	4.85856	14.84634	32.07971	180.54218
254	1.38504	1.09996	-2.53471	8.70855	6.17384	16.34097	48.87922	211.11961
021	1.42271	1.06229	-2.19650	9.88316	7.68666	17.74949	71.51392	240.27325
	14.22819	15.59181			30.43505	111.71839	196.21939	1154.88826
001	1.45251	1.03249	-1.69823	11.09628	9.39805	19.04075	101.00188	266.68455
3063	1.47313	1.01187	-1.07325	12.37696	11.30371	20.18080	138.26438	289.01953
117	1.48367	1.00133	-0.36707	13.75935	13.39228	21.13541	184.02426	306.04370
	18.63750	18.63750			64.52909	172.07535	619.50991	2016.63604

TABLE II (CONTINUED).

LOAD AT I

SEC.	m_{x_L}	m_{y_L}	$m_{x_L}b$	$m_{x_L}c$	$m_{x_L}D$	$m_{y_L}b$	$m_{y_L}d$	$m_{y_L}B$
1	0.	0.						
2	-1.50931	-0.15863	0.11311	-1.52723	-3.44393	0.01189	-0.23368	-0.01475
3	-2.99396	-0.47415	0.36302	-3.09123	-11.42172	0.05749	-0.68871	-0.12448
4	-4.43744	-0.94322	0.72002	-4.71385	-23.80145	0.15305	-1.34193	-0.49711
5	-5.82393	-1.56049	1.14260	-6.40609	-40.36467	0.30615	-2.16134	-1.40034
6	-7.13835	-2.31942	1.58143	-8.16534	-60.78462	0.51384	-3.11064	-3.21873
7	-8.36621	-3.21146	1.98447	-9.97319	-84.59435	0.76176	-4.15216	-6.46586
8	-9.49417	-4.22704	2.30234	-11.79651	-111.17293	1.02506	-5.25210	-11.79517
9	-10.50975	-5.35499	2.49291	-13.58827	-139.72271	1.27020	-6.38358	-19.99730
10	-11.40179	-6.58285	2.52595	-15.29128	-169.27485	1.45836	-7.52992	-31.98317
11	-12.16072	-7.89728	2.38581	-16.84308	-198.71796	1.54937	-8.68669	-48.75654
12	-12.77798	-9.28377	2.07336	-18.17936	-226.80263	1.50638	-9.86206	-71.36118
Σ			17.68502	-109.57543	-1070.10182	8.61355	-49.40281	-195.61463
13	-13.24706	-10.72724	1.60621	-19.24149	-252.23396	1.30068	-11.07577	-100.81514
14	-13.56258	-12.21190	1.01638	-19.97944	-273.70371	0.91516	-12.35686	-138.03978
15	-13.72121	-13.72120	0.34783	-20.35775	-290.00340	0.34783	-13.73945	-183.75815
Σ			20.65544	-169.15411	-1886.04289	11.17722	-86.57489	-618.22770

TABLE II (CONTINUED).

LOAD AT 2

SEC.	m_{x_L}	m_{y_L}	$m_{x_L}b$	$m_{x_L}c$	$m_{x_L}D$	$m_{y_L}b$	$m_{y_L}d$	$m_{y_L}B$
1	0.	0						
2	0.	0.						
3	-1.48465	-0.31552	0.18001	-1.53289	-5.66382	0.03826	-0.45830	-0.08283
4	-2.92813	-0.78459	0.47512	-3.11052	-15.70585	0.12731	-1.11624	-0.41351
5	-4.31462	-1.40186	0.84649	-4.74591	-29.90390	0.27503	-1.94163	-1.25799
6	-5.62904	-2.16079	1.24706	-6.43889	-47.93251	0.47870	-2.89790	-2.99859
7	-6.85690	-3.05283	1.62646	-8.17397	-69.33306	0.72413	-3.94706	-6.14648
8	-7.98486	-4.06841	1.93633	-9.92119	-93.49952	0.98659	-5.05500	-11.35253
9	-9.00044	-5.19636	2.13490	-11.63685	-119.65707	1.23258	-6.19448	-19.40492
10	-9.89248	-6.42422	2.19158	-13.26710	-146.86712	1.42322	-7.34847	-31.21246
11	-10.65141	-7.73865	2.08970	-14.75263	-174.05437	1.51825	-8.51221	-47.77719
12	-11.26867	-9.12514	1.82845	-16.03205	-200.01315	1.48065	-9.69354	-70.14185
Σ			14.55610	-89.61200	-902.63037	8.28472	-47.16483	-190.78835
13	-11.73775	-10.56861	1.42320	-17.04920	-223.49556	1.28144	-10.91198	-99.32433
14	-12.05327	-12.05327	0.90327	-17.75603	-243.24463	0.90327	-12.19634	-136.24667
15	-12.21190	-13.56257	0.30957	-18.11843	-258.10351	0.34381	-13.58061	-181.63373
Σ			17.19214	-142.53566	-1627.47407	10.81324	-83.85376	-607.99308

TABLE II (CONTINUED).

LOAD AT 3

SEC.	m_{x_L}	m_{y_L}	$m_{x_L}b$	$m_{x_L}c$	$m_{x_L}D$	$m_{y_L}b$	$m_{y_L}d$	$m_{y_L}B$
1	0.	0.						
2	0.	0.						
3	0.	0.						
4	-1.44348	-0.46907	0.23422	-1.53339	-7.74251	0.07611	-0.66735	-0.24722
5	-2.82997	-1.08634	0.55521	-3.11285	-19.61404	0.21313	-1.50462	-0.97485
6	-4.14439	-1.84527	0.91815	-4.74064	-35.29039	0.40880	-2.47475	-2.56074
7	-5.37225	-2.73731	1.27430	-6.40415	-54.32113	0.64929	-3.53912	-5.51122
8	-6.50021	-3.75289	1.57630	-8.07651	-76.11486	0.91008	-4.66297	-10.47210
9	-7.51579	-4.88084	1.78275	-9.71732	-99.91927	1.15774	-5.81835	-18.22667
10	-8.40783	-6.10870	1.86267	-11.27599	-124.82550	1.35332	-6.98756	-29.67949
11	-9.16676	-7.42313	1.79843	-12.69633	-149.79375	1.45634	-8.16515	-45.82922
12	-9.78402	-8.80962	1.58756	-13.91982	-173.66137	1.42945	-9.35837	-67.71655
Σ			11.58959	-71.47700	-741.28282	7.65426	-43.17824	-181.21806
13	-10.25310	-10.25309	1.24319	-14.89273	-195.22671	1.24319	-10.58621	-96.35905
14	-10.56862	-11.73775	0.79201	-15.56895	-213.28321	0.87963	-11.87708	-132.68012
15	-10.72725	-13.24705	0.27194	-15.91570	-226.72483	0.33581	-13.26467	-177.40820
Σ			13.89673	-117.85438	-1376.51757	10.11289	-78.90620	-587.66543

TABLE II (CONTINUED).

LOAD AT 4

SEC.	m_{x_L}	m_{y_L}	$m_{x_L b}$	$m_{x_L c}$	$m_{x_L D}$	$m_{y_L b}$	$m_{y_L d}$	$m_{y_L B}$
1	0.	0.						
2	0.	0.						
3	0.	0.						
4	0.	0.						
5	-1.38649	-0.61727	0.27202	-1.52508	-9.60953	0.12110	-0.85494	-0.55392
6	-2.70091	-1.37620	0.59836	-3.08949	-22.99884	0.30488	-1.84566	-1.90979
7	-3.92877	-2.26824	0.93190	-4.68341	-39.72548	0.53803	-2.93265	-4.56681
8	-5.05673	-3.28382	1.22626	-6.28299	-59.21229	0.79633	-4.08015	-9.16320
9	-6.07231	-4.41177	1.44035	-7.85101	-80.72881	1.04647	-5.25918	-16.47501
10	-6.96435	-5.63963	1.54288	-9.34010	-103.39511	1.24940	-6.45100	-27.40048
11	-7.72328	-6.95406	1.51523	-10.69705	-126.20589	1.36432	-7.64919	-42.93325
12	-8.34054	-8.34055	1.35334	-11.86617	-148.04033	1.35334	-8.86008	-64.11097
Σ			8.86034	-55.33530	-589.91628	6.77387	-37.93285	-167.11343
13	-8.80962	-9.78402	1.06817	-12.79606	-167.74177	1.18631	-10.10190	-91.95071
14	-9.12514	-11.26868	0.68384	-13.44252	-184.15263	0.84447	-11.40244	-127.37789
15	-9.28377	-12.77798	0.23534	-13.77405	-196.21629	0.32392	-12.79497	-171.12629
Σ			10.86769	-95.34793	-1138.02697	9.12857	-72.23216	-557.56832

TABLE II (CONTINUED).

LOAD AT 6

SEC.	m_{x_L}	m_{y_L}	$m_{x_L}b$	$m_{x_L}c$	$m_{x_L}D$	$m_{y_L}b$	$m_{y_L}d$	$m_{y_L}B$
1	0.	0.						
2	0.	0.						
3	0.	0.						
4	0.	0.						
5	0.	0.						
6	0.	0.						
7	-1.22786	-0.89204	0.29125	-1.46371	-12.41542	0.21159	-1.15334	-1.79601
8	-2.35582	-1.90762	0.57129	-2.92711	-27.58571	0.46260	-2.37022	-5.32304
9	-3.37140	-3.03557	0.79970	-4.35895	-44.82135	0.72004	-3.61864	-11.33582
10	-4.26344	-4.26343	0.94452	-5.71783	-63.29648	0.94452	-4.87681	-20.71413
11	-5.02237	-5.57786	0.98534	-6.95618	-82.07040	1.09432	-6.13542	-34.43682
12	-5.63963	-6.96435	0.91509	-8.02356	-100.10056	1.13004	-7.39816	-53.53259
Σ			4.50719	-29.44734	-330.26992	4.56311	-25.55259	-127.13841
13	-6.10871	-8.40782	0.74068	-8.87296	-116.31442	1.01945	-8.68099	-79.01711
14	-6.42423	-9.89248	0.48143	-9.46373	-129.64610	0.74134	-10.00990	-111.82173
15	-6.58286	-11.40178	0.16688	-9.76679	-139.13145	0.28904	-11.41694	-152.69583
Σ			5.89618	-57.55082	-715.38189	6.61294	-55.66042	-470.67308

TABLE II (CONTINUED).

LOAD AT 8

SEC.	m_{x_L}	m_{y_L}	$m_{x_L} b$	$m_{x_L} C$	$m_{x_L} D$	$m_{y_L} b$	$m_{y_L} d$	$m_{y_L} B$
8	0.	0.						
9	-1.01558	-1.12795	0.24090	-1.31306	-13.50171	0.26755	-1.34461	-4.21214
10	-1.90762	-2.35581	0.42261	-2.55837	-28.32118	0.52191	-2.69474	-11.44584
11	-2.66655	-3.67024	0.52315	-3.69328	-43.57401	0.72006	-4.03712	-22.65947
12	-3.28381	-5.05673	0.53283	-4.67191	-58.28595	0.82051	-5.37171	-38.86936
Σ			1.71949	-12.23662	-143.68285	2.33003	-13.44818	-77.18681
13	-3.75289	-6.50020	0.45504	-5.45111	-71.45784	0.78815	-6.71139	-61.08920
14	-4.06841	-7.98486	0.30489	-5.99330	-82.10377	0.59839	-8.07964	-90.25854
15	-4.22704	-9.49416	0.10716	-6.27153	-89.34022	0.24068	-9.50679	-127.14845
Σ			2.58658	-29.95256	-386.58468	3.95725	-37.74600	-355.68300

LOAD AT 9

9	0.	0.						
10	-0.89204	-1.22786	0.19762	-1.19634	-13.24353	0.27202	-1.40451	-5.96563
11	-1.65097	-2.54229	0.32390	-2.28666	-26.97845	0.49877	-2.79642	-15.69569
12	-2.26823	-3.92878	0.36804	-3.22703	-40.25993	0.63748	-4.17350	-30.19920
Σ			0.88956	-6.71003	-80.48191	1.40827	-8.37443	-51.86052
13	-2.73731	-5.37225	0.33190	-3.97597	-52.12044	0.65139	-5.54679	-50.48867
14	-3.05283	-6.85691	0.22878	-4.49722	-61.60855	0.51386	-6.93830	-77.50852
15	-3.21146	-8.36621	0.08141	-4.76475	-67.87552	0.21208	-8.37734	-112.04263
Σ			1.53165	-19.94797	-262.08642	2.78560	-29.23686	-291.90034

TABLE II (CONTINUED).

LOAD AT II

SEC.	m_{x_L}	m_{y_L}	$m_{x_L} b$	$m_{x_L} c$	$m_{x_L} D$	$m_{y_L} b$	$m_{y_L} d$	$m_{y_L} B$
11	0.	0.						
12	-0.61726	-1.38649	0.10016	-0.87818	-10.95605	0.22497	-1.47285	-10.65748
Σ			0.10016	-0.87818	-10.95605	0.22497	-1.47285	-10.65748
13	-1.08634	-2.82996	0.13172	-1.57792	-20.68473	0.34313	-2.92191	-26.59611
14	-1.40186	-4.31462	0.10506	-2.06512	-28.29066	0.32334	-4.36583	-48.77121
15	-1.56049	-5.82392	0.03956	-2.31525	-32.98160	0.14764	-5.83167	-77.99557
Σ			0.37650	-6.83647	-92.91304	1.03908	-14.59226	-164.02037

LOAD AT 13

13	0.	0.						
14	-0.31552	-1.48466	0.02365	-0.46480	-6.36745	0.11126	-1.50228	-16.78217
15	-0.47415	-2.99396	0.01202	-0.70348	-10.02135	0.07590	-2.99794	-40.09595
Σ			0.03567	-1.16828	-16.38880	0.18716	-4.50022	-56.87812

TABLE III. VALUES OF INFLUENCE ORDINATE
AND TWISTING MOMENT AT $\frac{1}{4}$ POINT

$\theta = 45^\circ$ $\sin \theta = 0.70711$, $\cos \theta = 0.70711$, $x = 10.25310$
 $\frac{1}{4}$ - point $x \sin \theta = 7.25007$, $x \cos \theta = 7.25007$, $y = 10.25310$
 $x \sin \theta + y \cos \theta = 10.25310$, $x \cos \theta - y \sin \theta = 0$

	Unit Load A				
	C	1	2	3	4
M_c	+4.61637	+4.23815	+3.53381	+2.89045	+2.31300
$M_c \sin \theta$	+3.26429	+2.99684	+2.49879	+2.04387	+1.63550
$M_c \cos \theta$	+3.26429	+2.99684	+2.49879	+2.04387	+1.63550
V_c		+0.47167	+0.41597	+0.36041	+0.30700
$V_c(x \sin \theta + y \cos \theta)$		+4.83608	+4.26498	+3.69532	+3.15100
$V_c(x \cos \theta - y \sin \theta)$		+2.00314	+1.76659	+1.53063	+1.30500
T_c		+0.13538	+0.35000	+0.49622	+0.58200
$T_c \sin \theta$		+0.09573	+0.24749	+0.35088	+0.41160
$T_c \cos \theta$		+0.09573	+0.24749	+0.35088	+0.41160
M_{x_L}	-5.12655	-9.49417	-7.98486	-6.50021	-5.05600
$M_{x_L} \sin \theta$	-3.62503	-6.71342	-5.64617	-4.59636	-3.57500
$M_{x_L} \cos \theta$	-3.62503	-6.71342	-5.64617	-4.59636	-3.57500
M_{y_L}	-2.12346	-4.22704	-4.06841	-3.75289	-3.28300
$M_{y_L} \sin \theta$	-1.50152	-2.98898	-2.87681	-2.65371	-2.32200
$M_{y_L} \cos \theta$	-1.50152	-2.98898	-2.87681	-2.65371	-2.32200
$M_{\frac{1}{4}} \text{ Left}$	-1.86226	-1.77375	-1.51172	-1.16000	-0.69900
$T_{\frac{1}{4}} \text{ Left}$	-1.14078	-1.17981	-1.24853	-1.28097	-1.27500
$M_{\frac{1}{4}} \text{ Right}$	-1.86226	-1.93497	-2.01368	-2.00233	-1.92740
$T_{\frac{1}{4}} \text{ Right}$	-1.14078	-1.08943	-0.97969	-0.86412	-0.74100

FLUENCE ORDINATES FOR BENDING MOMENT
 AT $\frac{1}{4}$ POINT \sim ARC 180° .

$0.70711, x = 10.25310, y = 4.24691$

$5\theta = 725007, y \sin \theta = 3.00303, y \cos \theta = 3.00303$

$310, x \cos \theta - y \sin \theta = 4.24691$

Unit Load At						
3	4	6	8	9	11	13
2.89045	+2.31306	+1.36654	+0.69739	+0.46043	+0.15553	+0.02632
2.04387	+1.63559	+0.96629	+0.49313	+0.32557	+0.10998	+0.01861
2.04387	+1.63599	+0.96629	+0.49313	+0.32557	+0.10998	+0.01861
0.36041	+0.30736	+0.21009	+0.12860	+0.09493	+0.04305	+0.01198
3.69532	+3.15139	+2.15407	+1.31855	+0.97333	+0.44140	+0.12283
1.53063	+1.30533	+0.89223	+0.54615	+0.40316	+0.18283	+0.05088
0.49622	+0.58210	+0.60767	+0.49800	+0.41460	+0.23234	+0.07118
0.35088	+0.41161	+0.42969	+0.35214	+0.29317	+0.16429	+0.05033
0.35088	+0.41161	+0.42969	+0.35214	+0.29317	+0.16429	+0.05033
6.50021	-5.05673	-2.35582				
4.59636	-3.57566	-1.66582				
4.59636	-3.57566	-1.66582				
3.75289	-3.28382	-1.90762				
2.65371	-2.32202	-1.34890				
2.65371	-2.32202	-0.63077				
-1.16000	-0.69909	+0.53533	+2.16382	+1.59207	+0.71567	+0.19177
-1.28097	-1.27567	-1.11191	-0.68714	-0.43556	-0.12852	-0.01916
-2.00233	-1.92741	-1.61747	-1.17756	-0.94093	-0.49571	-0.15455
-0.86412	-0.74187	-0.50375	-0.29908	-0.21558	-0.09144	-0.01806

TABLE IV. VALUES OF INFLUENCE ORDINATES
AND TWISTING MOMENT AT $\frac{1}{4}$ POINT

$\theta = 54^\circ$ $\sin \theta = 0.80902$, $\cos \theta = 0.58779$, $x = 8.52296$,
 $\frac{1}{4}$ - point $x \sin \theta = 6.89525$, $x \cos \theta = 5.00971$, $y \sin \theta$
 $x \sin \theta + y \cos \theta = 8.52296$, $x \cos \theta - y \sin \theta$

	Unit Load at				
	C	1	2	3	4
M_c	+3.92595	+3.54795	+2.85796	+2.24283	+1.70652
$M_c \sin \theta$	3.17617	2.87036	2.31215	1.81449	1.38061
$M_c \cos \theta$	2.30763	2.08545	1.67988	1.31831	1.00300
V_c		0.46598	0.39861	0.33322	0.27108
$V_c(x \sin \theta + y \cos \theta)$		3.97153	3.39734	2.84002	2.31041
$V_c(x \cos \theta - y \sin \theta)$		1.29040	1.10383	0.92276	0.75066
T_c		0.10755	0.26762	0.36255	0.40255
$T_c \sin \theta$		0.08701	0.21651	0.29331	0.32566
$T_c \cos \theta$		0.06322	0.15730	0.21310	0.23655
M_{xL}	-4.26148	-7.76403	-6.25472	-4.77007	-3.32655
$M_{xL} \sin \theta$	-3.44762	-6.28126	-5.06019	-3.85908	-2.69120
$M_{xL} \cos \theta$	-2.50486	-4.56362	-3.67646	-2.80380	-1.95530
M_{yL}	-1.38461	-2.74934	-2.59071	-2.27519	-1.80610
$M_{yL} \sin \theta$	-1.12018	-2.22427	-2.09594	-1.84067	-1.46115
$M_{yL} \cos \theta$	-0.81386	-1.61603	-1.52279	-1.33733	-1.06160
$M_{\frac{1}{4}} \text{ Left}$	-1.08531	-0.99218	-0.71619	-0.32880	+0.17470
$T_{\frac{1}{4}} \text{ Left}$	-0.92295	-0.94949	-0.98668	-0.98463	-0.93350
$M_{\frac{1}{4}} \text{ Right}$	-1.08531	-1.16439	-1.24249	-1.23863	-1.16630
$T_{\frac{1}{4}} \text{ Right}$	-0.92295	-0.88206	-0.79256	-0.68886	-0.57800

* For circular arcs $x \sin \theta + y \cos \theta = x$ and $x \cos \theta - y \sin \theta = y$. Corr

INFLUENCE ORDINATES FOR BENDING MOMENT
 MOMENT AT $\frac{1}{4}$ POINT \sim ARC 144°

$\sin \theta = 0.58779$, $x = 8.52296$, $y = 2.76921$

$x \cos \theta = 5.00971$, $y \sin \theta = 2.24035$, $y \cos \theta = 1.62771$

3.52296 , $x \cos \theta - y \sin \theta = 2.76921$ *

Unit Load at						
2	3	4	6	8	9	11
2.85796	+2.24283	+1.70652	+0.87447	+0.34813	+0.18631	+0.02295
2.31215	1.81449	1.38061	0.70746	0.28164	0.15073	0.01857
1.67988	1.31831	1.00308	0.51400	0.20463	0.10951	0.01349
0.39861	0.33322	0.27108	0.16116	0.07663	0.04557	0.00733
3.39734	2.84002	2.31040	1.37356	0.65311	0.38839	0.06247
1.10383	0.92276	0.75068	0.44629	0.21220	0.12619	0.02030
0.26762	0.36255	0.40250	0.36030	0.22653	0.15107	0.02971
0.21651	0.29331	0.32563	0.29149	0.18327	0.12222	0.02404
0.15730	0.21310	0.23659	0.21178	0.13315	0.08880	0.01746
6.25472	-4.77007	-3.32659	-0.62568			
5.06019	-3.85908	-2.69128	-0.50619			
3.67646	-2.80380	-1.95534	-0.36777			
2.59071	-2.27519	-1.80612	-0.42992			
2.09594	-1.84067	-1.46119	-0.34781			
-1.52279	-1.33733	-1.06162	-0.25270			
-0.71619	-0.32880	+0.17470	+1.53391	+1.06790	+0.62792	+0.09850
-0.98668	-0.98463	-0.93398	-0.64884	-0.23356	-0.11348	-0.00975
-1.24249	-1.23863	-1.16638	-0.87788	-0.50462	-0.32646	-0.06136
-0.79256	-0.68886	-0.57803	-0.35920	-0.17570	-0.10554	-0.01723

$x \cos \theta - y \sin \theta = y$. Correct only to five significant figures.

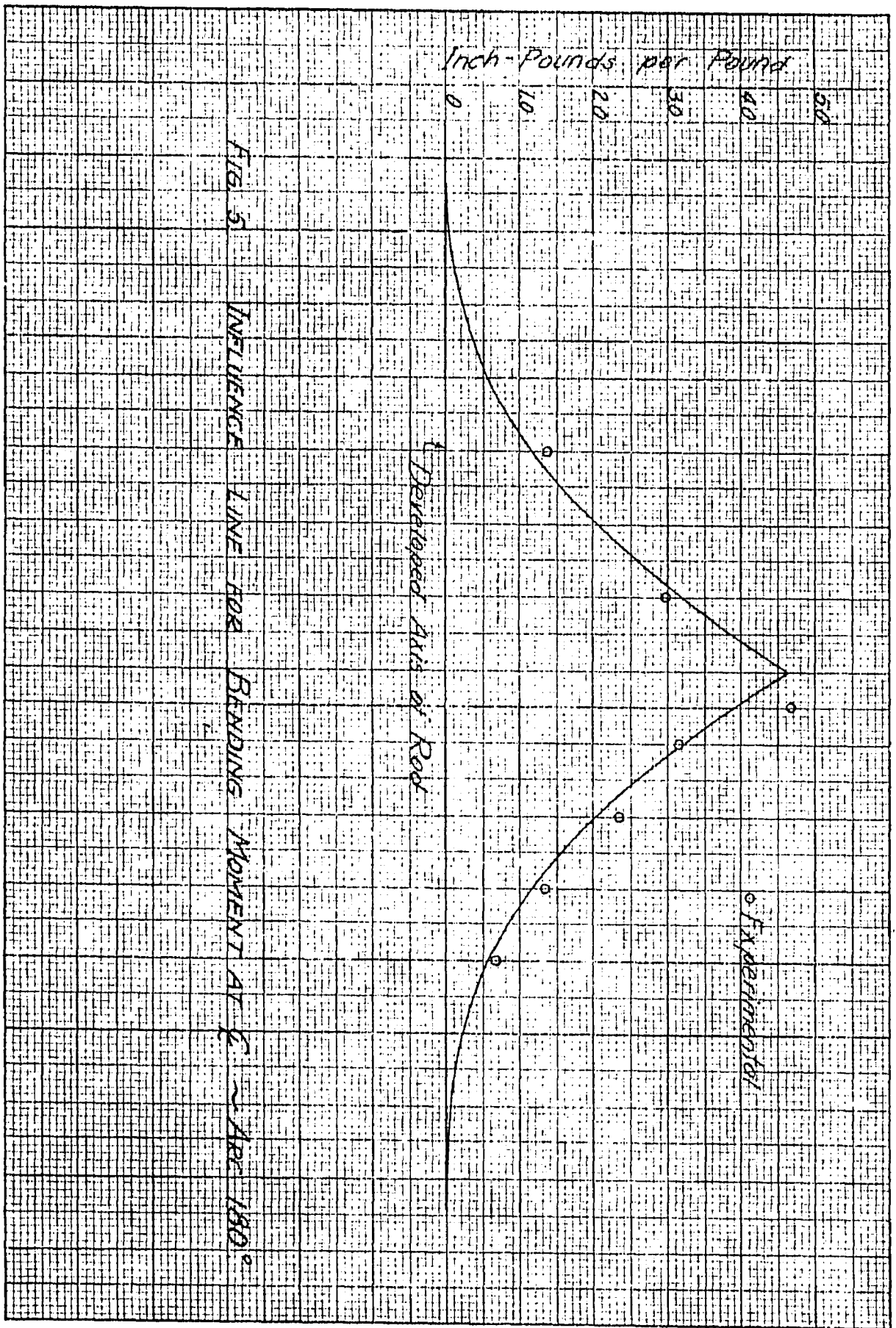


FIG. 5

INFLUENCE LINE FOR BENDING MOMENT AT C - APR 1900

Developed Axis of Rod

EXPERIMENTAL

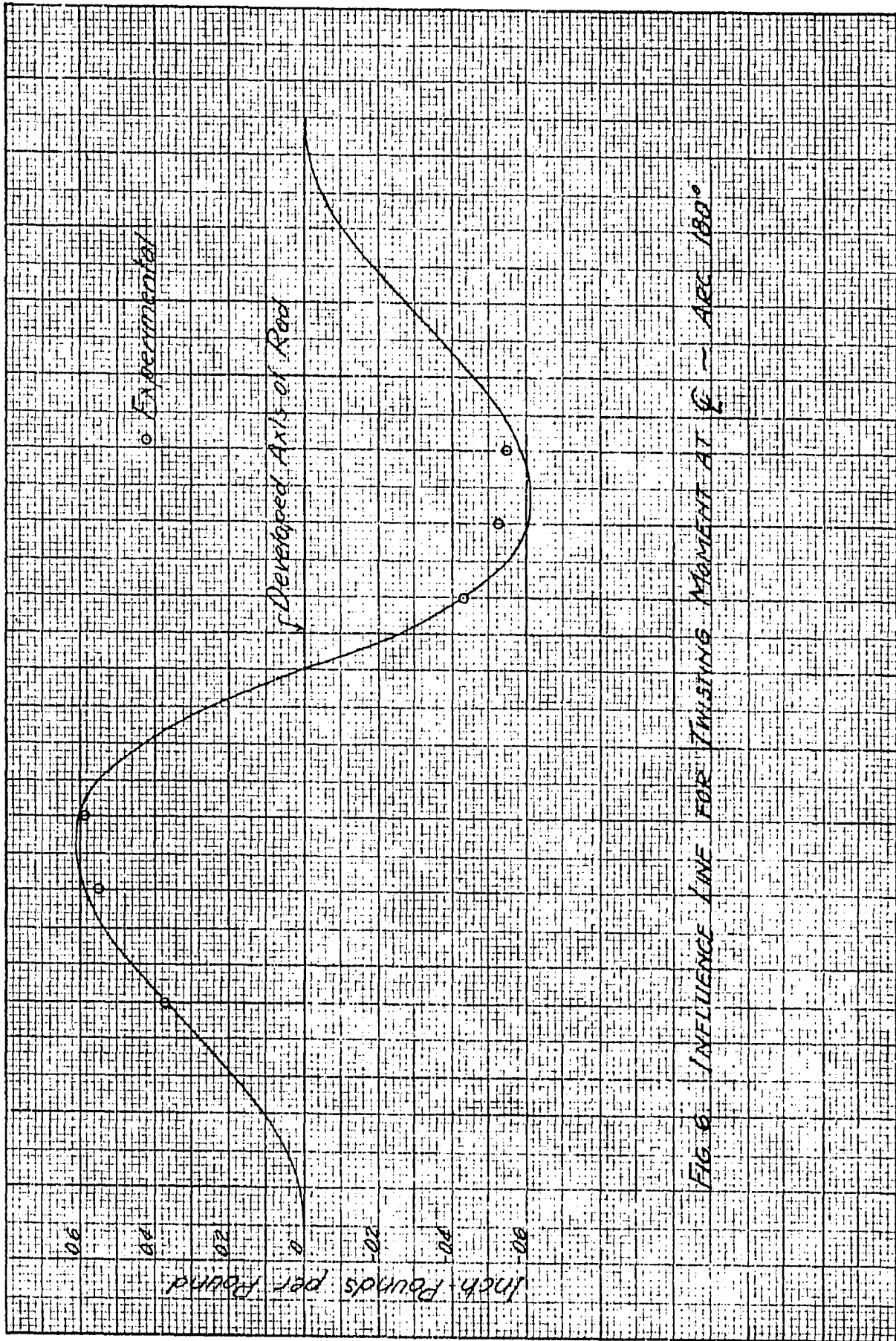


FIG. 6 INFLUENCE LINE FOR TWISTING MOMENT AT $\phi = 180^\circ$

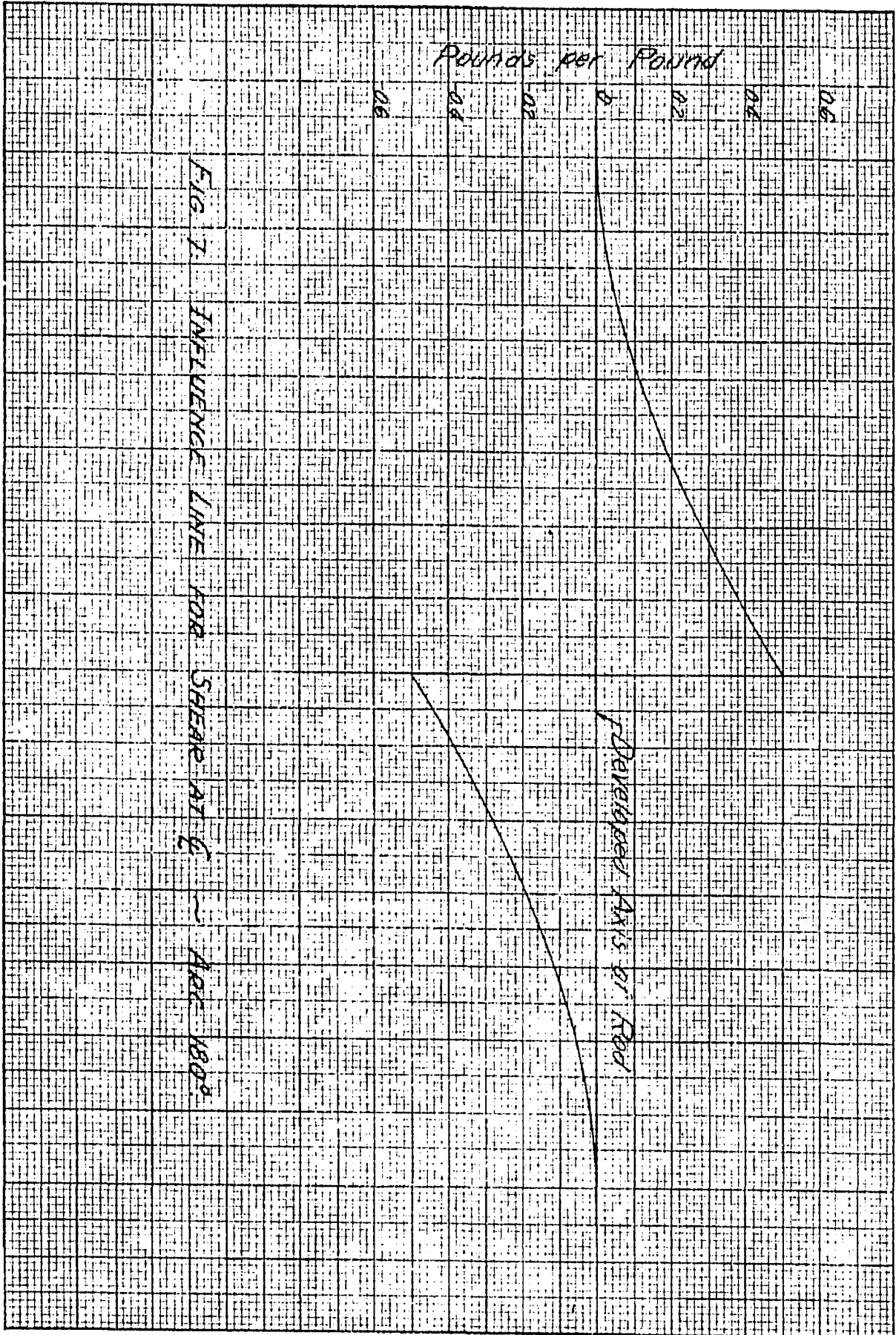


FIG. 1. INFLUENCE LINE FOR SHEAR AT C
 APC 180°

Pounds per Pound

0.8
 0.6
 0.4
 0.2
 0

Developed Axis of Rod

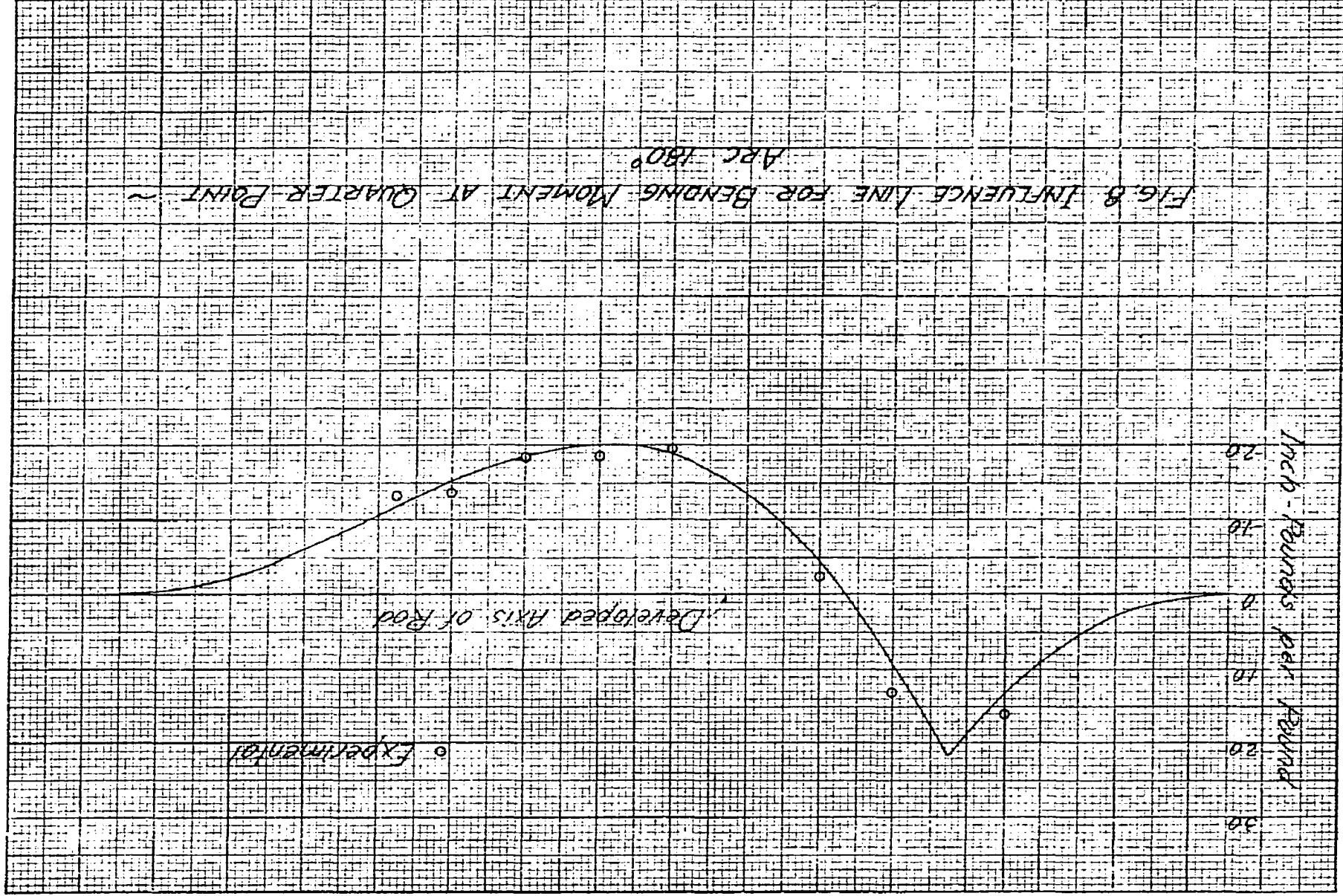


FIG. 8. INFLUENCE LINE FOR BENDING MOMENT AT QUARTER POINT ~
ARC 180°

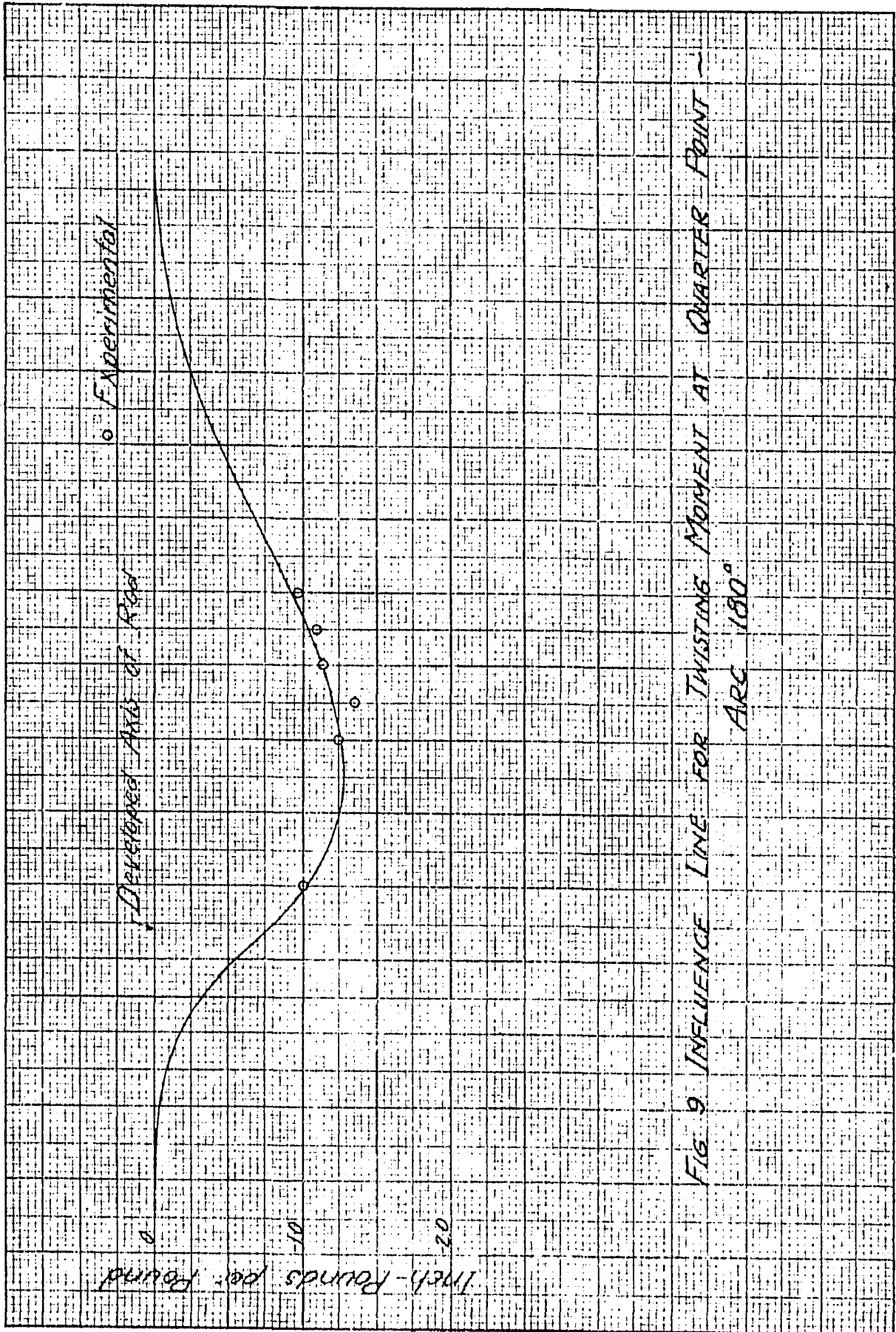
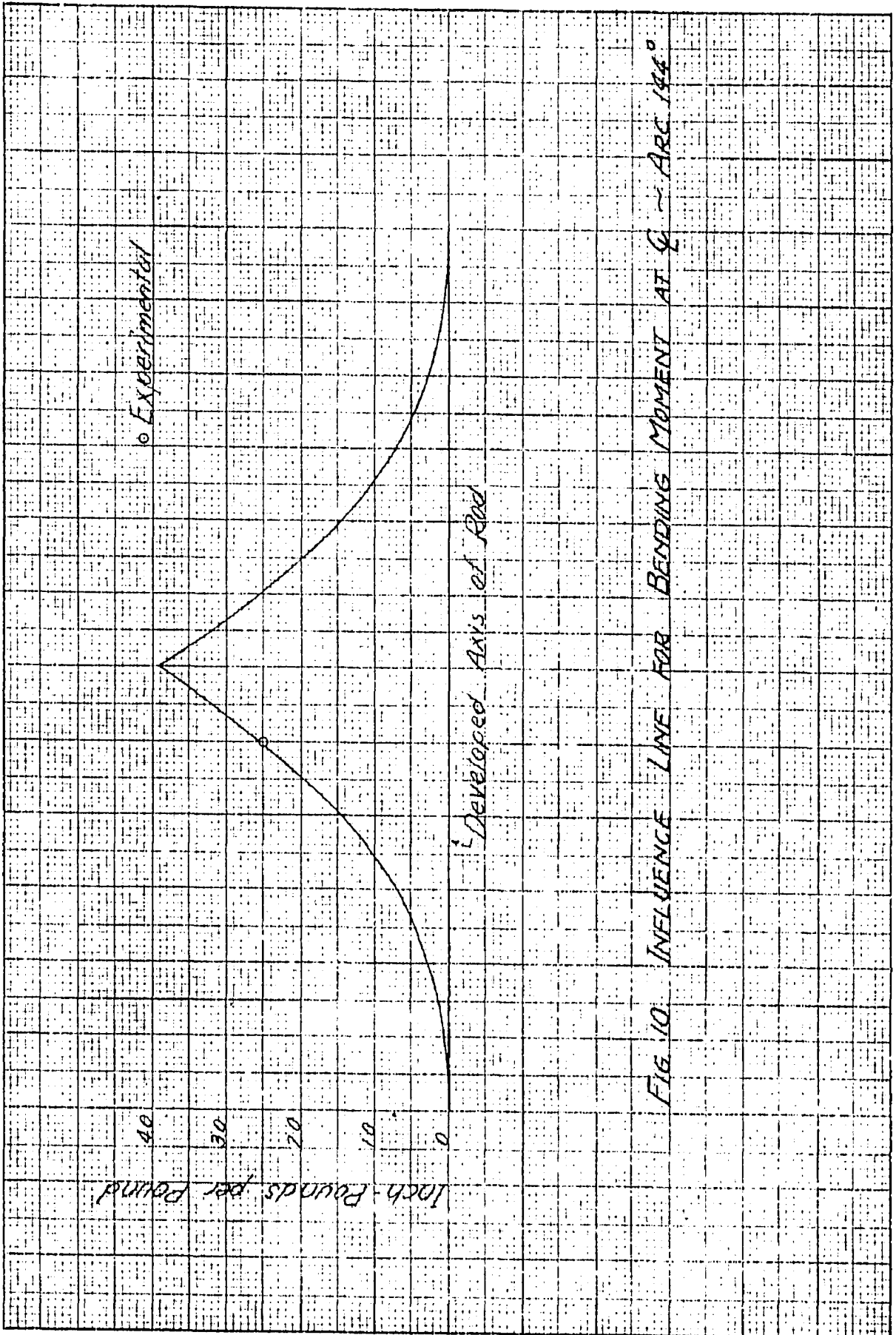


FIG. 9 INFLUENCE LINE FOR TWISTING MOMENT AT QUARTER POINT -
ARC 180°



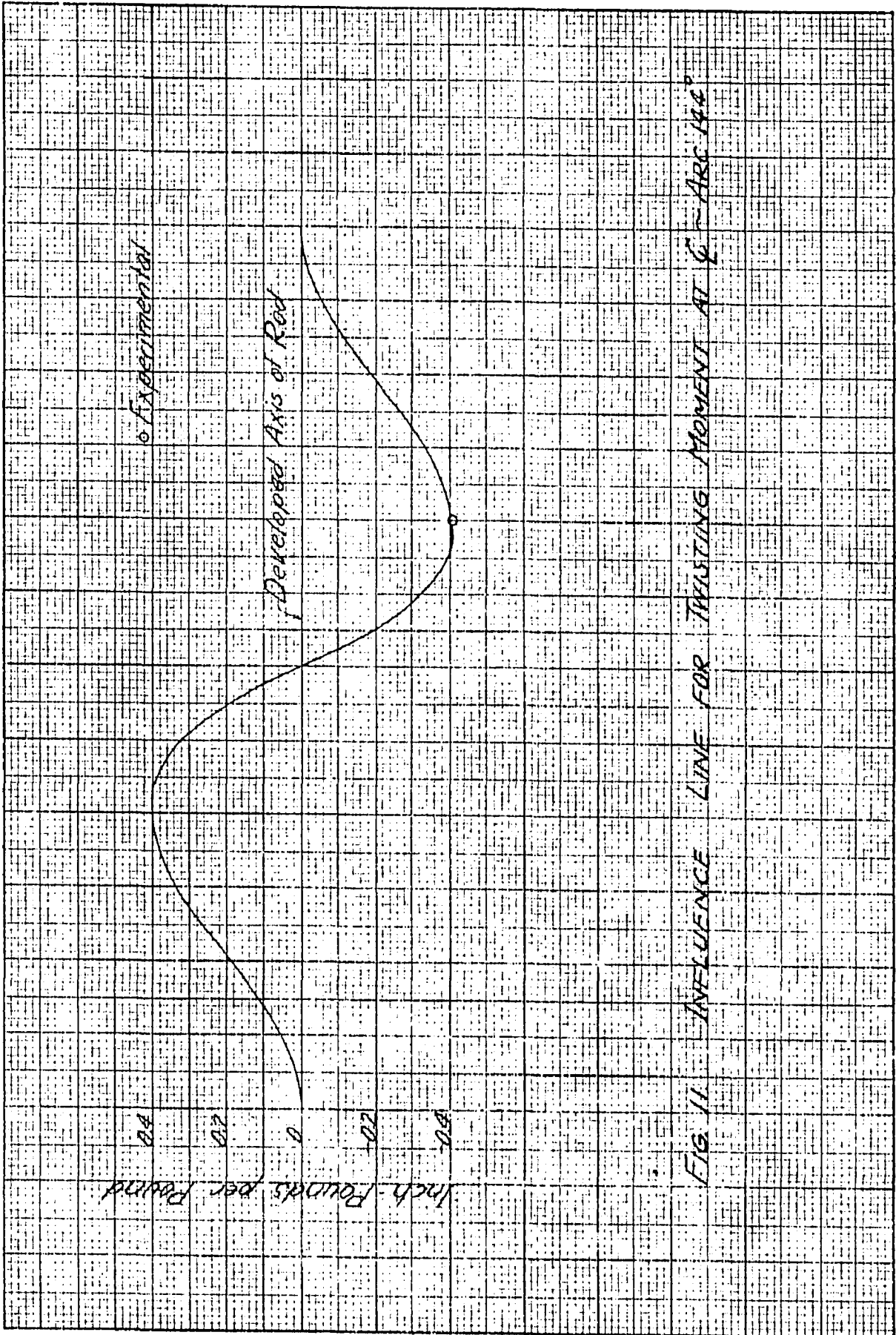
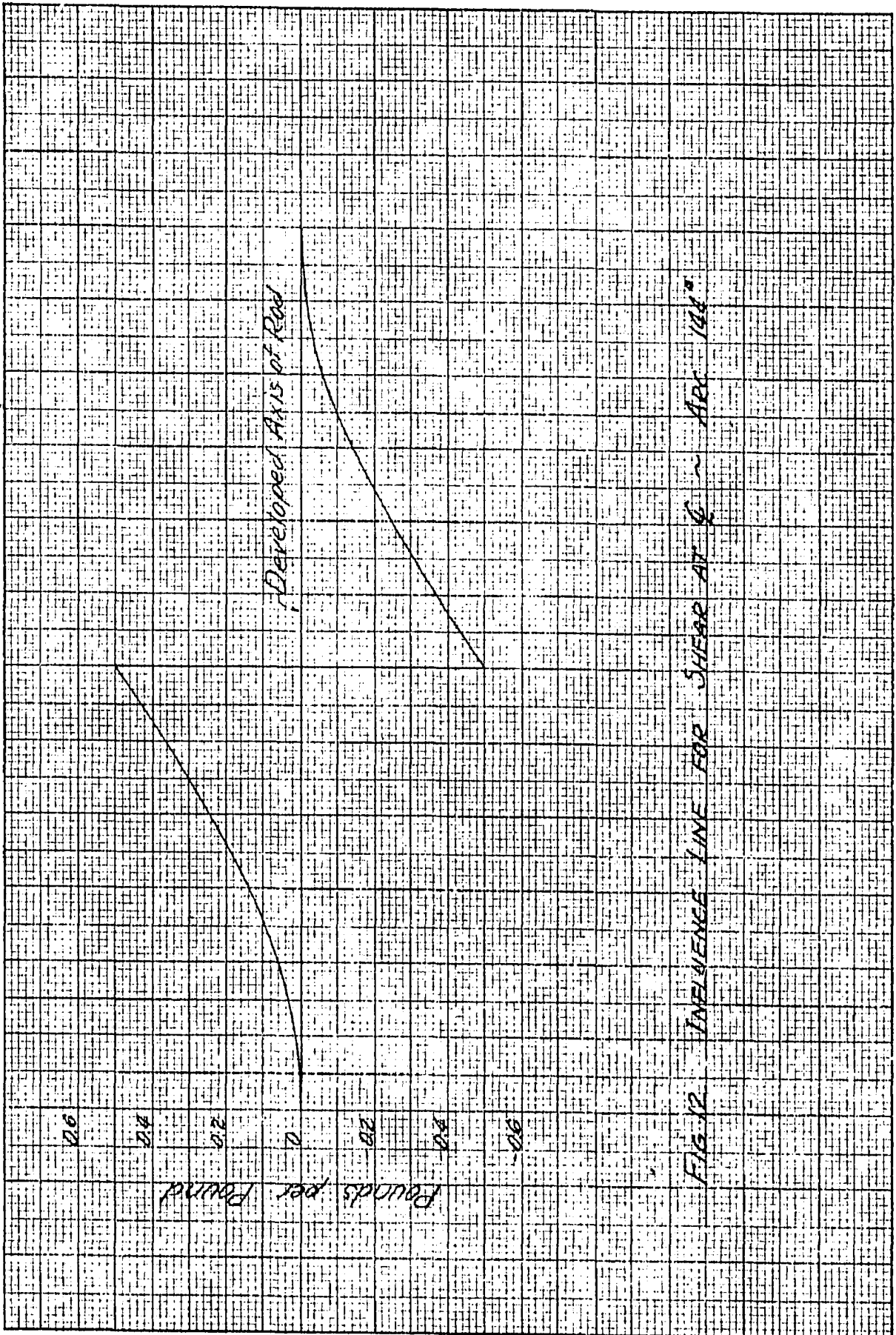


FIG. 11 INFLUENCE LINE FOR TWISTING MOMENT AT C - ARC 144°



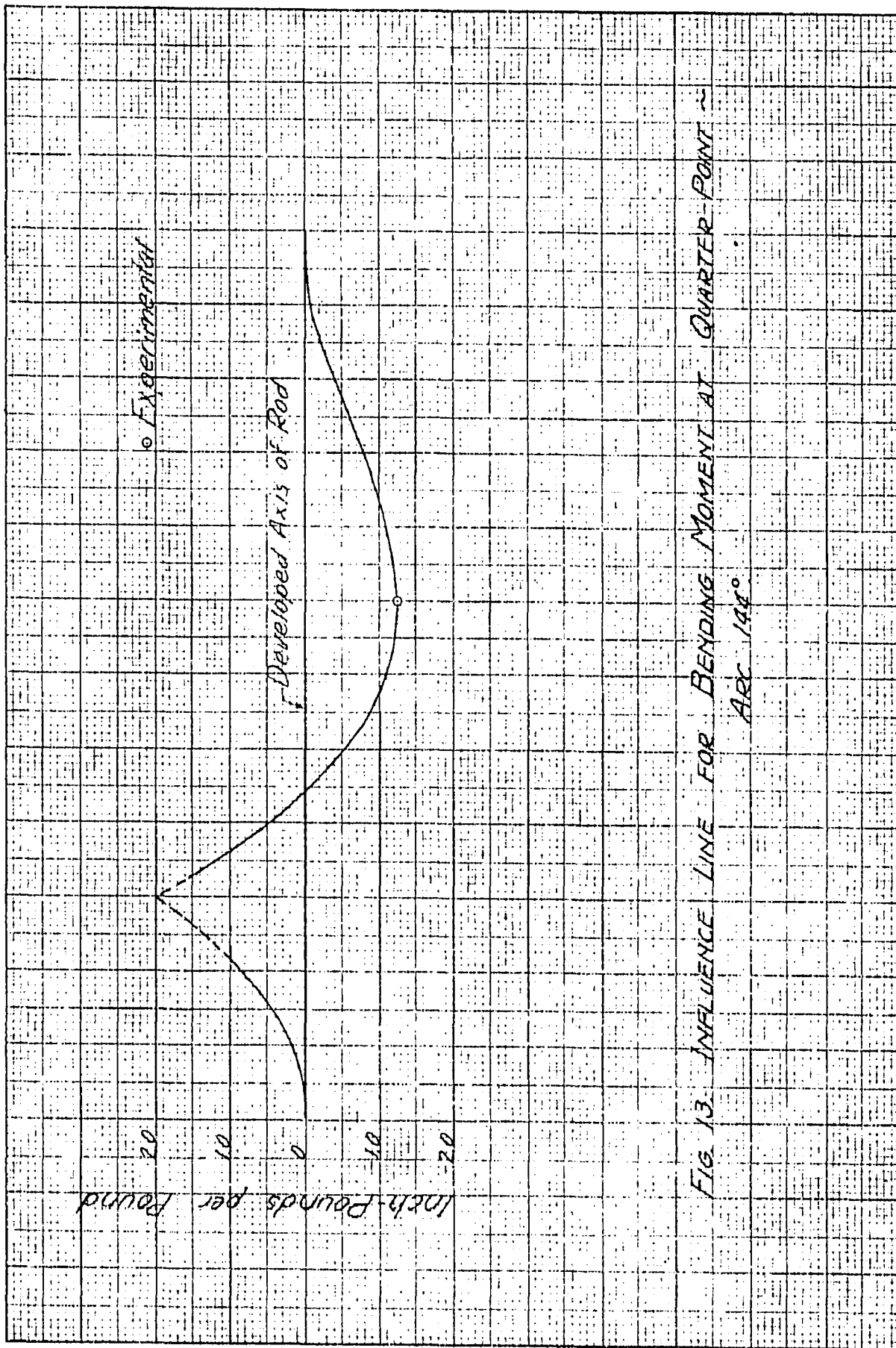


FIG. 13. INFLUENCE LINE FOR BENDING MOMENT AT QUARTER-POINT ~
ARC 144°

Page 55

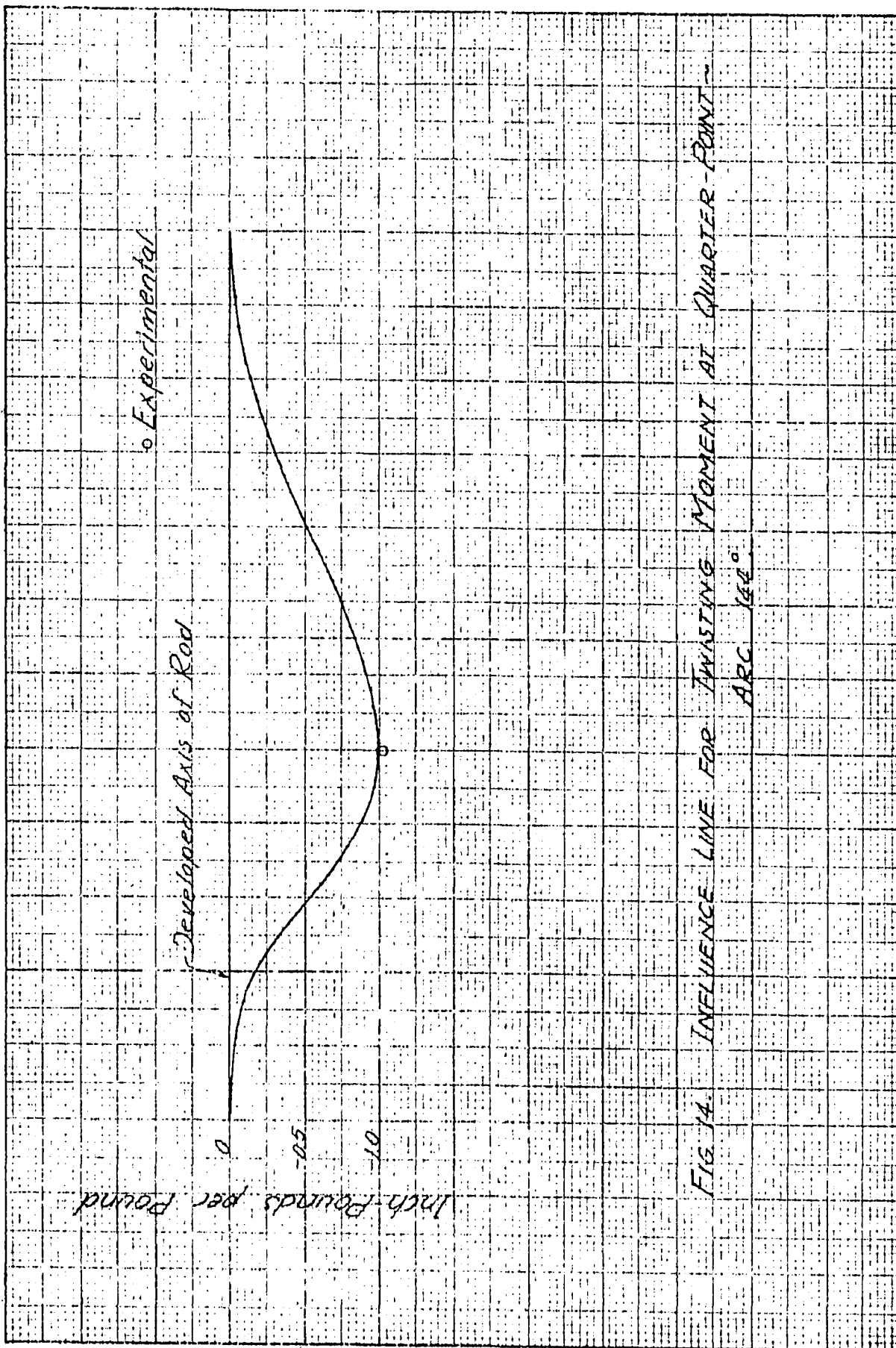


FIG. 14. INFLUENCE LINE FOR TWISTING MOMENT AT QUARTER-POINT - ARC 144°

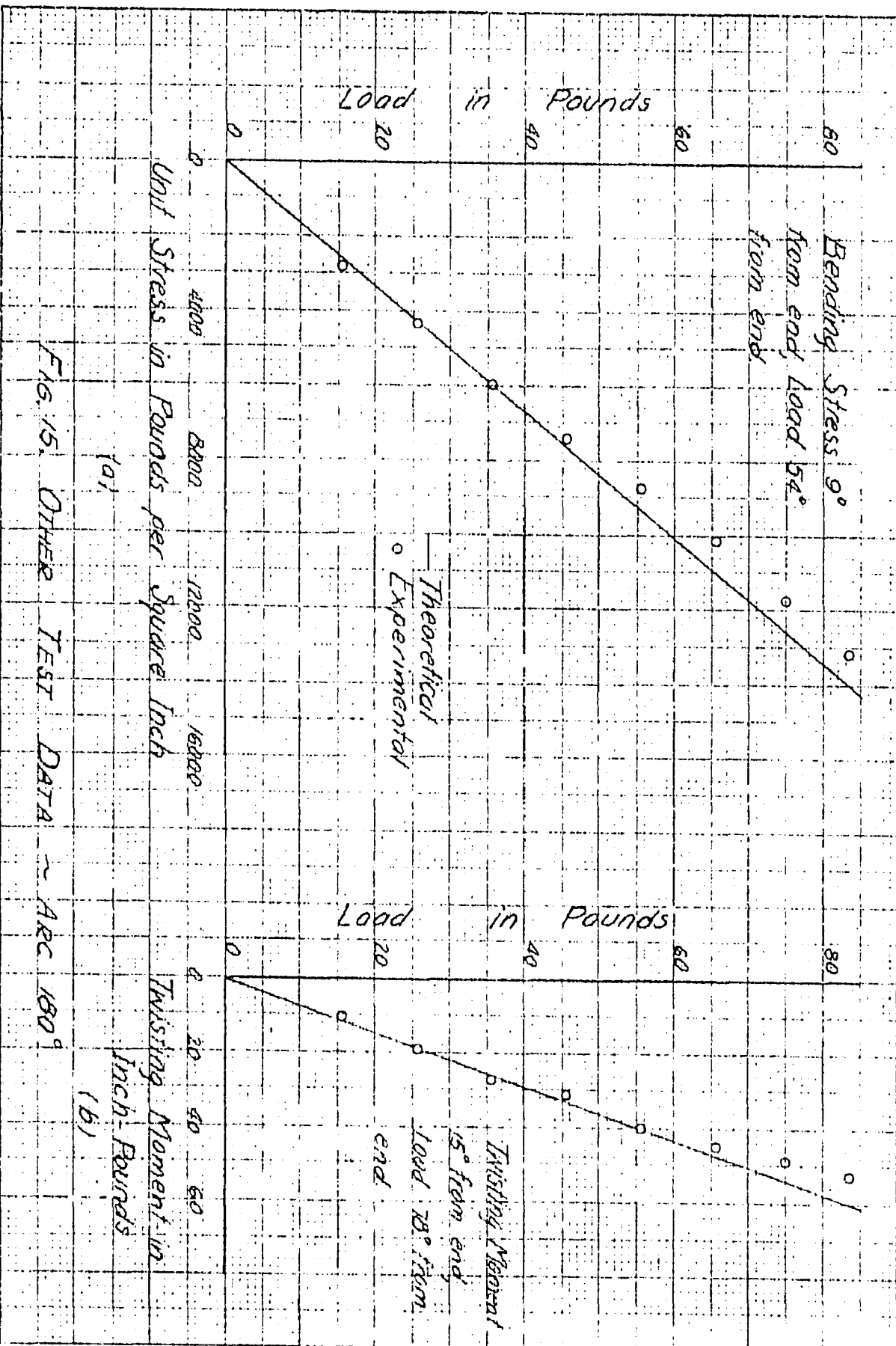


FIG. 15. OTHER TEST DATA ~ ARC 180°

C. Discussion

In general, the test results on the rod showed close agreement with the analysis. For the 180° arc the relatively high experimental values for bending moment at \mathcal{C} and at the quarter-point were probably due to the ends of the rod not being perfectly fixed. Other slight discrepancies may be explained by the fact that the rod was cold bent, was not turned in a lathe to a perfect circular section, and had mill scale on it except at the points of fastening the gages.

V. ANALYSIS OF CIRCULAR-ARC CURVED BEAM OF I-FORM

A. General

Because of the shape of its cross-section the curved beam of I-form must have special treatment. It is a recognized fact (8) that when an I-beam is fixed at its ends and then twisted, direct stresses are produced in the edges of the beam. These stresses are caused by each flange acting as a beam. The bending moments induced in the top and bottom flanges by twisting are equal but of opposite signs.

In the case of a curved I-beam fixed at its ends this stress becomes of primary importance. It was found that it might be as much as seven times as great as the stress the designer would ordinarily compute due to the bending moment about the major axis of the I-beam. The redeeming feature of this condition is that the stresses caused by these induced bending moments are of a localized nature and the signs of these stresses are the same at diagonally opposite corners of the I-beam.

Since this is true one finds that the stress due to twisting may be either added to or subtracted from what we might call the ordinary bending stress.

The analysis used here is essentially that of Unold (14), but in this chapter the principles of analysis are extended to include non-symmetrical concentrated loads. The origin of coordinates is taken at the applied load. This means that the origin varies according to the position of the load.

B. Notation

The following notation is used in Chapters V and VI:

- v displacement of center line of top flange in circumferential direction; positive when movement is toward the origin.
- z displacement of center line of top flange in radial direction, positive for outward movement.
- y displacement of axis of I-beam in vertical direction; positive for upward movement.
- M bending moment at any section of I-beam; positive for compression in top flange.
- T twisting moment developing shearing stresses on

- I-beam; positive as shown in Fig. 16.
- V vertical shear at any section; positive as shown in Fig. 16.
- M bending moment in flange induced by twist of I-beam; positive for compression on the inside of the top flange.
- \mathcal{V} shear accompanying M .
- θ angle of twist per unit length of I-beam.
- r radius of curved I-beam.
- x distance along axis of I-beam.
- E modulus of elasticity of I-beam.
- P concentrated load on I-beam.
- a one-half the depth of the beam.
- I moment of inertia of the I-beam about the horizontal axis.
- I_{2-2} moment of inertia of the I-beam about the vertical axis.
- H one-half of I_{2-2} .
- G modulus of elasticity of I-beam in shear.
- K torsion constant, comparable to the polar moment of inertia for circular sections.
- $C_1, C_2, \text{ etc.}$ and $D_1, D_2, \text{ etc.}$, constants of integration.

The derivatives of functions such as $M, y, z, \text{ etc.}$

with respect to ϕ are indicated by use of primes, eg.

$$\frac{dM}{d\phi} = M', \quad \frac{d^2 z}{d\phi^2} = z'', \quad \frac{d^4 y}{d\phi^4} = y'''' , \text{ etc.}$$

The sense of the moment when represented by an arrow-head on a vector is such as to direct the arrow-head away from the plane of the couple in the direction from which the rotation appears counter-clockwise.

C. Assumptions

The following assumptions are made:

1. Hooke's law applies.
2. The ends of the beam are fixed.
3. Angular deflections are small compared with the dimensions of the beam.
4. I is the moment of inertia of one flange about the vertical axis of the beam.
5. The transverse shear in each flange may be considered to act along the outside edge of the flange.

D. Derivation

Figure 16 shows a portion of a curved I-beam with

Note:

○ indicates V acts down

● indicates V acts up

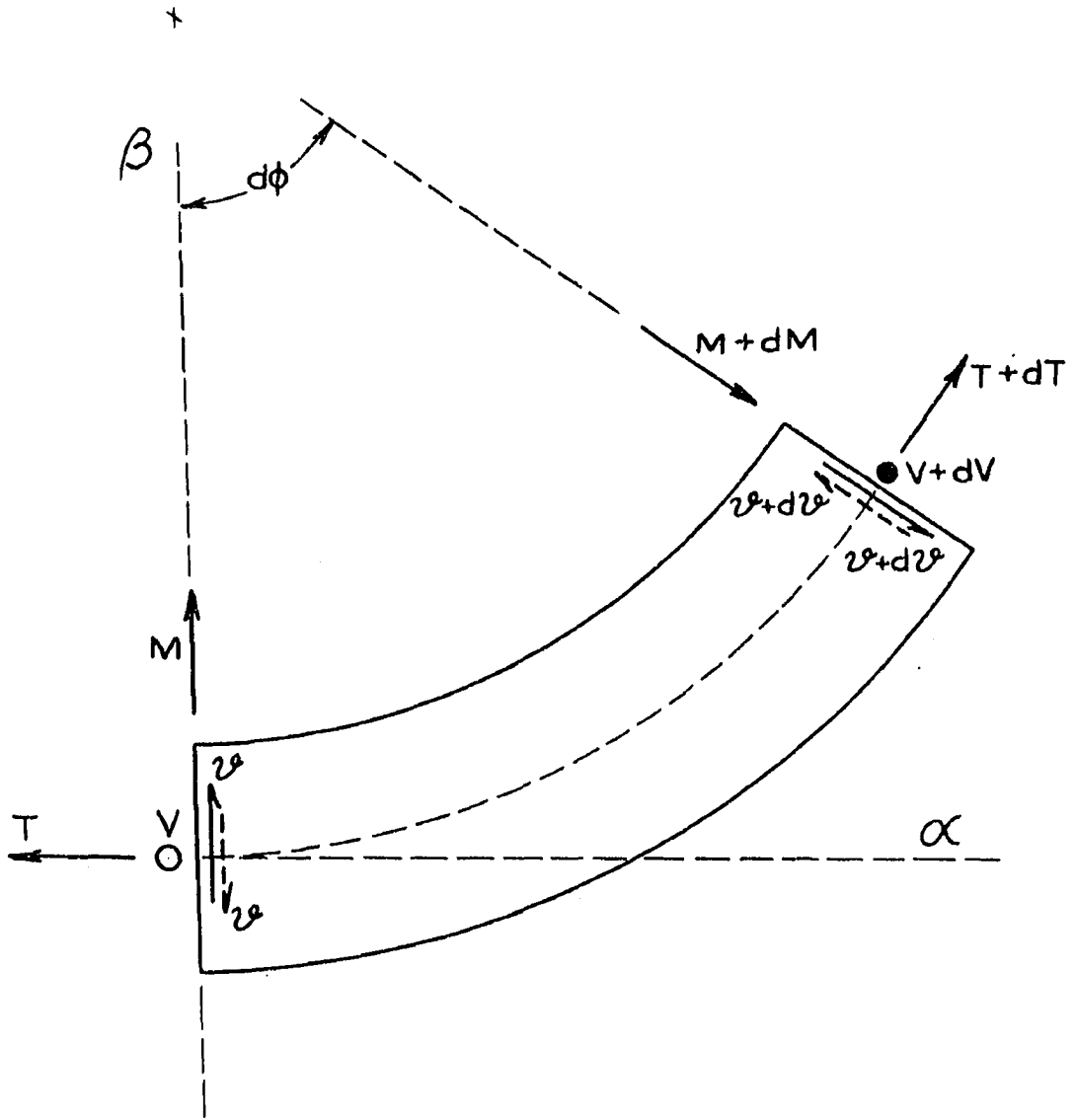


FIG. 16. FORCES ACTING ON ELEMENTAL LENGTH OF I-BEAM.

the forces acting thereon. The beam is assumed to be loaded with a single concentrated load.

Then from

$$\begin{aligned} \sum \text{Vertical Forces} = 0 \text{ is obtained} \\ dV = 0, \quad \therefore V = \text{constant} \end{aligned}$$

Moments about the line α give

$$\sum M_{\alpha} = 0$$

$$T + \mathcal{V} 2a - (T + dT) - (\mathcal{V} + d\mathcal{V}) 2a - (M + dM) d\phi = 0$$

Neglecting differentials higher than the first degree

$$Md\phi + dT + d\mathcal{V} 2a = 0$$

$$M + T' + \mathcal{V}' 2a = 0 \quad (37)$$

Moments about the line β give

$$\sum M_{\beta} = 0$$

$$\begin{aligned} M - (M + dM) + (T + dT) d\phi + (\mathcal{V} + d\mathcal{V}) 2ad\phi \\ -(V + dV) dx = 0 \end{aligned}$$

Since $dx = rd\phi$

$$- M' + T + \mathcal{V} 2a - Vr = 0 \quad (38)$$

The coordinates at one point and at a distance $dx = rd\phi$ from this point are in the case of displace-

ments expressed by

$$y, v, z \quad \text{and} \quad y + dy, \quad v + dv, \quad z + dz.$$

Now

$$v = a \frac{dy}{dx} = \frac{a}{r} \frac{dy}{d\phi} = \frac{a}{r} y' \quad (39)$$

(See Fig. 17).

The middle fiber of the upper flange shortens from the original length by a distance

$$\Delta dx = v + dv - v - (r + z) d\phi + rd\phi = dv - zd\phi$$

Therefore the unit strain is

$$\epsilon = \frac{\Delta dx}{dx} = \frac{dv}{dx} - z \frac{d\phi}{dx} = \frac{dv}{rd\phi} - \frac{z}{r} = \frac{v' - z}{r}$$

The corresponding bending moment is

$$M = \frac{(\epsilon E) I}{a} = (v' - z) \frac{EI}{ar} \quad (40)$$

The angle of twist, $d\delta$, between the cross-section at I and the cross-section at II may be obtained by considering the displacements on the center line of the top flange. (Figs. 17 and 18). The relative radial displacement between points 1 and 2, which are a distance dx apart, is ads . Then

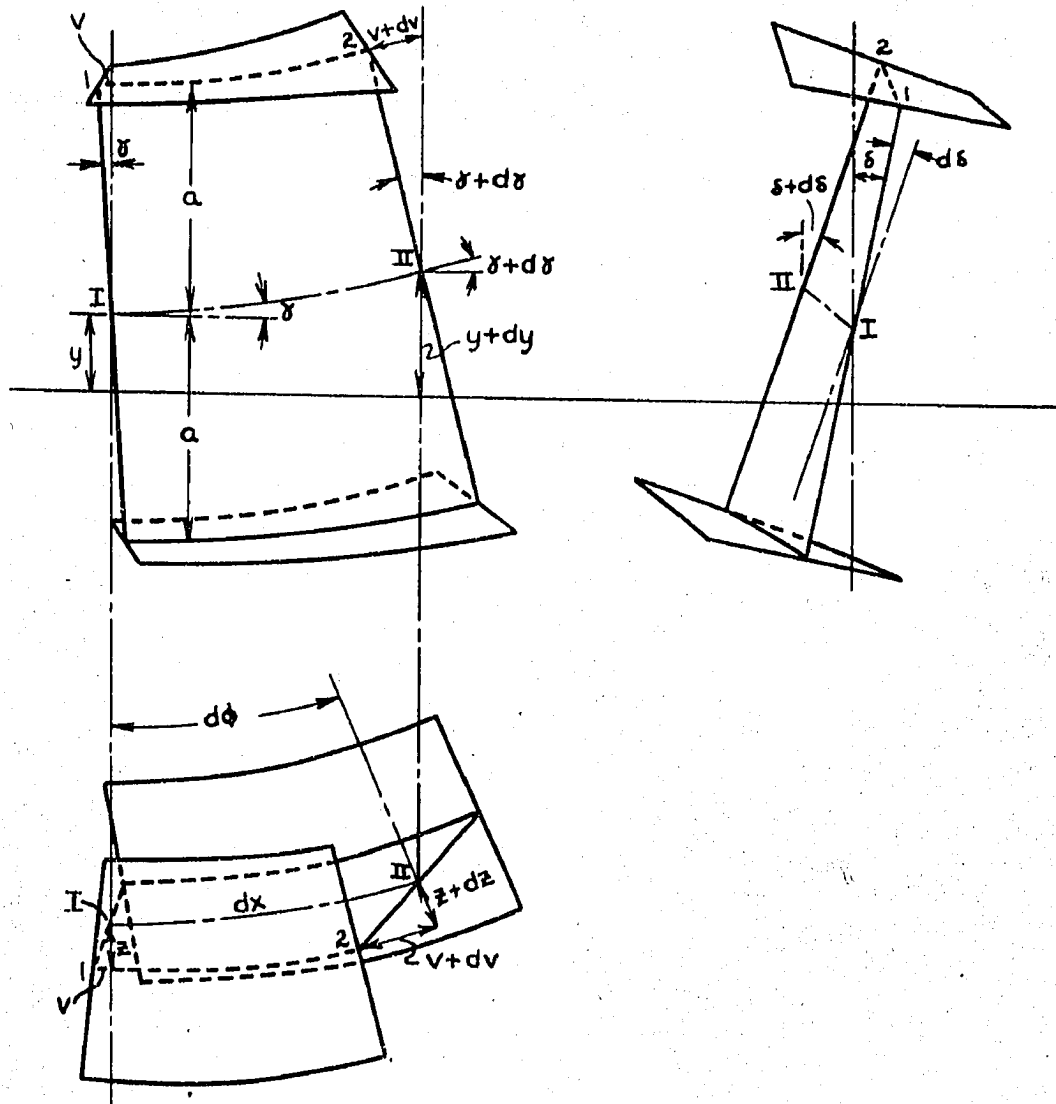


FIG. 17. DISPLACEMENTS v , y AND z .

$$d\delta = \frac{v d\phi + dz}{a},$$

$$\delta' = \frac{v}{a} + \frac{z'}{a}$$

and the rotation per unit length is

$$\theta = \frac{d\delta}{dx} = \frac{d\delta}{rd\phi} = \frac{\delta'}{r}$$

Also

$$\theta = \frac{T}{GK}$$

Let

$$q = \frac{GK}{EI} \text{ then}$$

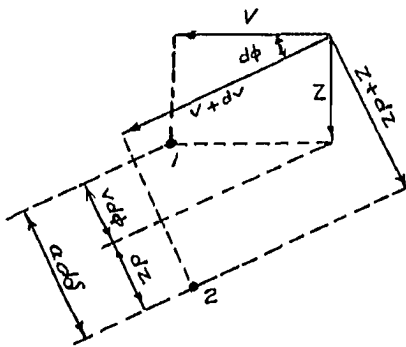


Fig. 18. Relative Displacements of points 1 and 2.

$$\frac{\delta'}{r} = + \frac{T}{EI} \frac{1}{q} \text{ or}$$

$$T = +(v + z') \frac{EI}{ar} q \quad (41)$$

Let $\frac{I_{z,z}}{2} = H$. Then from the formula* for the relation between change in curvature and bending moment in the case of curved beams, we have for the bending moment on the top flange

* For derivation see Appendix A.

$$M = -EH \left(\frac{d^2 z}{dx^2} + \frac{z}{r^2} \right)$$

or

$$M = -\frac{EH}{r^2} (z'' + z) \quad (42)$$

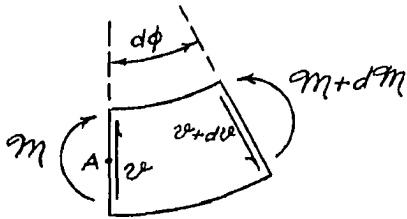


Fig. 19. M and z .

The relation between M and z may be found by taking moments about the vertical axis through A shown in Fig. 19.

$$M + dM - M - (z + dz) dx = 0$$

$$dM = z dx = z r d\phi \quad \text{or}$$

$$z = \frac{M'}{r} \quad (43)$$

The equations (37) to (43) form a system of simultaneous differential equations between the variable ϕ and the terms y, v, z, V, M, T, M and z . It is desirable to obtain a differential equation containing only ϕ and y .

From equations (39) and (40) we have

$$M = (v' - z) \frac{EI}{ar} = \left(\frac{a}{r} y'' - z\right) \frac{EI}{ar}$$

$$z = \frac{a}{r} y'' - \frac{ar}{EI} M$$

$$z' = \frac{a}{r} y''' - \frac{ar}{EI} M' \quad (44)$$

From equations (39) and (41) we obtain

$$T = +(v + z') \frac{EI}{ar} q = +\left(\frac{a}{r} y' + z'\right) \frac{EI}{ar} q$$

$$z' = \frac{ar}{EIq} T - \frac{a}{r} y' \quad (45)$$

Equating equations (44) and (45) and solving for T

$$\frac{a}{r} y''' - \frac{ar}{EI} M' = \frac{ar}{EIq} T - \frac{a}{r} y'$$

$$T = \frac{EIq}{r^2} (y' + y''') - M' q \quad (46)$$

Now

$$\mathcal{V} = \frac{M'}{r} = -\frac{EH}{r^3} (z' + z''')$$

$$= -\frac{EH}{r^3} \left(\frac{a}{r} y''' - \frac{ar}{EI} M' + \frac{a}{r} y^{(5)} - \frac{ar}{EI} M'' \right)$$

$$\mathcal{V} = -\frac{EHa}{r^4} (y'''' + y^{(5)}) + \frac{Ha}{Ir^2} (M' + M''') \quad (47)$$

From equations (37) and (38)

$$\begin{aligned} M + T' + \mathcal{V}' 2a &= 0 \\ -M'' + T' + \mathcal{V}' 2a - V' r &= 0 \\ \hline M + M'' + V' r &= 0 \end{aligned}$$

Since $V = a$ constant, $V' = 0$ and

$$M + M'' = 0 \quad (48)$$

Rewriting equation (47)

$$\mathcal{V} = -\frac{EHa}{r^4} (y'''' + y^{(5)}) \quad (49)$$

Equation (37)

$$M + T' + \mathcal{V}' 2a = 0$$

Substituting for T' (derivative of equation (46))
and \mathcal{V}' (derivative of equation (49)) we obtain

$$M + \frac{EIq}{r^2} (y'' + y''''') - M''q - \frac{2EHa^2}{r^4} (y'''' + y^{(6)}) = 0 \quad (50)$$

Differentiating equation (50) twice we have

$$M'' + \frac{EIq}{r^2} (y'''' + y^{(6)}) - M'''' q - \frac{2EHa^2}{r^4} (y^{(6)} + y^{(8)}) = 0 \quad (51)$$

Adding equations (50) and (51) and noting

$$M + M'' = 0 \quad \text{we have}$$

$$\frac{EIq}{r^2} (y'' + 2y'''' + y^{(6)}) - \frac{2EHa^2}{r^4} (y'''' + 2y^{(6)} + y^{(8)}) = 0 \quad (52)$$

$$\text{Let } \frac{EIq}{r^2} = A, \quad \frac{2EHa^2}{r^4} = B \quad \text{and} \quad \sqrt{\frac{A}{B}} = \rho \quad \text{then}$$

$$(y'' + 2y'''' + y^{(6)}) A - (y'''' + 2y^{(6)} + y^{(8)}) B = 0 \quad (53)$$

The solution of equation (53) is

$$y = C_1 + C_2 \rho + C_3 \sinh \rho \rho + C_4 \cosh \rho \rho + C_5 \sin \rho + C_6 \cos \rho \\ + C_7 \rho \sin \rho + C_8 \rho \cos \rho \quad (54)$$

The following is a summary of the equations used in determining the constants of integration:

$$y = C_1 + C_2 \phi + C_3 \sinh \rho \phi + C_4 \cosh \rho \phi + C_5 \sin \phi + C_6 \cos \phi + C_7 \phi \sin \phi + C_8 \phi \cos \phi$$

$$y' = C_2 + C_3 \rho \cosh \rho \phi + C_4 \rho \sinh \rho \phi + C_5 \cos \phi - C_6 \sin \phi + C_7 (\sin \phi + \phi \cos \phi) + C_8 (\cos \phi - \phi \sin \phi)$$

$$M = -\frac{A}{1+q} (y'' + y''''') + \frac{B}{1+q} (y'''' + y^{(6)}) = \frac{2B(1+\rho^2)}{1+q} [C_7 \cos \phi - C_8 \sin \phi]$$

$$T = A(y' + y''''') - M'q = A[C_2 + C_3 \rho(1+\rho^2) \cosh \rho \phi + C_4 \rho(1+\rho^2) \sinh \rho \phi - C_7 2 \sin \phi$$

$$- C_8 2 \cos \phi] + \frac{2B(1+\rho^2)q}{1+q} [C_7 \sin \phi + C_8 \cos \phi]$$

$$U = -\frac{B}{2a} (y'''' + y^{(6)}) = -\frac{B}{2a} [C_3 \rho^3(1+\rho^2) \cosh \rho \phi + C_4 \rho^3(1+\rho^2) \sinh \rho \phi + C_7 2 \sin \phi + C_8 2 \cos \phi]$$

$$W = -\frac{Br}{2a} (y'' + y''''') = -\frac{Br}{2a} [C_3 \rho^2(1+\rho^2) \sinh \rho \phi + C_4 \rho^2(1+\rho^2) \cosh \rho \phi - C_7 2 \cos \phi + C_8 2 \sin \phi]$$

$$V = \frac{1}{r} [-M' + T + U 2a] = \frac{1}{r} [A(y'''' + y^{(6)}) - B(y^{(5)} + y^{(7)}) + A(y' + y''''') - B(y'''' + y^{(6)})]$$

$$= \frac{B\rho^2}{r} C_2 = \frac{A}{r} C_2$$

$$Z = \frac{a}{r} y'' - \frac{ar}{EI} M$$

$$= \frac{a}{r} [C_3 \rho^2 \sinh \rho \phi + C_4 \rho^2 \cosh \rho \phi - C_5 \sin \phi - C_6 \cos \phi + C_7 (2 \cos \phi - \phi \sin \phi)$$

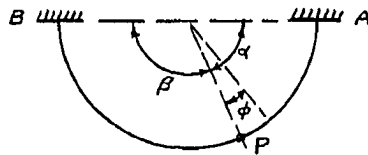
$$+ C_8 (-2 \sin \phi - \phi \cos \phi)] - \frac{2Bar(1+\rho^2)}{(1+q)EI} [C_7 \cos \phi - C_8 \sin \phi]$$

$$Z' = \frac{a}{r} [C_3 \rho^3 \cosh \rho \phi + C_4 \rho^3 \sinh \rho \phi - C_5 \cos \phi + C_6 \sin \phi + C_7 (-3 \sin \phi - \phi \cos \phi)$$

$$+ C_8 (-3 \cos \phi + \phi \sin \phi)] + \frac{2Bar(1+\rho^2)}{(1+q)EI} [C_7 \sin \phi + C_8 \cos \phi]$$

The necessary boundary conditions for determining the constants of integration are tabulated below. The origin is to be taken under the load and ϕ is positive, measured in either direction.

When	<u>$\phi = \alpha$</u>	<u>$\phi = \beta$</u>	<u>$\phi = 0$</u>
	$y = 0$	$y = 0$	$v_{\alpha}^{\prime} = -v_{\beta}^{\prime}$
	$y' = 0$	$y' = 0$	$V_{\alpha} + V_{\beta} = P$
	$z = 0$	$z = 0$	$y_{\alpha} = y_{\beta}$
	$z' = 0$	$z' = 0$	$y'_{\alpha} = -y'_{\beta}$
			$z_{\alpha} = z_{\beta}$
			$z'_{\alpha} = -z'_{\beta}$
			$m_{\alpha} = m_{\beta}$
			$M_{\alpha} = M_{\beta}$



The constants of integration are designated as C for the α segment and D for the β segment.

The necessary boundary conditions for determining the constants of integration in the case of symmetrical loading, i.e., for $\alpha = \beta$, are

when	<u>$\phi = \alpha$</u>	<u>$\phi = 0$</u>
	$y = 0$	$V = \frac{P}{2}$
	$y' = 0$	$T = 0$ or $\mathcal{V} = 0$
	$z = 0$	$y' = 0$
	$z' = 0$	$z' = 0$

After the constants of integration are determined by the solution of simultaneous equations, the constants should be substituted in the equation for the particular function desired. The constants of integration are expressed in terms of the load P.

In the determination of the outer fiber stress the bending moment M is substituted in the flexure formula, $S_1 = \frac{Ma}{I}$, and the bending moment \mathcal{M} is substituted in the flexure formula, $S_2 = \frac{\mathcal{M} b}{I}$, where b is one-half the width of the flange. The unit stress in the outer fiber is then $S = S_1 \pm S_2$.

VI. EXPERIMENTS ON AN I-BEAM BENT TO A SEMI-CIRCLE.

A. General

For the purpose of comparison of the analysis developed in Chapter V with experimental values the strains, deflections and rotations were measured on a 6 inch 12.5 lb. American Standard I-beam, bent in the shape of a semi-circle about the vertical axis with a 6 foot radius. Figure 20 is a general view of the experimental set-up.

B. Materials

Since the I-beam was bent cold it had initial stresses and more or less permanent set. However, the beam was not tested until one year after the cold bending, and it is possible that some sort of recovery had taken place in the interim. Later the beam was annealed and tested again.

The modulus of elasticity in tension and shear were determined from coupons cut from an 18 inch length

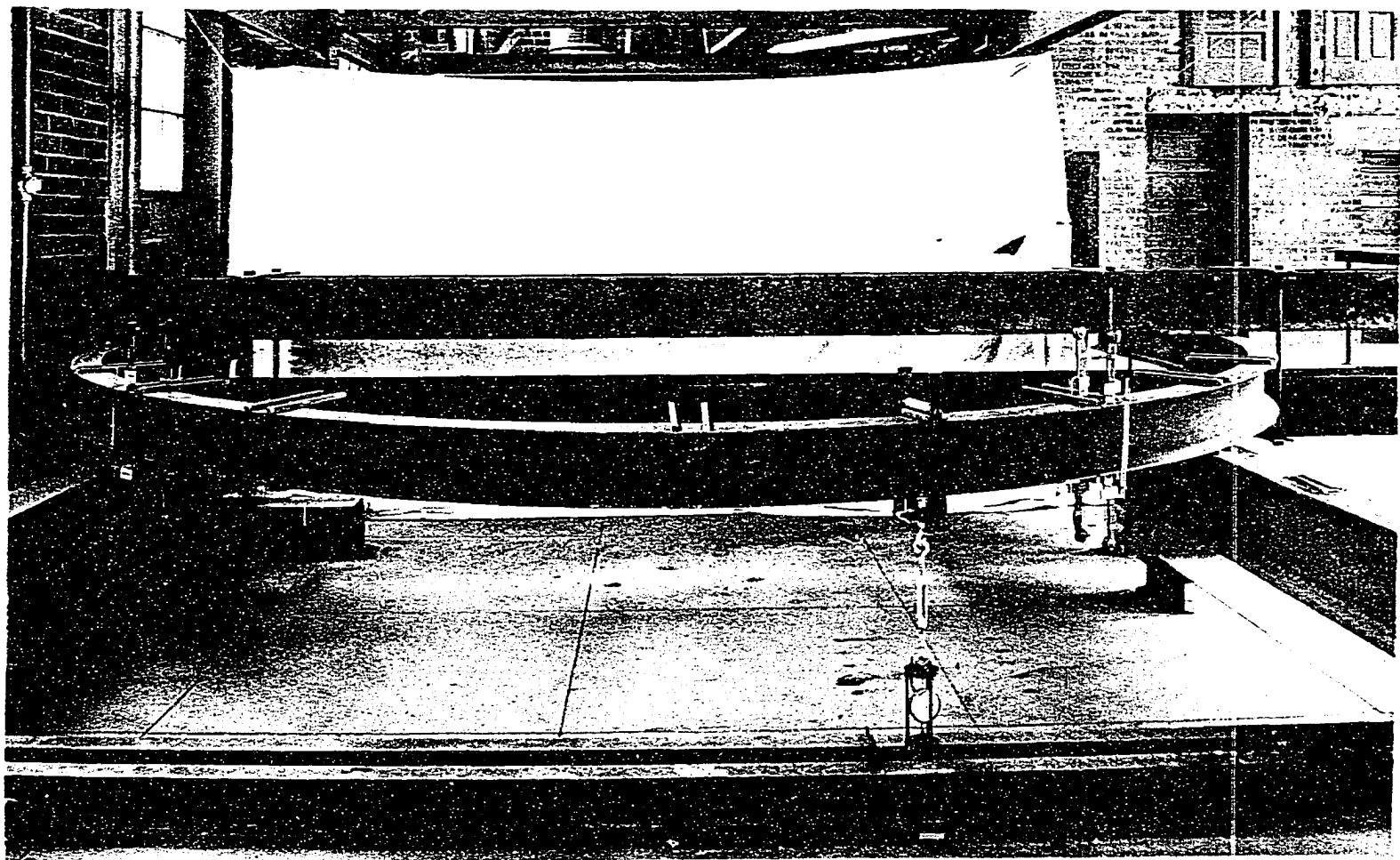


Fig. 20. General View of Experimental Set-up.

of I-beam from the same stock length as the curved beam.

C. Constants

The constants necessary for the analysis of this I-beam are listed below. The values of E and G were determined from coupons from the beam. The values I, H and a may be found in any steel handbook. The value of K was taken from the Bethlehem Manual of Steel Construction and was also checked by the membrane analogy. The beam was bent to the radius r.

E	28 300 000 lbs. per sq. in.
G	11 750 000 lbs. per sq. in.
K	0.171 inches ⁴
I	21.8 inches ⁴
H	0.9 inches ⁴
a	3 inches
r	72 inches

The constants of integration are given in Table V.

TABLE V. CONSTANTS OF INTEGRATION
IN TERMS OF P TO BE USED IN EQUATION(54).

CONSTANT	$\alpha = 90^\circ, \beta = 90^\circ$	$\alpha = 75^\circ, \beta = 105^\circ$	$\alpha = 45^\circ, \beta = 135^\circ$
C_1	-0.0480812	-0.0433519	-0.0166528
C_2	+0.0928224	+0.124401	+0.170947
C_3	-0.0000347487	-0.0000355729	-0.0000429580
C_4	+0.000034330	+0.0000338351	+0.0000265369
C_5	-0.137345	-0.186165	-0.255516
C_6	+0.0464008	+0.0419313	+0.0163286
C_7	+0.0254015	+0.0226310	+0.00788787
C_8	+0.0446281	+0.0628516	+0.0855084
D_1		-0.0433519	-0.0166528
D_2		+0.0613636	+0.0148180
D_3		-0.0000339245	-0.0000265394
D_4		+0.0000338351	+0.0000265369
D_5		-0.0885249	-0.0191737
D_6		+0.0419313	+0.0163286
D_7		+0.0226310	+0.00788787
D_8		+0.0264047	+0.00374785

D. Method of Procedure

The beam was clamped into position, as shown in Fig. 20, between two 12 inch wide flange sections which in turn rested on two other 12 inch beams. The 4 foot straight ends of the curved beam were anchored so as to prevent, as much as possible, any rotation of the supporting beams. This was to simulate fixed-end conditions.

The load was applied direct to the beam through a quarter-inch square steel bar 1 inch long, running tangential to the curve of the beam. A dynamometer consisting of a single spring, turnbuckle, and $\frac{1}{1000}$ inch dial was used to apply the load to the beam.

The beam was loaded at the center, at $\alpha = 75^\circ$ and at $\alpha = 45^\circ$. An initial load of about 125 lbs. was placed on the beam for the zero readings. The load was then increased 500 lbs. in 100 lb. increments. In all cases at least one check test was run.

Huggenberger tensometers were used for measuring strains at the edges of the beam, as shown in Fig. 21. These strains were produced by combinations of the bending moments M and m .

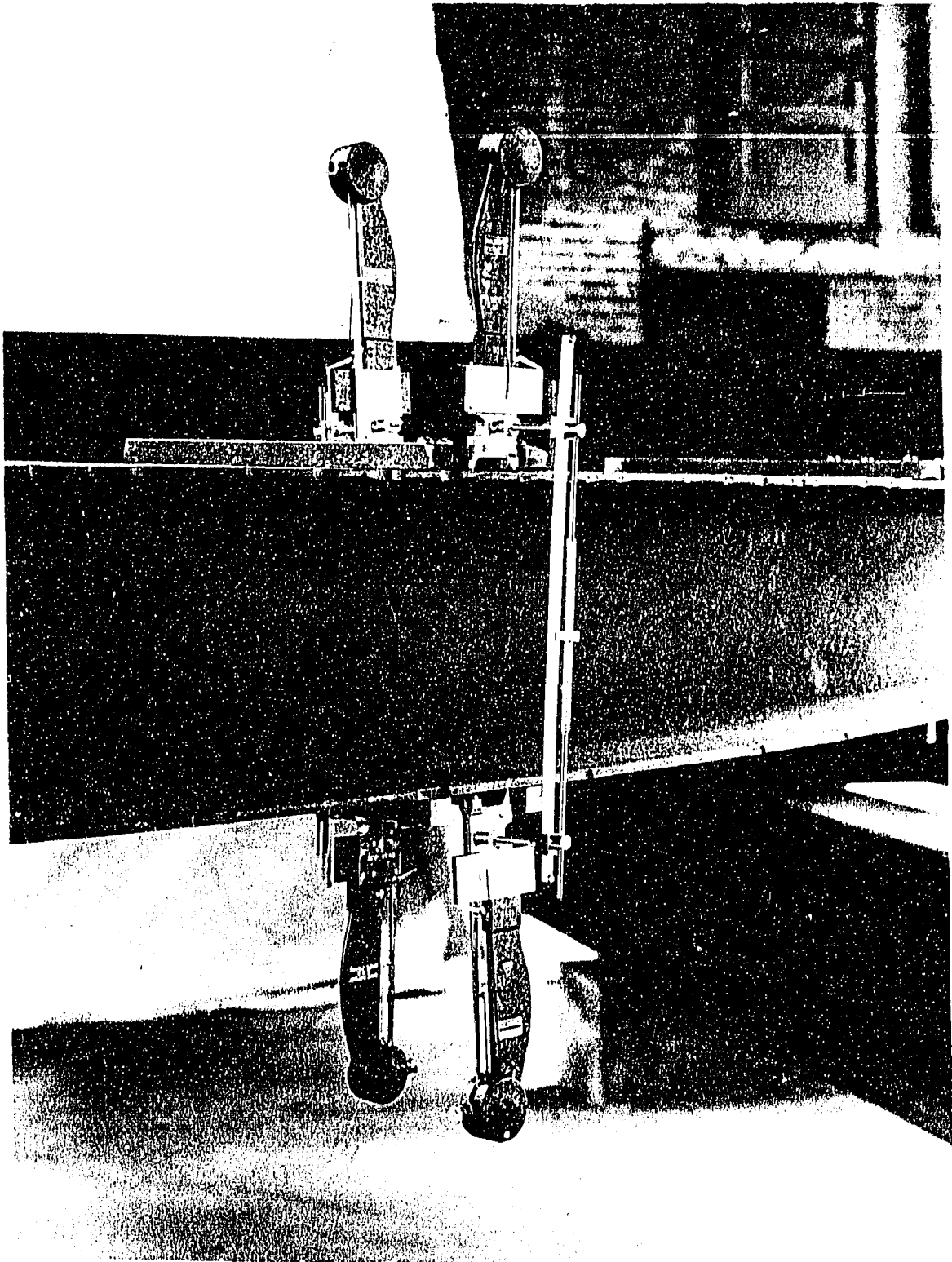


Fig. 21. Huggenberger Tensometers in Place.

A clinometer or level bar built to measure the change in relative altitude of two points 8 inches apart was used to measure rotation of the beam and also of the supports. One-half inch square steel bars were attached to the top and bottom flanges of the I-beam in groups of four at 9 different positions along the beam, as shown in Fig. 20. The changes of altitude of two points eight inches apart on each bar were measured and in this way the amount of twist of the beam was obtained. These observations were corrected for the slight rotation observed at the supports.

To measure the deflections $\frac{1}{1000}$ inch dials were attached, one at each of the supports and one at the center of the beam. The plungers of the dials made contact with plate glass which was supported by the floor. Corrections were made for deflection and rotation at the supports in determining the deflection at the center of the beam.

E. Annealing of I-Beam.

After the first series of tests the I-beam was annealed and the tests repeated. The annealing was done in the foundry at Iowa State College. A kiln of fire

brick was built around the beam. Openings were left for gas and air nozzles and also for inserting a pyrometer for temperature readings. The beam was heated uniformly to a temperature of about 1535° F. and held at this temperature for two hours. The burners were then shut off and foundry sand piled on the kiln. The beam was left this way to cool for 20 hours. During the annealing and subsequent handling of the beam the diameter at the support decreased $1\frac{1}{4}$ inches. Figure 22 shows a general view during the annealing of the beam.

F. Results

The results of the tests are shown in Figs. 23 to 40, inclusive. The stresses in the edge of the beam (Fig. 21) are designated as follows: for the top flange T is used, for the bottom flange B, for the inside edge I and for the outside edge O. The top outside edge of the flange is then designated as TO and the bottom inside edge as BI.

Figures 23 to 34, inclusive, show the theoretical stress along the edge of the beam for loads at $\alpha = 90^{\circ}$, $\alpha = 75^{\circ}$ and $\alpha = 45^{\circ}$. The stress is shown for the beam

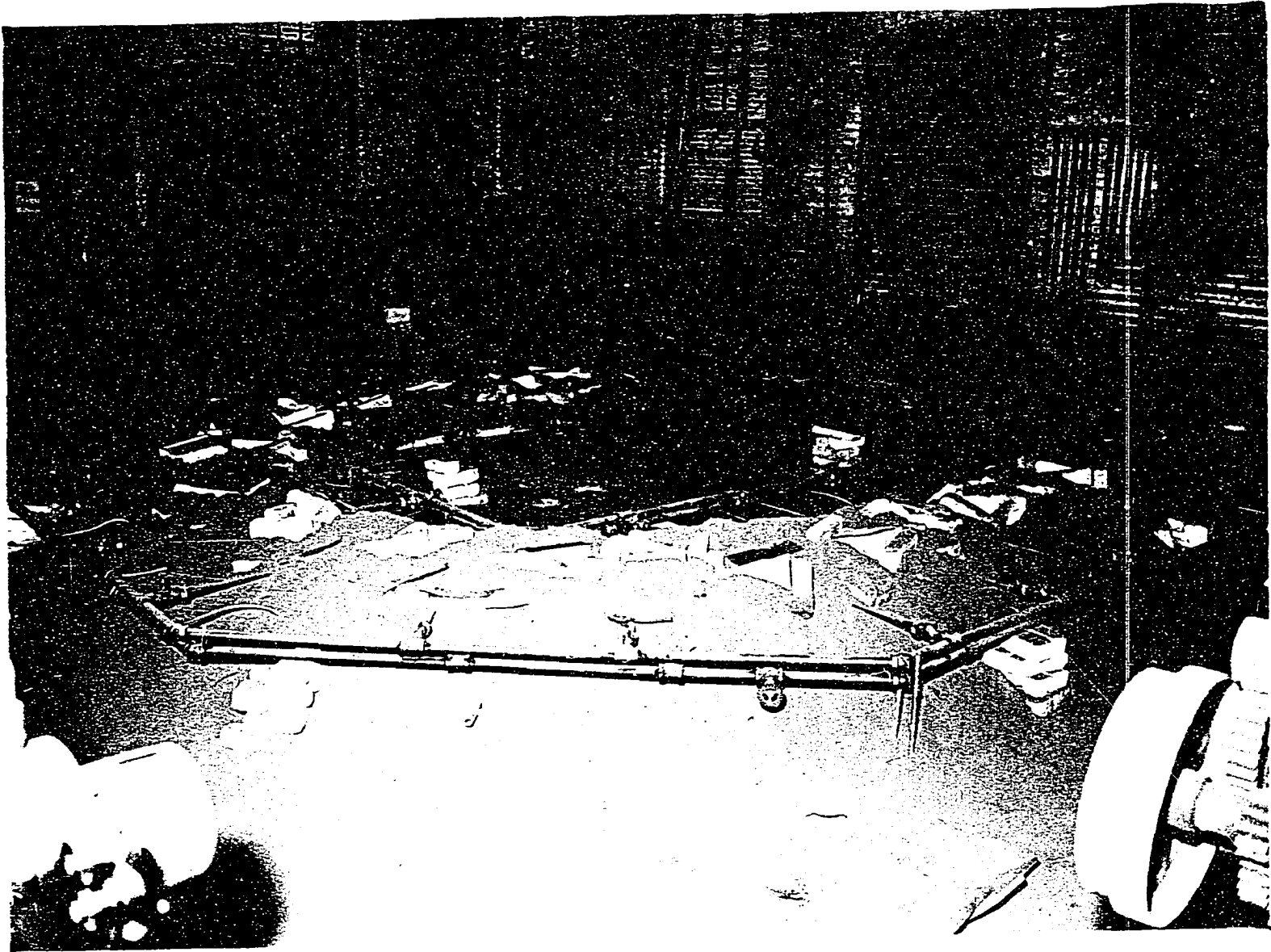


Fig. 22. General View During Annealing of Beam.

developed into a straight line. The experimental values for both before and after annealing the beam are also shown. There is very close agreement between the analytical and experimental values, and it seems to make little difference whether the beam was annealed or unannealed. However, there was one difference noticed during the testing. While testing the annealed beam the experimental results could be reproduced exactly each time, but with the unannealed beam the check tests in most instances varied slightly from the first readings. This was probably due to the initial stresses existing in the beam.

It will be noticed that there is a rapid increase in stress as one approaches the support. This stress even though it reached the yield point of the material would probably do little, if any, damage inasmuch as it is of a localized nature. If the material did yield the vertical deflection would naturally be increased.

Figures 35, 36 and 37 show the values of z , the radial displacement of the top flange. The experimental values are greater than the theoretical. This can be explained by the fact that the flanges of the beam had been warped slightly during the original bending; that the beam weighed 12.4 lbs. per foot instead of 12.5 lbs.; and, that in the bending of the beam the

bulldozer altered the section at various points along the flanges, as can be seen in Fig. 21. In addition to this the section of the beam was reduced at various points by holes which were tapped $1/8$ inch in diameter and $3/16$ inch deep. This was necessary in order to fasten the clinometer bars. All these factors tend to increase the rotation and deflection of the beam over the theoretical values.

Figures 38, 39 and 40 show curves for twisting moment along the beam. The experimental values were obtained by using the difference in rotation of two bars placed $2\frac{1}{8}$ inches apart and from this rotation the angle of twist was determined. The twisting moment was computed by multiplying the angle of twist by the torsional rigidity and dividing by the distance between the bars. In other words, the experimental value for twisting moment is taken as the product of the angle of twist per unit length of beam and the torsional rigidity. The experimental values are not in as close agreement with the theoretical values as might be desirable. One reason for these discrepancies is that the differences in readings were small for large readings of the clinometer. Large readings of the clinometer are likely to be in error, since the legs of the clinometer are rigid and

are perpendicular to its length. A difference between the zero reading and the one taken after the maximum loading, amount to 0.3 or 0.4 of an inch, is considered large. It will be noted that the theoretical values of T are zero at the supports. Since the beam was firmly clamped at the supports the twisting tendency at the ends was absorbed by the flanges of the beam acting as short cantilevers. The total twisting moment at these points is equal to the shear τ times the depth of the beam $2a$.

For the load at $\alpha = 75^\circ$ measurements of strains, 30° from the load on the α segment, were made on the top and bottom flanges along four intersecting gage lines each making an angle of 45° with the adjacent one. The unit shearing stress determined from the readings was 7510 p.s.i. The computed unit shearing stress at this point was 5390 p.s.i. The computed value was made up of two parts, one due to the pure torsion T and the other due to the flange shear τ . A unit shearing stress of 5120 p.s.i. in the flange was computed for T by the method of Lyse and Johnston (8) and a unit shearing stress of 270 p.s.i. was computed due to the shear τ .

Table VI gives the deflections at the center

of the beam. It will be seen that the annealing of the beam reduced the deflections slightly. The measured deflections were greater than the theoretical values. This may be explained by the following facts; the flanges of the beam had been slightly warped during the original bending; the beam was 0.1 lb. lighter than its nominal weight; the flanges were reduced in width by the bulldozer; at certain points along the beam the section was reduced by the holes which it was necessary to tap in order to fasten the clinometer bars; and, compression on the supporting beams would tend to increase the measured deflection.

In Appendix B are discussed the theoretical stresses in the outer fibers and center fiber of the flanges for quarter-point loads. Loads of 200 lbs. were placed on the beam spaced at 45 degrees.

Table VI. Deflections of Center of Beam Due to a Load of 500 pounds.

Deflection in Inches			
α	Calculated	Before Annealing	After Annealing
90°	0.82	1.17	1.05
75°	0.74	0.93	0.89
45°	0.28	0.36	0.36

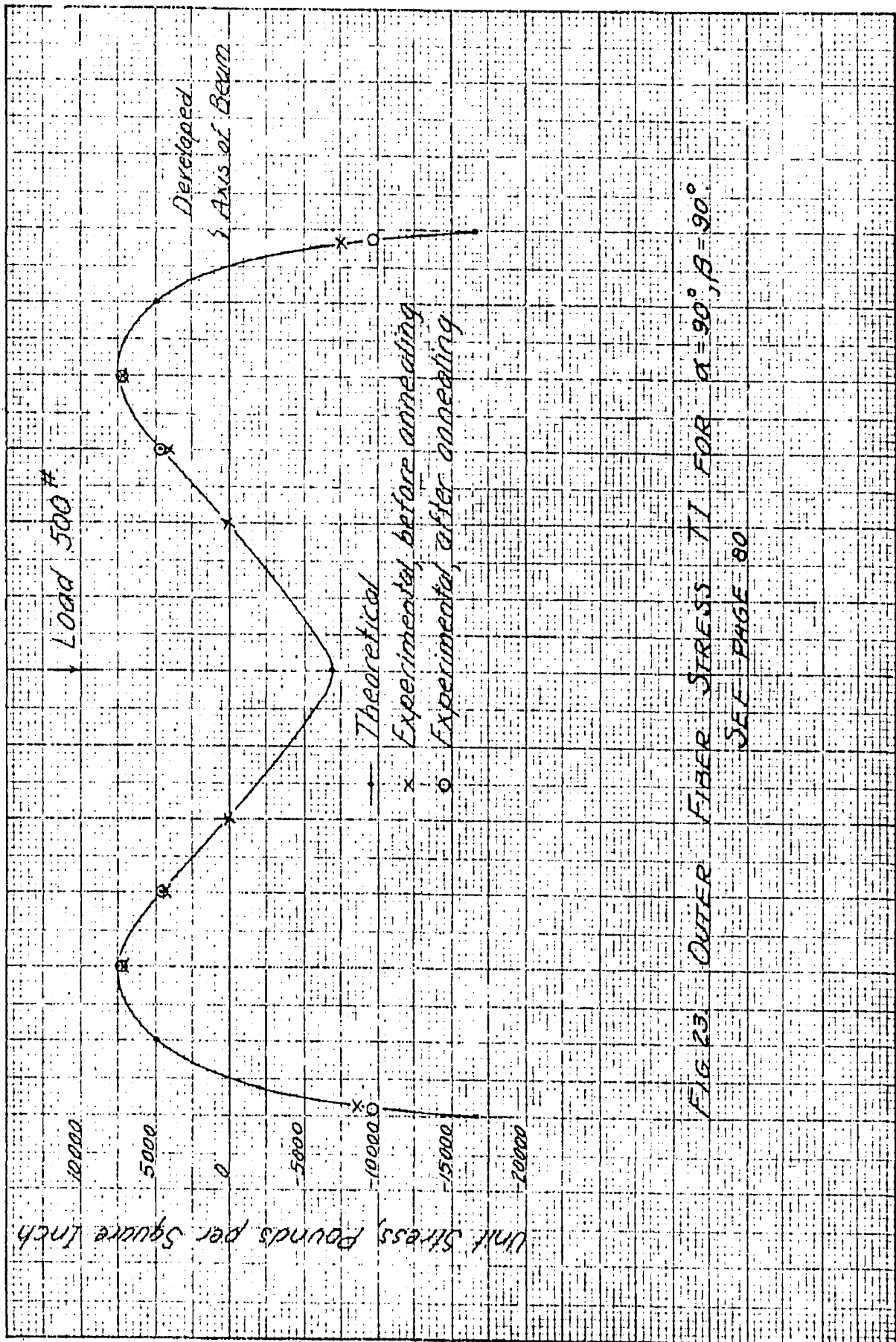


FIG. 23. OUTER FIBER STRESS T_1 FOR $\alpha = 90^\circ, \beta = 90^\circ$.
SEE PAGE 80

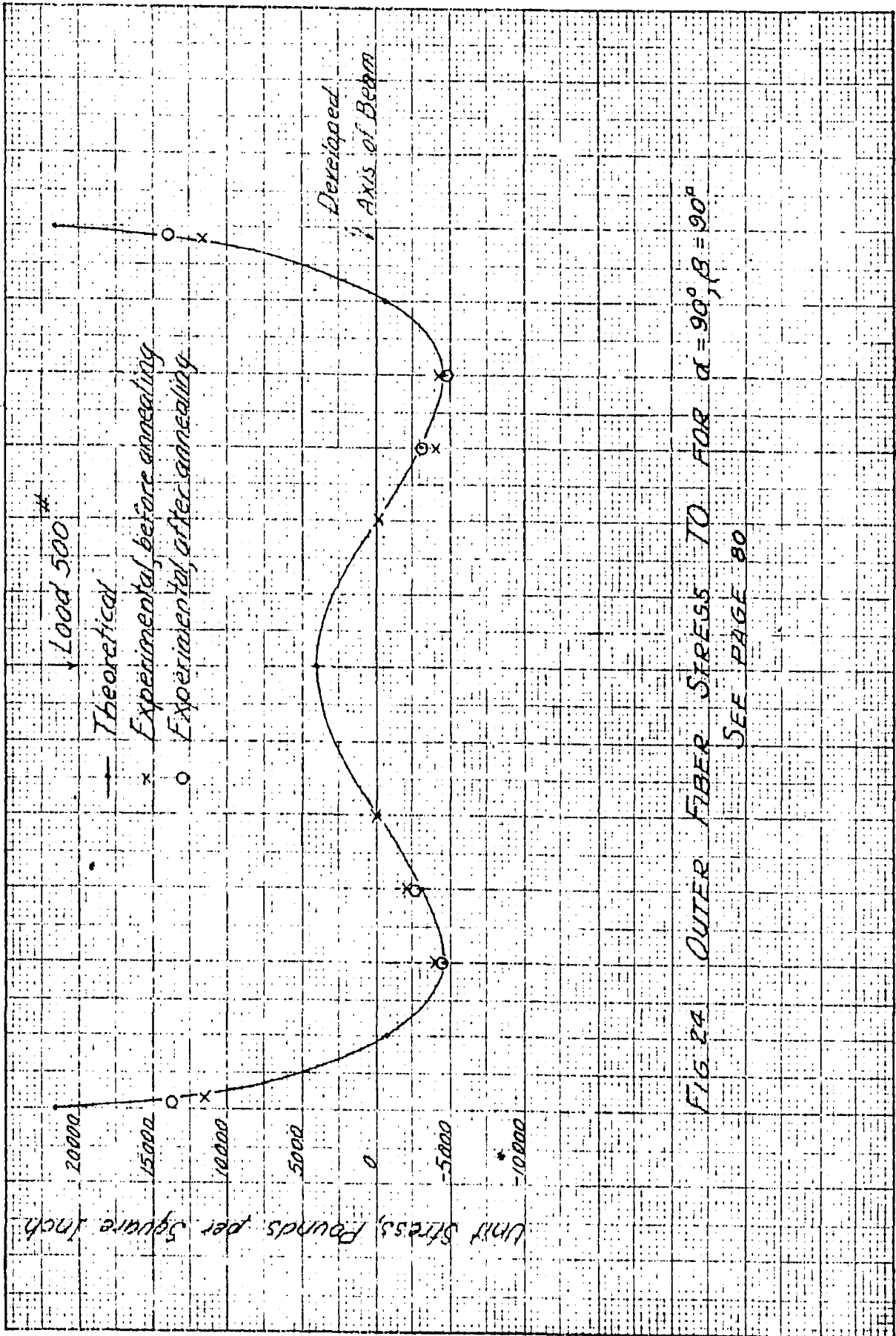


FIG. 24 OUTER FIBER STRESS TO FOR $\alpha = 90^\circ, \beta = 90^\circ$

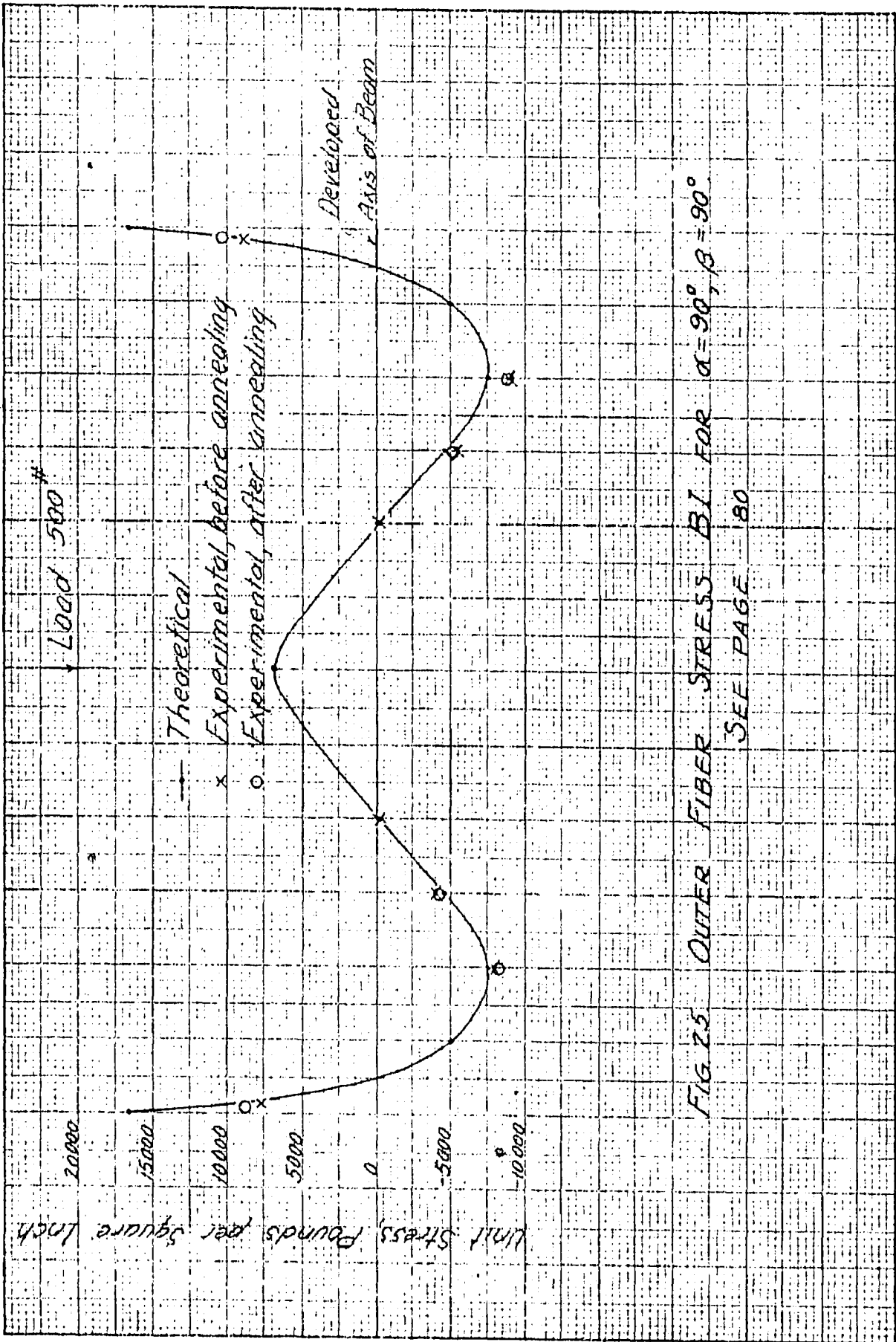


FIG. 25 OUTER FIBER STRESS BI FOR $\alpha = 90^\circ, \beta = 90^\circ$
SEE PAGE 80

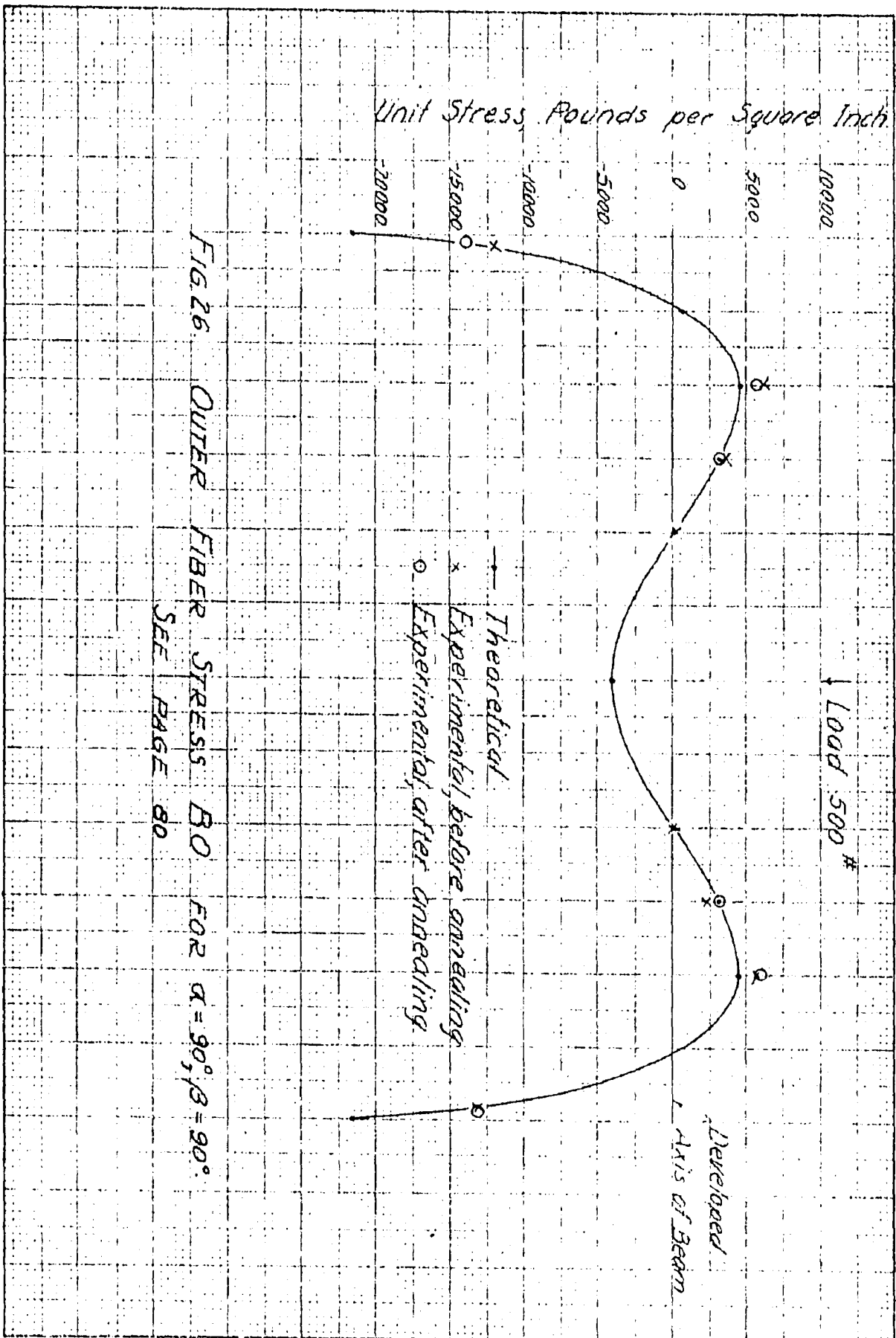


FIG. 26 OUTER FIBER STRESS BO FOR $\alpha = 90^\circ; \beta = 90^\circ$
SEE PAGE 80

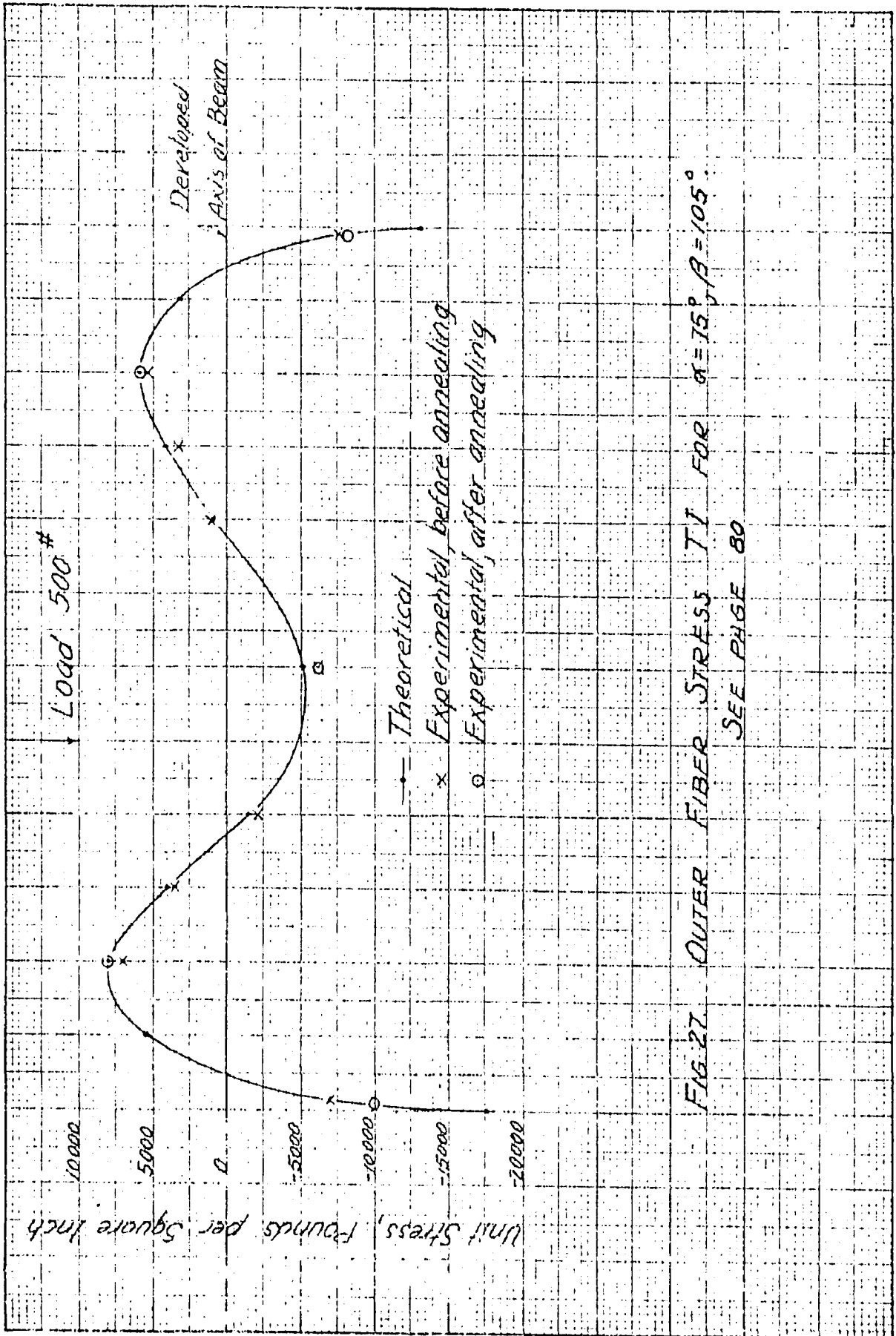


FIG. 27. OUTER FIBER STRESS T_I FOR $\alpha = 15^\circ, \beta = 105^\circ$.
SEE PAGE 80

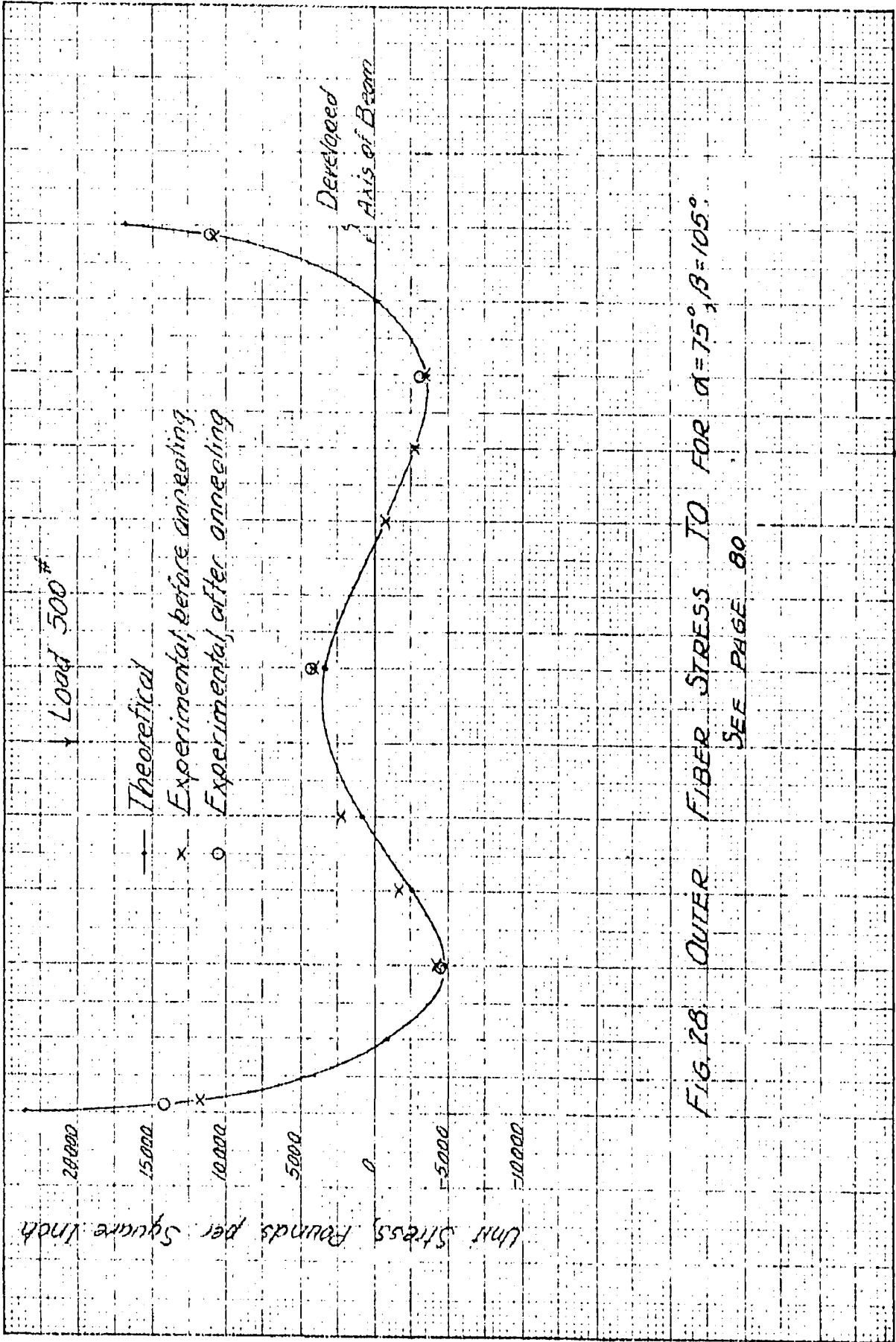


FIG. 28. OUTER FIBER STRESS TO FOR $\alpha = 75^\circ, \beta = 105^\circ$.
SEE PAGE 80

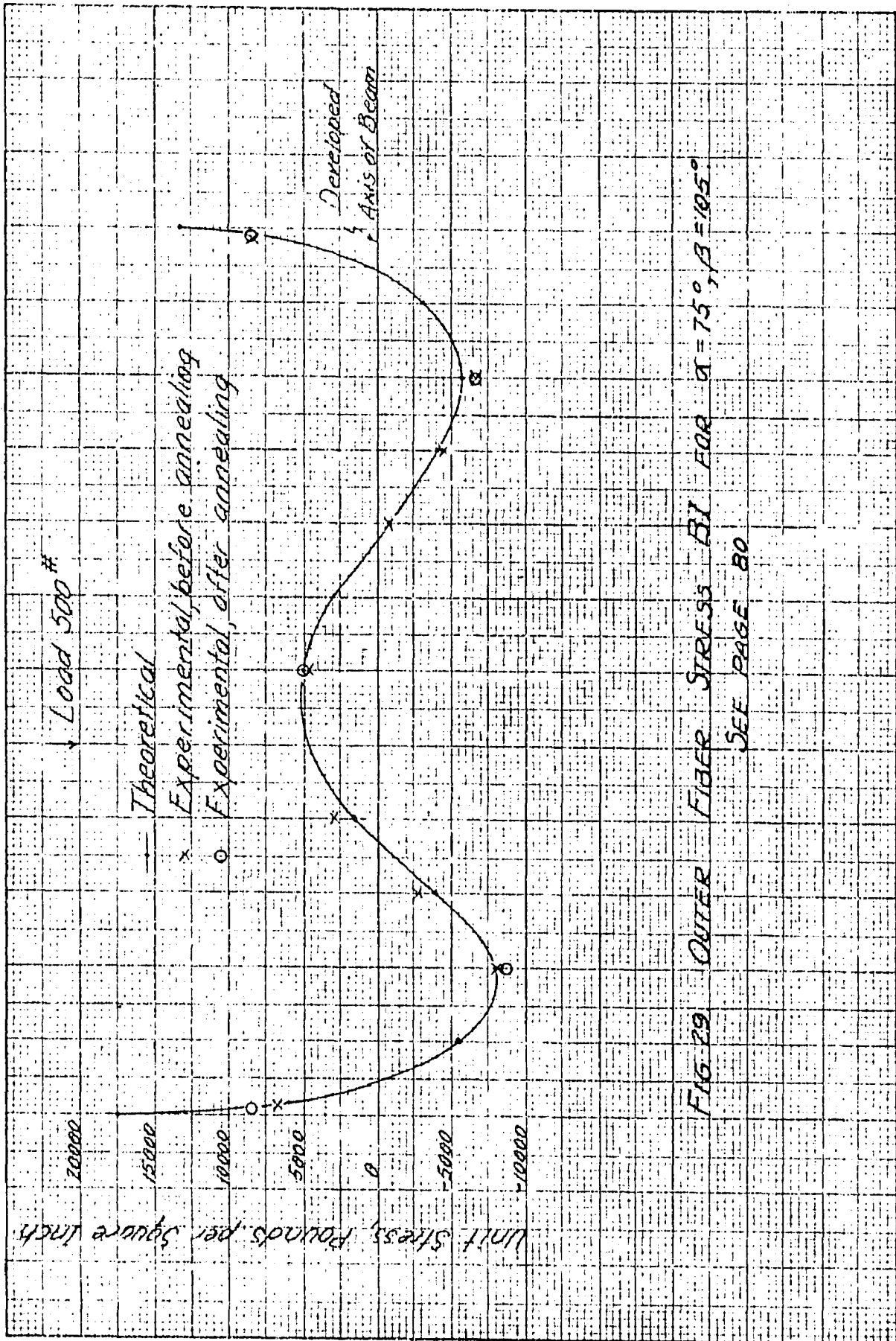


FIG. 29 OUTER FIBER STRESS BY FOR $\alpha = 75^\circ$, $\beta = 105^\circ$
SEE PAGE 80

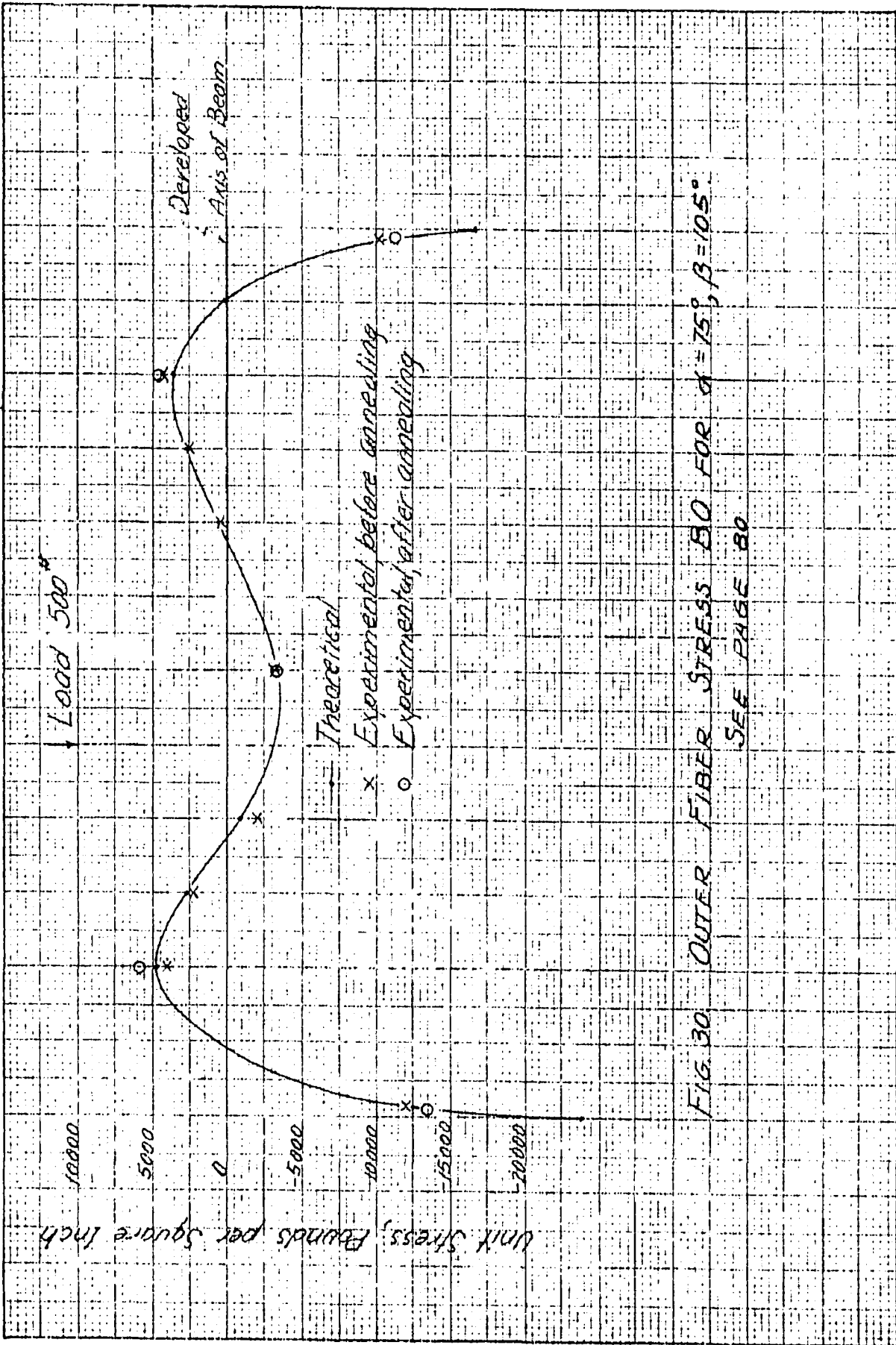


FIG. 30. OUTER FIBER STRESS 80 FOR $\alpha = 75^\circ$, $\beta = 105^\circ$.
SEE PAGE 80

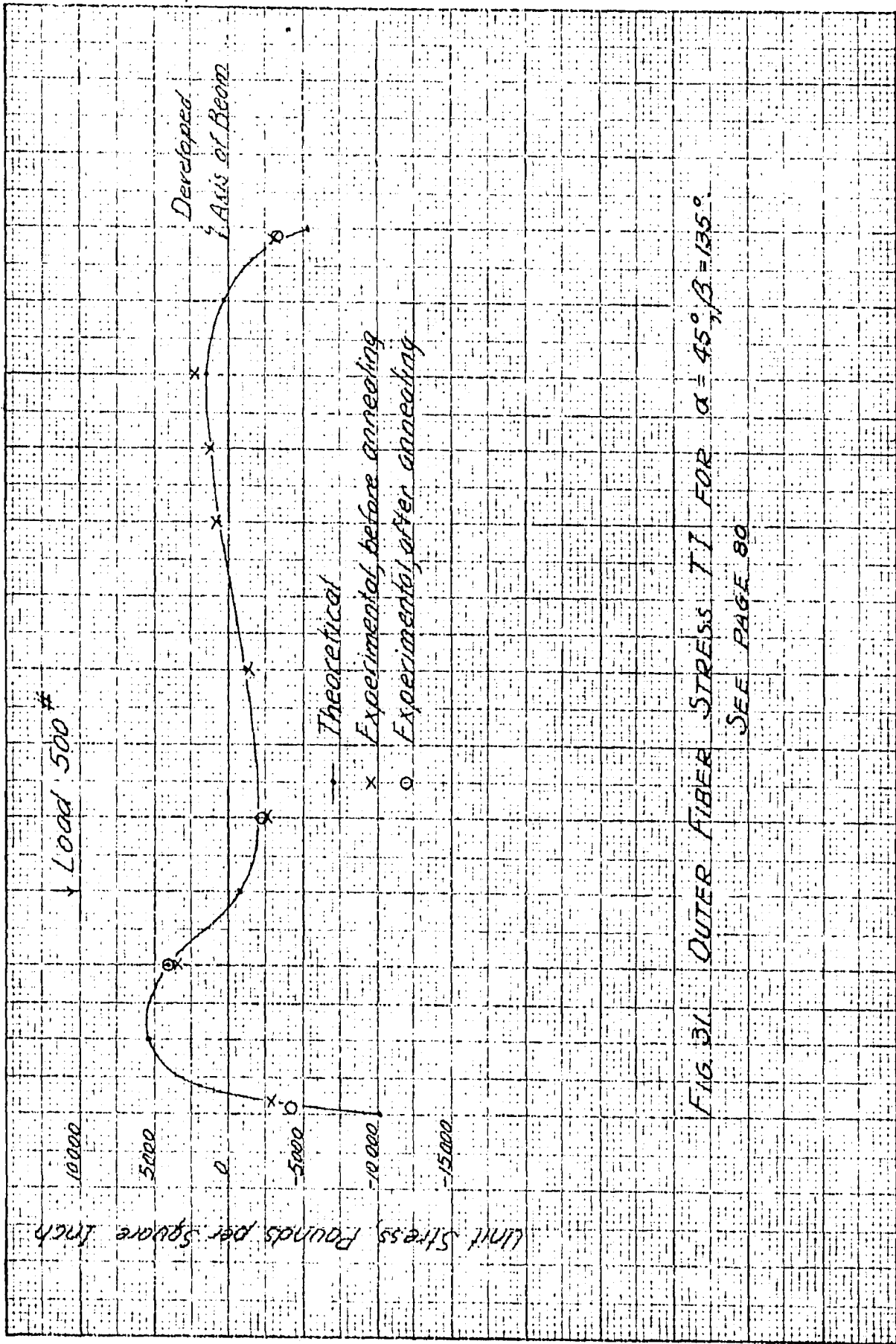


FIG. 31 OUTER FIBER STRESS T/I FOR $\alpha = 45^\circ, \beta = 135^\circ$
SEE PAGE 80

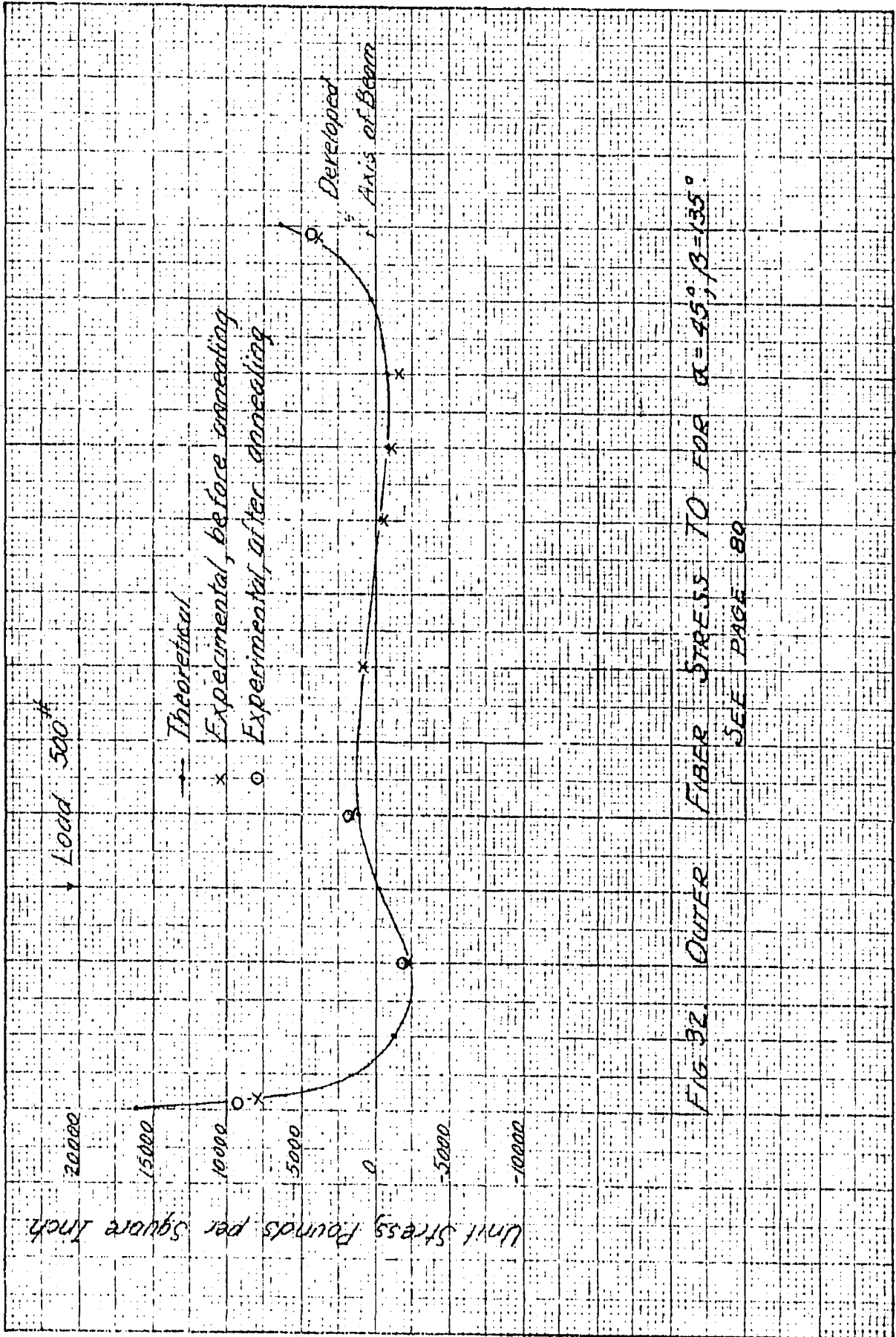


FIG. 32 OUTER FIBER STRESS TO FIBER $\alpha = 45^\circ, \beta = 135^\circ$
SEE PAGE 80

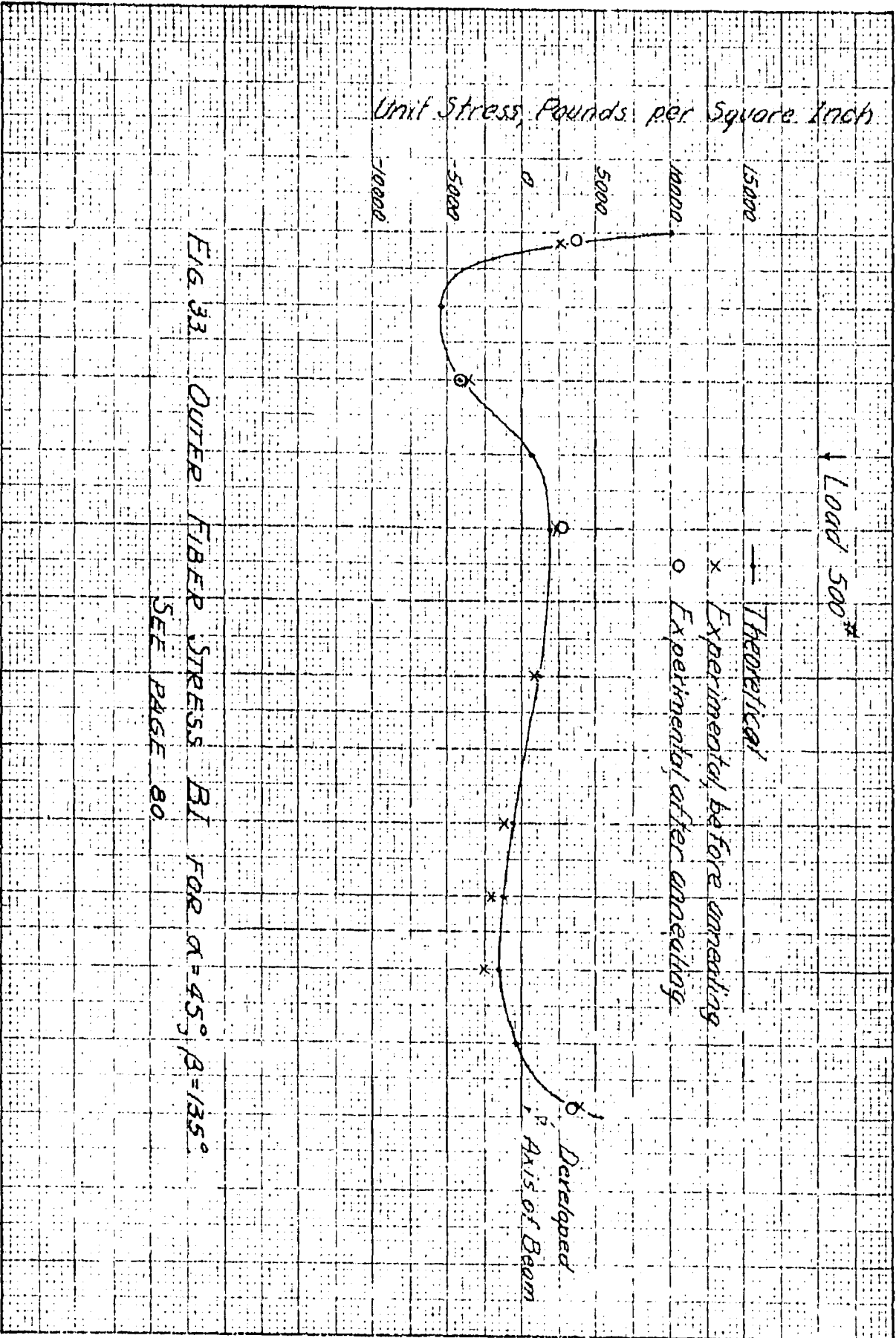


FIG. 33 OUTER FIBER STRESS BI FOR $\alpha = 45^\circ$, $\beta = 135^\circ$.

SEE PAGE 80

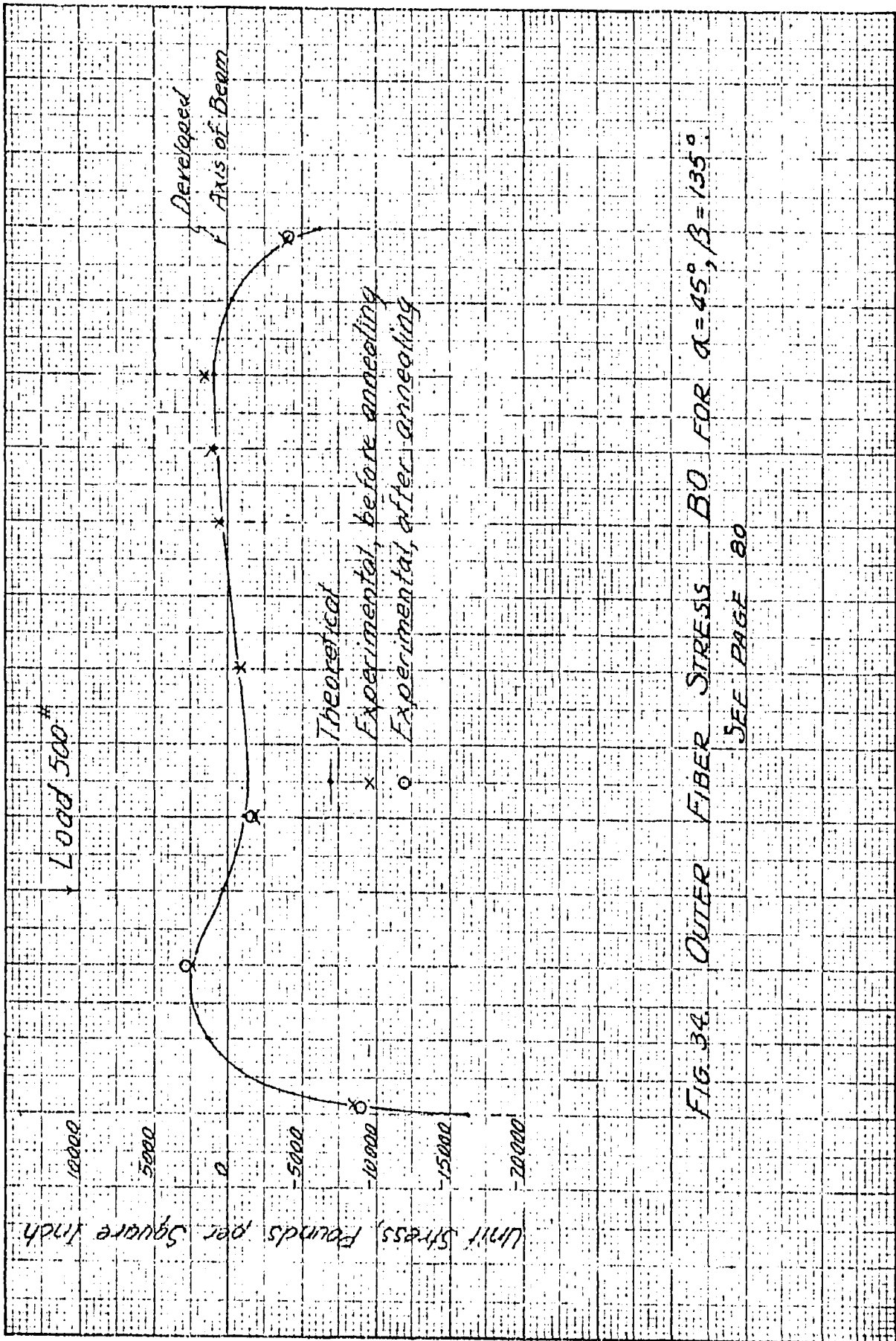


FIG. 34. OUTER FIBER STRESS BO FOR $\alpha = 45^\circ$, $\beta = 135^\circ$.
SEE PAGE 80

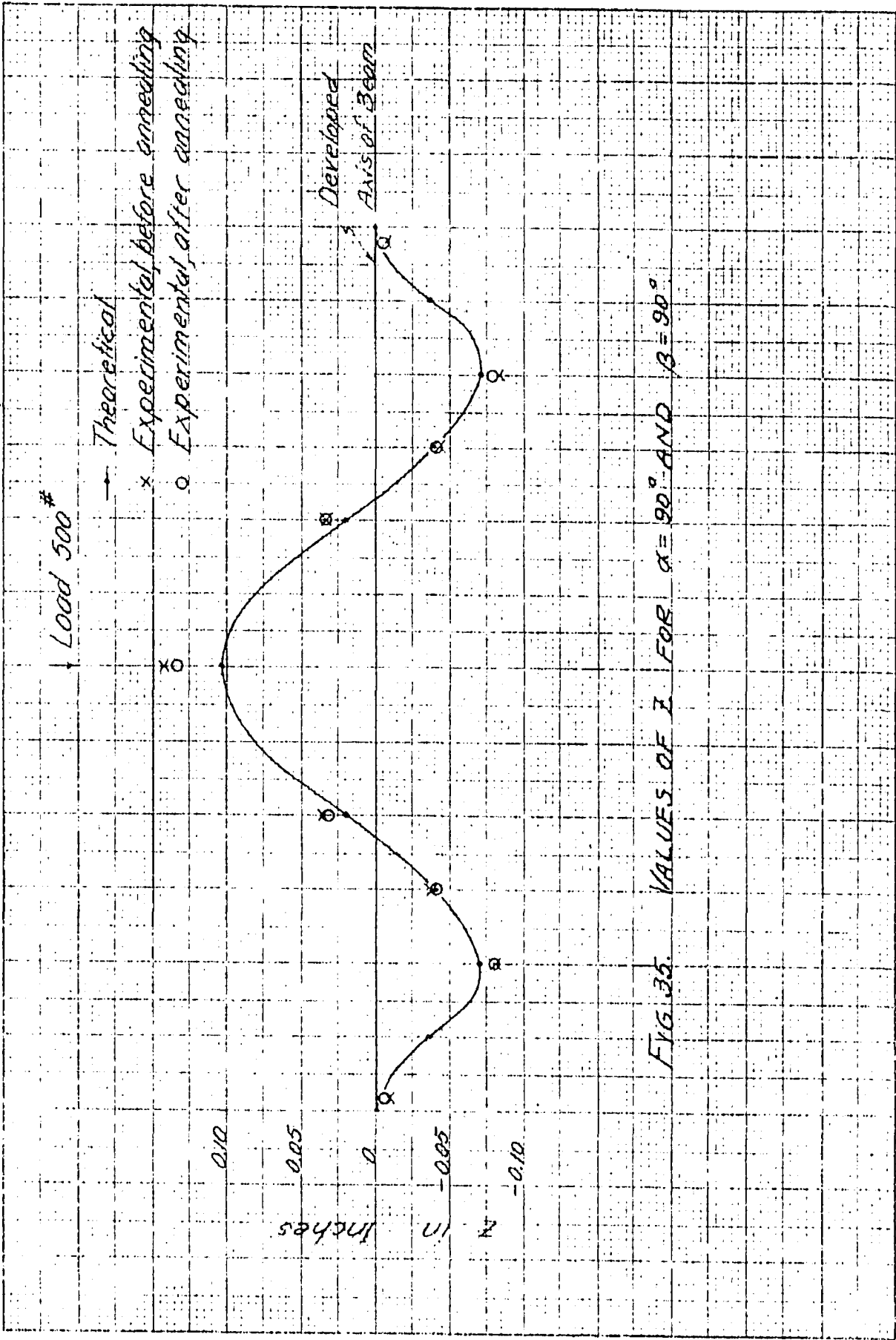
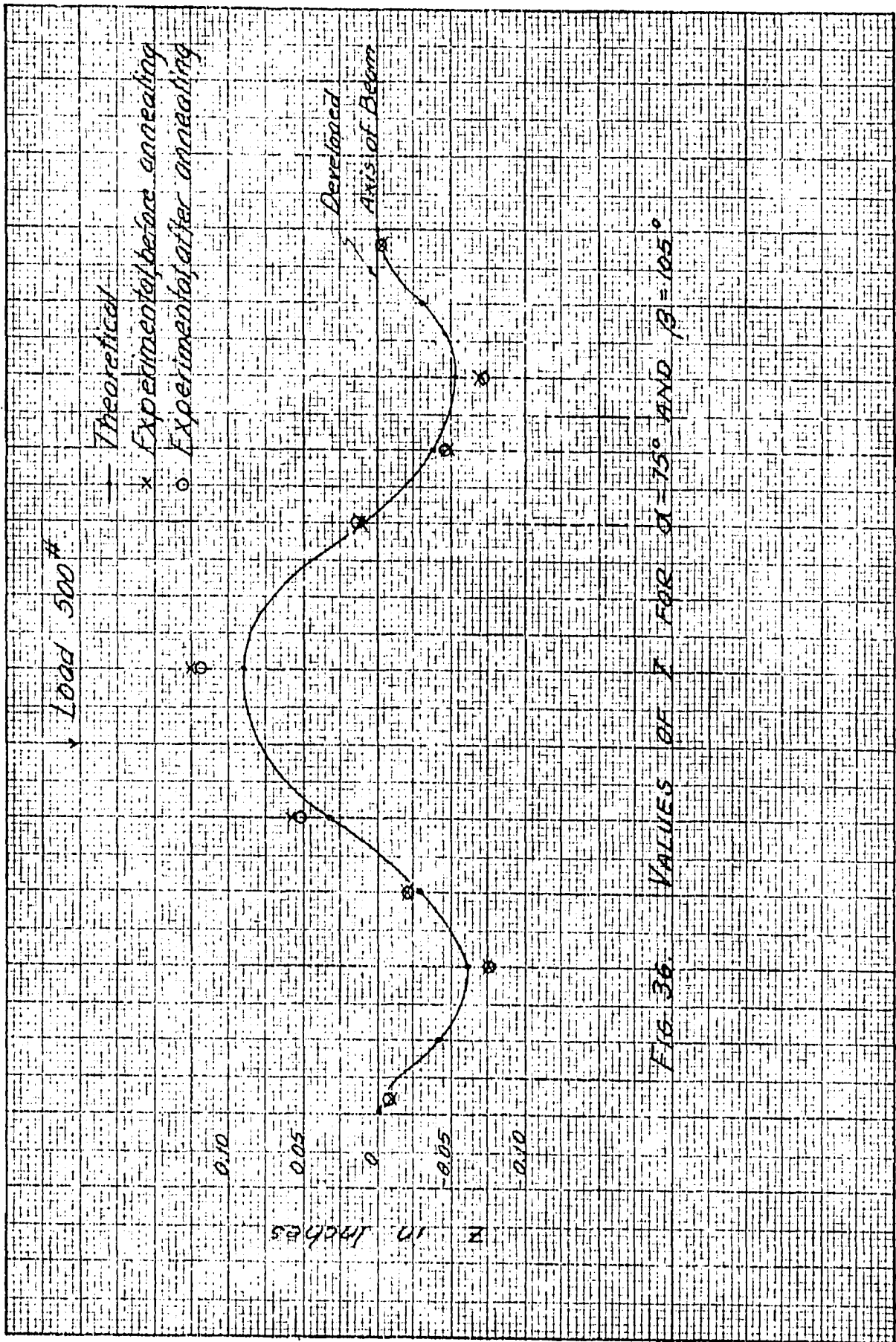


FIG. 35. VALUES OF I FOR $\alpha = 90^\circ$ AND $\beta = 90^\circ$



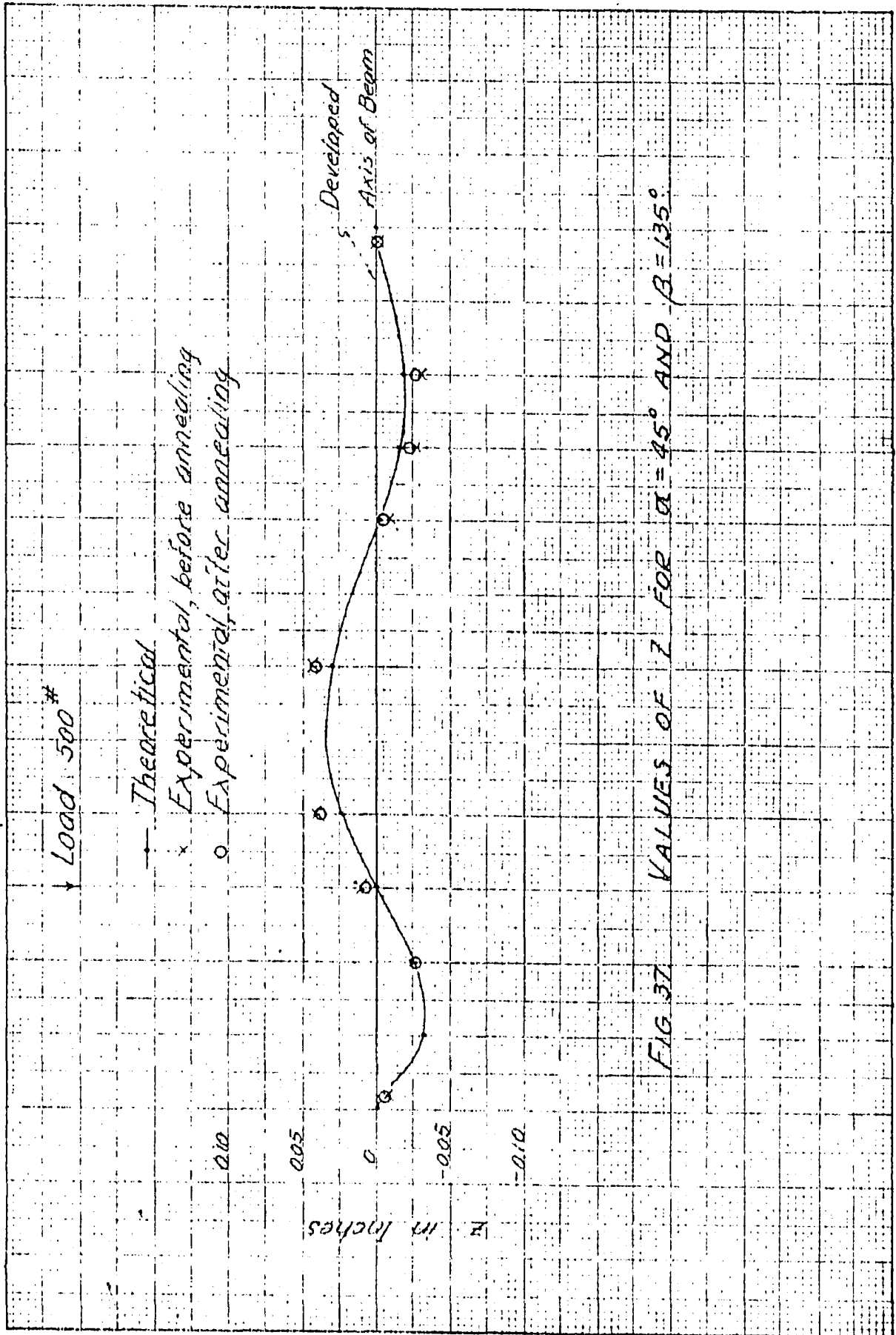


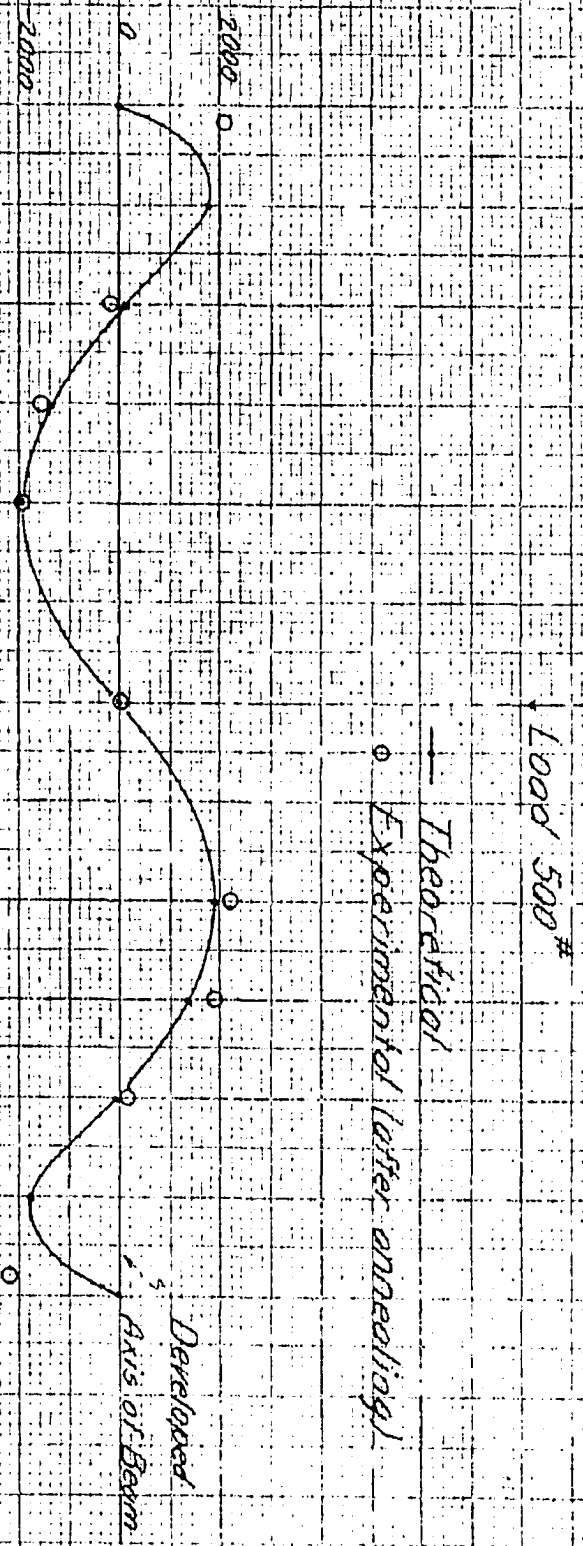
FIG. 37 VALUES OF I FOR $\alpha = 45^\circ$ AND $\beta = 135^\circ$

Twisting Moment
in Inch Pounds

FIG. 38

TWISTING MOMENT

$\alpha = 90^\circ$ AND $\beta = 90^\circ$



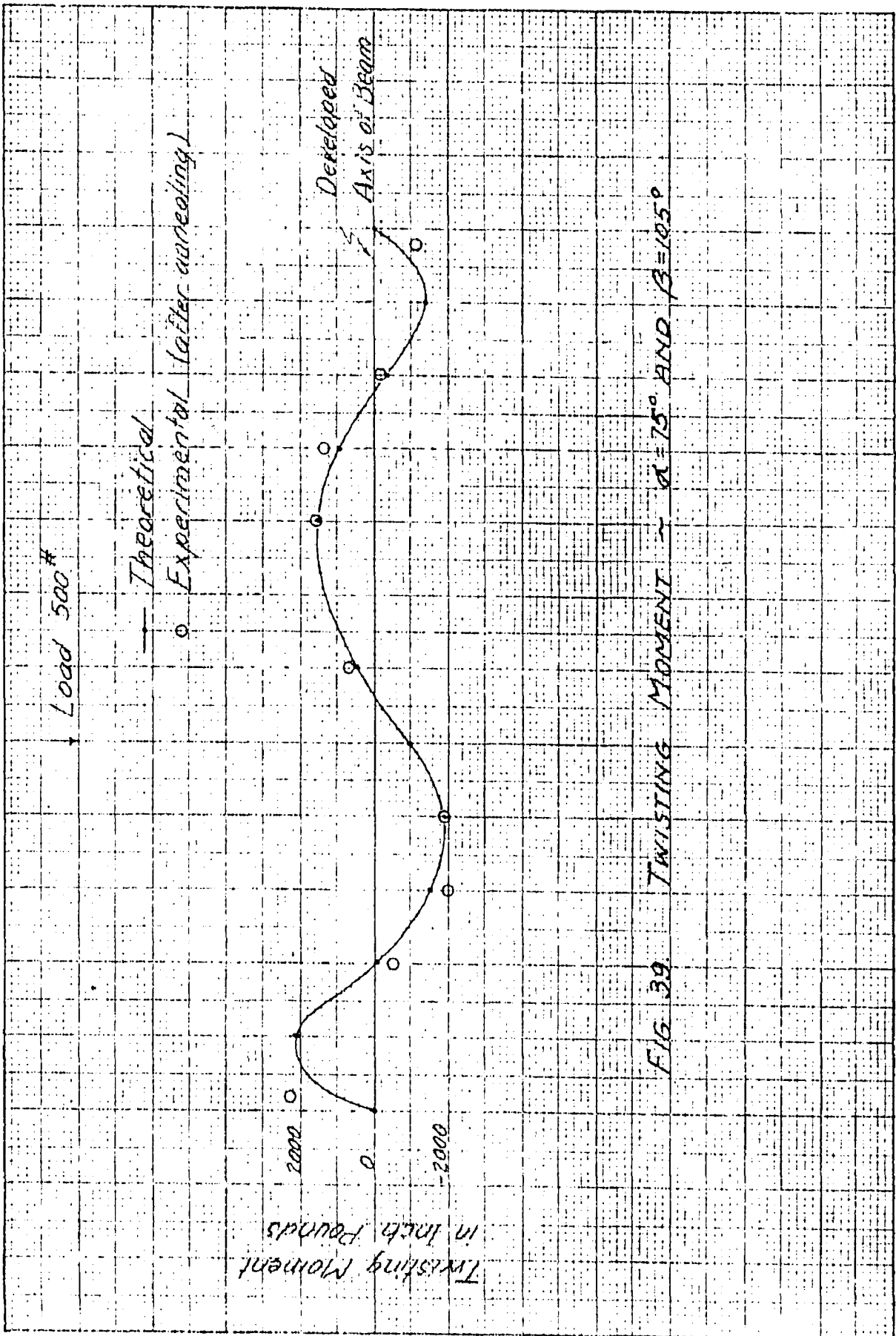


FIG. 39. TWISTING MOMENT - $\alpha = 75^\circ$ AND $\beta = 105^\circ$

Form F-5

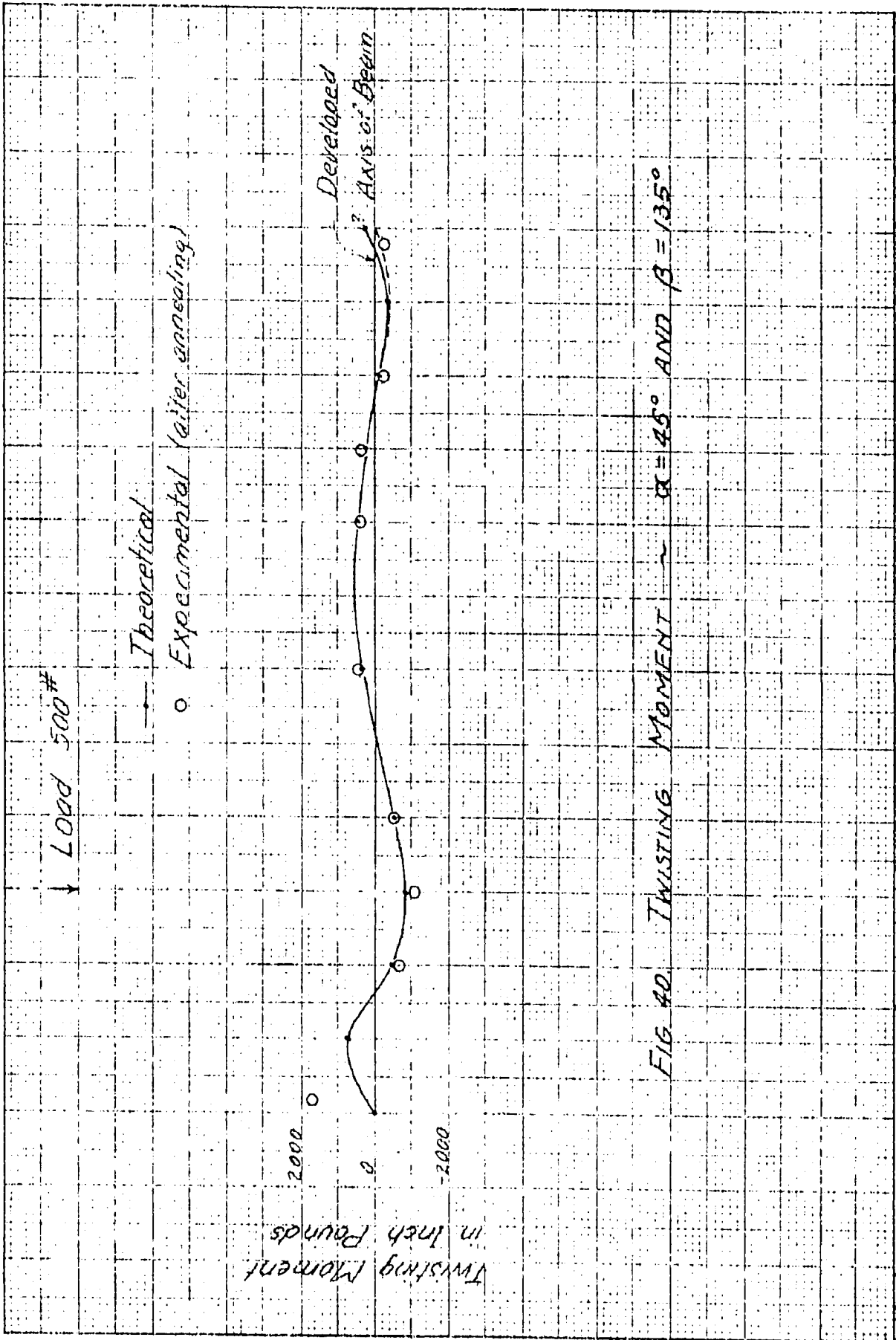


FIG. 40. TWISTING MOMENT ~ $\alpha = 45^\circ$ AND $\beta = 135^\circ$

VII. CONCLUSIONS

A. Analysis of Curved Beam by Method of Work Involving Only Bending Moment, Twisting Moment and Shear, with Tests on a Curved Rod.

1. This analysis may be used for beams of circular cross-section or of such cross sections that little or no bending moment is induced in planes parallel to the plane of the axis of the beam when the beam is twisted.
2. This analysis may be used for a horizontally curved beam of any plan.
3. This analysis may be used for unsymmetrical loads.
4. The computed bending stresses are in close agreement with the experimental values in the case of a round steel rod used as a curved beam and loaded perpendicularly to the plane of its axis.
5. The computed twisting moments are in close agreement with the experimental values.

B. Analysis of the Circular-Arc Beam of I-form and
Tests on the I-Beam.

1. The analysis given is satisfactory for computing stresses in a circular-arc beam of I-form.
2. This analysis may be used in the case of any circular-arc fixed-end beam of I-form. To determine the constants of integration it is necessary to substitute the boundary conditions for the particular case in the equations on page 70 and solve the equations simultaneously.
3. Relatively high stresses occur near and at the fixed ends of a circular-arc curved beam of I-form.
4. The twisting moment producing pure torsion is zero at the supports.
5. The measured deflections of the I-beam are 20 to 43 percent greater than the theoretical values. These relatively large discrepancies may be accounted for by calling attention to the fact that about 95 percent of the deflection is due to the twisting of the beam. The irregularities of this particular beam have a greater influence on the deflections due to twisting than the deflections due to bending.

6. The computed stresses in the outer fibers are in very close agreement with the experimental values.
7. The experimental values of twisting moment producing pure torsion are in close agreement with the computed values, with the exception of a few values which were higher than the computed values.
8. Upon comparing the beam in the annealed condition with the beam in the unannealed condition it is noted that there is very slight difference in the observed readings for strain on the outer fibers.
9. In the case of check tests on the annealed beam the readings could be duplicated while for the beam in the unannealed condition they were slightly erratic. This would indicate that in the case of the annealed beam there was more uniformity in material structure.
10. The analysis shows that for quarter-point loads the stress at the supports due to the bending moment alone has a ratio to the outer fiber stress of about 1 to 7.
11. The working stress for the outer fibers can probably be taken just below the yield point of the material without serious damage except that the deflection might be excessive.

VIII. SUMMARY

Two analyses of the curved beam are presented here. The first analysis is developed by the method of work and involves only bending moment, twisting moment and shear. The beam may have any plan form, loaded with concentrated loads or distributed loads, and must have such a cross-section that there is little or no bending moment induced in planes parallel to the plane of the axis of the beam when the beam is twisted. The second analysis pertains to a beam of I-form with a circular-arc plan loaded with a single concentrated load.

Experiments were conducted in order that a comparison might be made with the theoretic results. Accompanying the first analysis are the results of tests made of a $3/4$ inch round steel rod bent into a circular-arc of $14\frac{1}{2}$ inch radius. For comparison with the second analysis are the results of tests on a 6 inch 12.5 lb. American Standard I-beam bent in a semi-circle to a radius of 6 feet. The experimental results for the beam bent cold are given together with the experimental results for the beam in the annealed condition.

IX. LITERATURE CITED

1. Andrée, W. L. Zur Berechnung gekrümmter Träger. Der Eisenbau, 9:184-190. 1918.
2. Bethlehem Manual of Steel Construction. pp. 279-289. 1934.
3. Federhofer, K. Berechnung des Senkrecht zu seiner Ebene belasteten Bogenträgers. Ztschr. f. Math. und Physik, 62:40-63. 1914.
4. Gibson, A. H. and Ritchie, E. G. The Circular-Arc Bow Girder. Constable & Co., London. 1914.
5. Grashof, F. Elasticität und Festigkeit. pp. 294-296. R. Gaertner, Berlin. 1878.
6. Hailer, J. Beitrag zur Berechnung gekrümmter Träger. Bautechnik, 10:372. 1932.
7. Kannenberg, B. G. Zur Theorie torsion^sfester Ringe. Der Eisenbau, 4:329-334. 1913.
8. Lyse, I. and Johnston, B. G. Structural Beams in Torsion. Trans. Am. Soc. Civil Engr., 101:857-896. 1936.
9. Mayer, R. Über Elastizität und Stabilität des geschlossenen und offenen Kreisbogens. Ztschr. f. Math. und Physik, 61:302-308. 1913.
10. Oesterblom, I. Bending and Torsion in Horizontally Curved Beams. Jour. Am. Concrete Inst., 3:597-606. 1932.
11. Pippard, A. J. S. and Barrow, F. L. The Stress Analysis of Bow Girders. Gt. Brit. Dept. of Sci. and Indus. Res. Bldg. Res. Bd. Tech. Paper No. 1. Royal Sta. Off., London. 1926.

12. St. Hessler. Der nach einen Kreisbogen gekrümmte beiderseits eingespannte Eisenbetonträger mit rechteckigem Querschnitt. Beton und Eisen, 26:425-433. 1927.
13. St. Hessler. Der kontinuierliche, halbkreisförmig gebogene und gleichmäßig belastete Eisenbetonträger mit rechteckigen Querschnitt auf drei und vier gleich weit entfernten Stützen. Beton und Eisen, 29:149-154. 1930.
14. Unold, Georg. Der Kreisträger. Forschungsarbeiten, Ver. Deut. Ing., No. 255. Berlin. 1922.
15. Young, C. R. and Hughes, C. A. Torsional Strength of Steel I-Sections. Univ. of Toronto, School of Engineering Research Bul. No. 4, Sec. 3. pp. 131-144. 1924.
16. Worch, G. Beitrag zur Ermittlung der Formänderungen ebener Stabzüge mit räumlicher Stützung. Beton und Eisen, 29:167-173, 183-189, 200-205. 1930.

X. ACKNOWLEDGMENT

The author wishes to express his appreciation to Professor R. A. Caughey, Chairman, and the other members of his Committee for the many helpful suggestions offered during the progress of the investigation. Acknowledgment is also due Professor H. L. Daasch of the Mechanical Engineering Department for supervising the annealing of the I-beam, and to Doctor Archie Higdon of the Department of Theoretical and Applied Mechanics for his assistance in checking part of the mathematical solutions.

APPENDIX A

Derivation of the Expression of the Relation Between
Change in Curvature and Bending Moment
in the Case of Curved Rods.

The following is the derivation of the expression for the bending moment (M) in the flange due to the change in the curvature of the axis of the top flange. Figure 41 shows the points 1 and 2 in their original positions and 1' and 2' in their displaced positions.

$$dx = r d\phi ; \quad \frac{d\phi}{dx} = \frac{d\phi}{r d\phi} = \frac{1}{r}$$

The new curvature may be expressed as

$$\frac{1}{r_1} = \frac{d\phi + \Delta d\phi}{dx + \Delta dx} \quad (a)$$

where r_1 is the new radius.

The angle between the tangent to the center line at

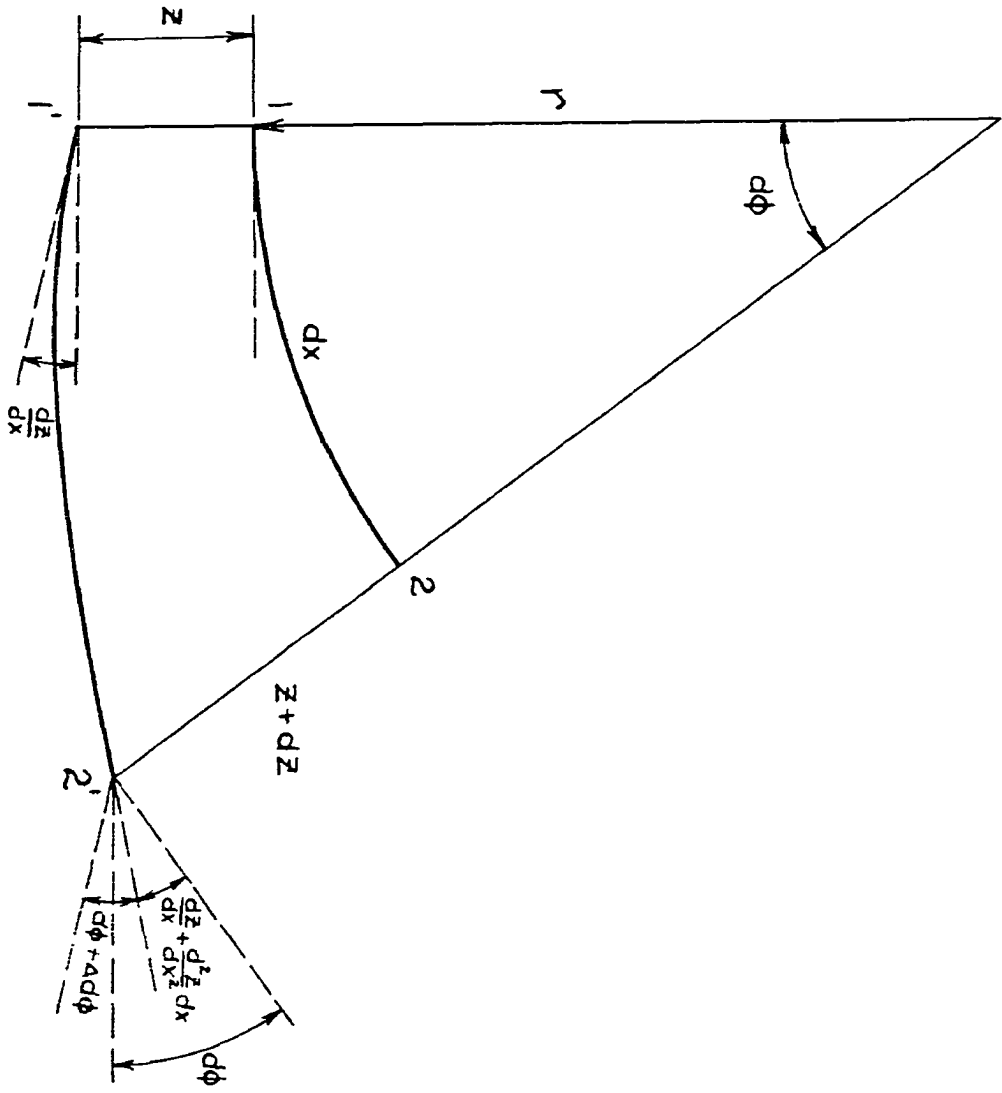


FIG. 41. CHANGE IN CURVATURE.

l' and the normal to the radius at l' is $\frac{dz}{dx}$. The corresponding angle at $2'$ is

$$\frac{dz}{dx} + \frac{d^2z}{dx^2} dx$$

Then

$$\Delta d\phi = - \frac{d^2z}{dx^2} dx$$

and

$$\Delta dx = (r + z) d\phi - rd\phi = zd\phi = \frac{zdx}{r}$$

Substituting in equation (a) we have

$$\frac{1}{r_1} = \frac{d\phi - \frac{d^2z}{dx^2} dx}{dx + \frac{zdx}{r}} = \frac{\frac{1}{r} - \frac{d^2z}{dx^2}}{1 + \frac{z}{r}}$$

$$\frac{1}{r_1} \left(1 + \frac{z}{r}\right) = \frac{1}{r} - \frac{d^2z}{dx^2}$$

$$\frac{1}{r_1} + \frac{z}{r_1 r} = \frac{1}{r} - \frac{d^2z}{dx^2}$$

$$\frac{1}{r_1} - \frac{1}{r} = -\frac{z}{r_1 r} - \frac{d^2z}{dx^2} = -\left(\frac{z}{r^2} + \frac{d^2z}{dx^2}\right)$$

since r^2 can be taken equal to rr_1 for very small changes in the length of the radius. Also

$$\frac{1}{r_1} - \frac{1}{r} = + \frac{M}{EH}$$

The plus sign on the right side of the equation follows from the sign of the bending moment which is taken to be positive when it produces a decrease in the initial curvature.

We may then write

$$- \frac{M}{EH} = \frac{z}{r^2} + \frac{d^2 z}{dx^2} = \frac{1}{r^2} (z + z'')$$

APPENDIX B

Quarter-Point Loads.

In order to study the effect of several loads on the beam at one time the curves of Figs. 42, 43, 44 and 45 are plotted. The outer fiber stresses are obtained by the theoretical superposition of the previous individual loads at $\alpha=45^\circ$, $\alpha=90^\circ$ and $\alpha=135^\circ$. To keep the stresses within working limits loads of 200 lbs. each are placed at the quarter-points. These figures also show the stress due to the bending moment M . It is seen that this latter stress is very small compared with the outer fiber stress. In fact, on comparing the maximum values of each it is noted that they have a ratio of about 1 to 7.

Unless it is necessary to keep within certain limits of deflections it would seem best to take the working stress for the outer fibers near the yield point. If the yield point should be reached in the outer fibers the author believes little damage would be done except

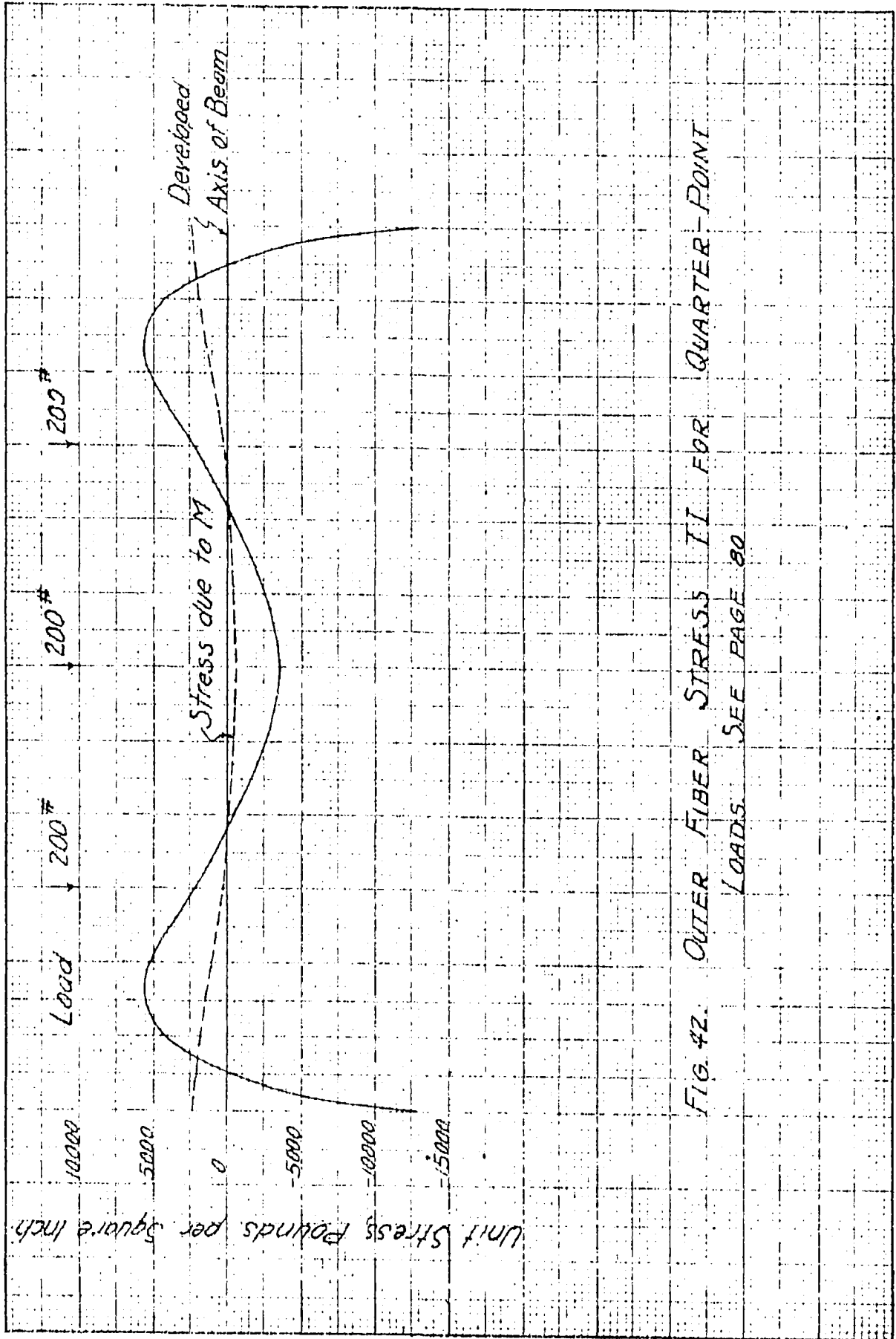
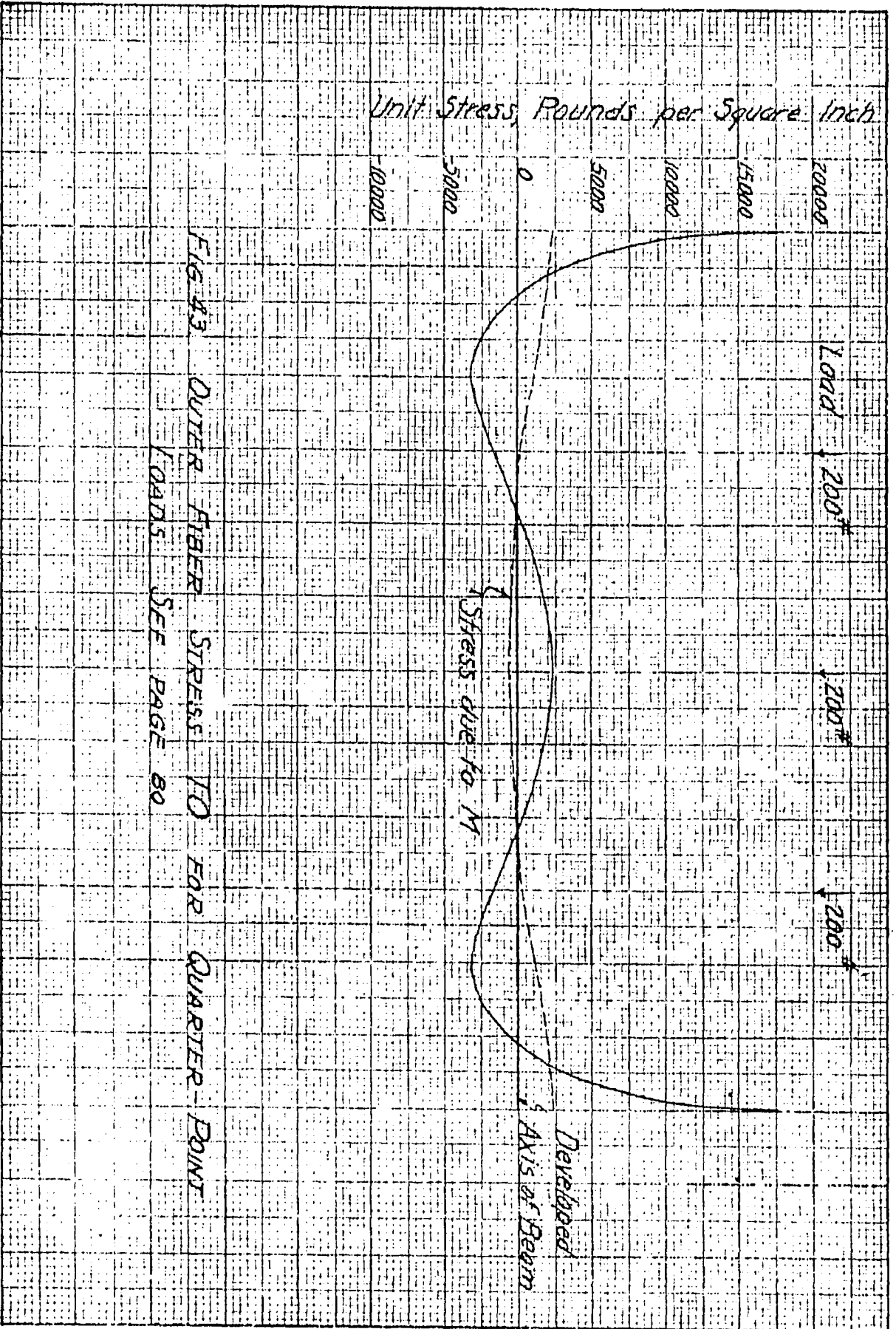


FIG. 42. OUTER FIBER STRESS T_I FOR QUARTER-POINT LOADS. SEE PAGE 80



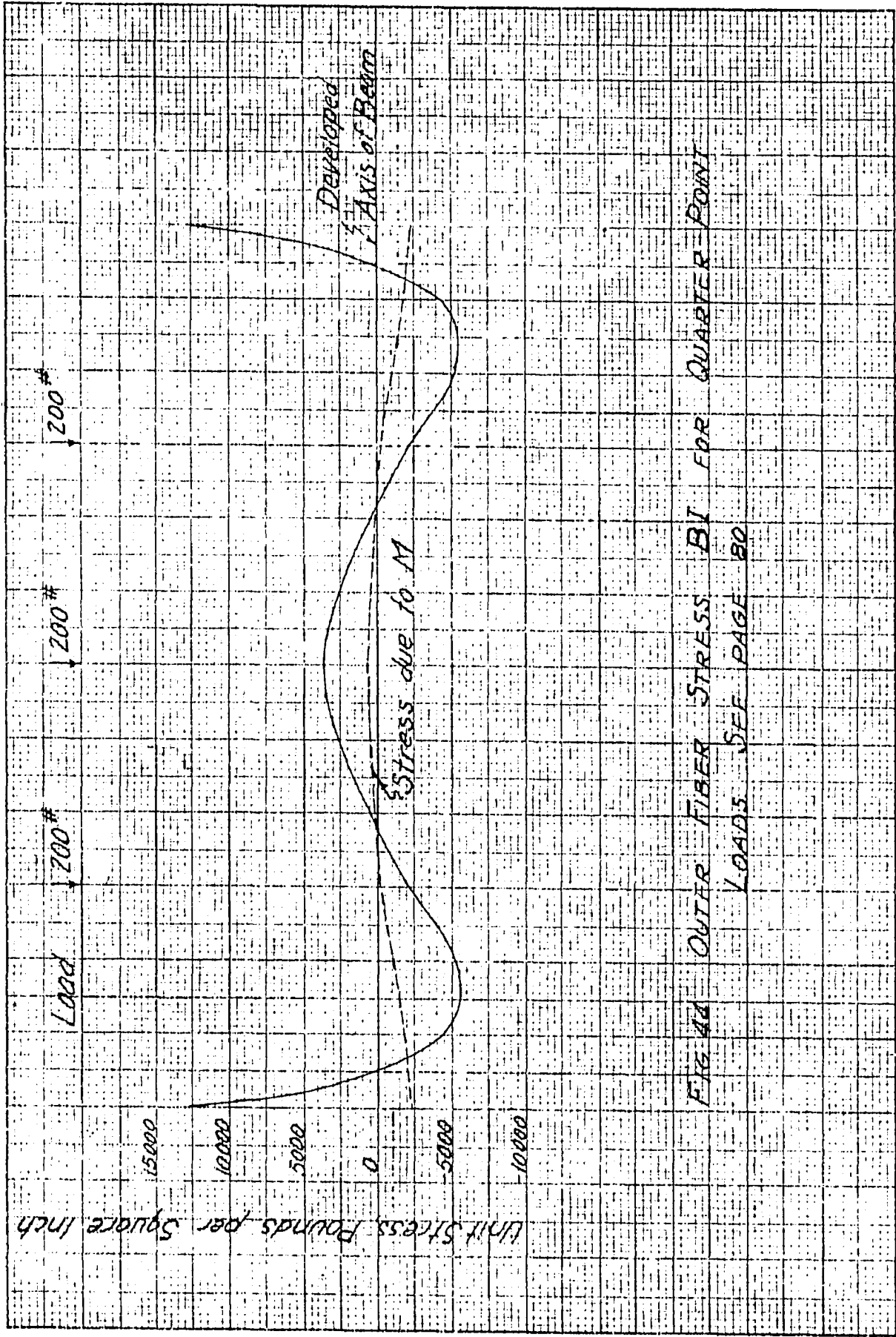


FIG 44 OUTER FIBER STRESS BI FOR QUARTER POINT LOADS SEE PAGE 80

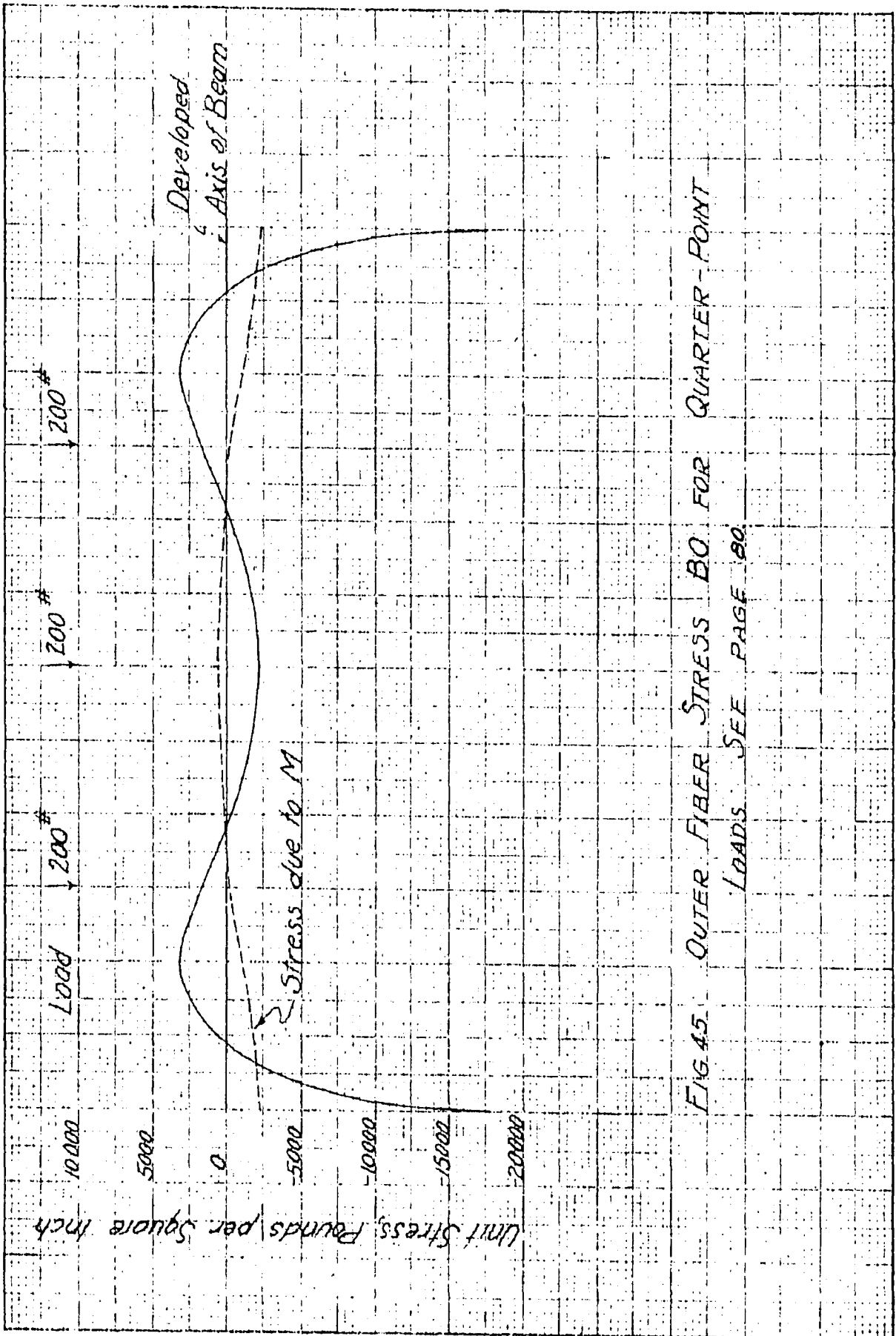


FIG. 45. OUTER FIBER STRESS B_0 FOR QUARTER-POINT LOADS. SEE PAGE 80.

that the deflection might be excessive. The reason for this belief is that although the stress due to the moment M is high it affects a localized portion of the beam. In other words this is another case of relatively high localized stress. As stated before, the stresses due to M are of the same sign in the outer edges of the beam diagonally opposite one another.